



Florida State University
Center for Advanced Power Systems

High Penetration Solar PV Deployment Sunshine State Solar Grid Initiative (SUNGRIN) Final Report



Rick Meeker*, Mischa Steurer, Omar Faruque, Hui Li
James Langston, Harsha Ravindra, Karl Schoder, Peter McLaren
Matthew Bosworth, Isaac Leonard, Raturaj Soman, Mike Sloderbeck,
Dionne Soto
Ali Hariri, Thierry Kayiranga, Ye Yang
Florida State University, Center for Advanced Power Systems

Houtan Moaveni, David Click, Bob Reedy
University of Central Florida, Florida Solar Energy Center

* Project Lead PI / Corresponding Author

May 2015

This material is based upon work supported by the U.S. Department of Energy (Office of Energy Efficiency and Renewable Energy, SunShot Program) under Award Numbers DE- EE0002063 and DE-EE0004682



Disclaimer

This report was prepared as an account of work sponsored by an agency of the United States Government. Neither the United States Government nor any agency thereof, nor any of their employees, makes any warranty, express or implied, or assumes any legal liability or responsibility for the accuracy, completeness, or usefulness of any information, apparatus, product, or process disclosed, or represents that its use would not infringe privately owned rights. Reference herein to any specific commercial product, process, or service by trade name, trademark, manufacturer, or otherwise does not necessarily constitute or imply its endorsement, recommendation, or favoring by the United States Government or any agency thereof. The views and opinions of authors expressed herein do not necessarily state or reflect those of the United States Government or any agency thereof.

Acknowledgments

The work described herein was made possible by the dedication and commitment of the SUNGRIN project's electric utility partners and industry suppliers who provided information on high penetration PV circuits for analysis, valuable input and perspective on real-world issues and challenges, review of project activities and results, and in-kind cost share contributions to completion of the total effort:

- **Florida Municipal Power Agency (FMPA)**
- **Florida Power and Light (FPL) / NextEra Energy, Inc.**
- **Florida Reliability Coordinating Council (FRCC)**
- **Gainesville Regional Utilities (GRU)**
- **Jacksonville Electric Authority (JEA)**
- **Lakeland Electric**
- **Orlando Utilities Commission (OUC)**
- **AMEC** (Phase 1, Phase 2 only)
- **OSISoft**
- **Satcon Technologies** (Phase 1 only)
- **SMA Americas** (Phase 2 only)

Special thanks go to electric utility partners **GRU, JEA, Lakeland Electric, and OUC**, who's committed and very capable team members made possible the detailed studies of the four distribution feeders and two substations described in the report.

University partners also played an important role, particularly in completing the research and analytical work. The **Florida Solar Energy Center (FSEC)** at the **University of Central Florida (UCF)** made major contributions in data collection and studies of the solar resource throughout the course of the project, and the **Power Center for Utility Explorations (PCUE)** at the **University of South Florida (USF)** contributed to the research activities in Phase 1.

Finally, this work was made possible through the support of the U.S. Department of Energy's Office of Energy Efficiency and Renewable Energy (EERE), SunShot Program.

Contact: R. H. (Rick) Meeker, Jr., P.E.
Florida State University
Center for Advanced Power Systems
2000 Levy Ave., Suite 140
Tallahassee, FL 32310
rmeeke@fsu.edu (or rmeeke@nhuenergy.com)
850.645.1711

CONTENTS

1	EXECUTIVE SUMMARY.....	1-1
1.1	IMPACT OF THE SOLAR RESOURCE IN PV INTEGRATION	1-1
1.2	ANALYTICAL APPROACHES	1-2
1.3	HIGH PENETRATION PV IMPACTS, FLORIDA CIRCUITS.....	1-2
1.4	OPEN-USE MODELS AND TOOLS	1-2
1.5	SYSTEMATIC IMPACT ASSESSMENT	1-3
1.6	VOLTAGE REGULATION	1-3
2	INTRODUCTION.....	2-1
2.1	SOLAR PV INTEGRATION CHALLENGES AND OPPORTUNITIES	2-1
2.1.1	<i>Voltage.....</i>	<i>2-1</i>
2.1.2	<i>Power quality.....</i>	<i>2-1</i>
2.1.3	<i>Protection</i>	<i>2-1</i>
2.1.4	<i>Reverse power flow.....</i>	<i>2-1</i>
2.1.5	<i>Island detection, anti-islanding, islanded operation.....</i>	<i>2-2</i>
2.2	THE SUNSHINE STATE SOLAR GRID INITIATIVE (SUNGRIN)	2-2
2.3	TOOLS AND DATA	2-3
2.4	REFERENCES.....	2-3
3	GRID-CONNECTED SOLAR PV	3-1
3.1	PV INTERCONNECTION PRACTICES.....	3-1
3.2	PV PENETRATION AND LOAD.....	3-1
3.3	REFERENCES.....	3-2
4	UNDERSTANDING THE SOLAR RESOURCE.....	4-1
4.1	THE SOLAR RESOURCE FROM A SYSTEM INTEGRATION PERSPECTIVE.....	4-1
4.2	SOLAR PV MEASUREMENTS AND METRICS	4-1
4.2.1	<i>Data from Existing Field Instrumentation.....</i>	<i>4-1</i>
4.2.2	<i>High-speed Data from SUNGRIN-installed Irradiance Sensor Network.....</i>	<i>4-2</i>
4.2.3	<i>Variability Metrics.....</i>	<i>4-3</i>
4.2.4	<i>Spatial and Temporal Studies with Satellite-Derived Irradiance Data</i>	<i>4-4</i>
4.2.5	<i>Variability of Small and Large PV systems</i>	<i>4-6</i>
4.2.6	<i>Ramp Rates for a 3 MW Central Florida Location.....</i>	<i>4-7</i>
4.2.7	<i>Comparing Florida Variability to Western U.S. and Hawaii</i>	<i>4-7</i>
4.3	REFERENCES.....	4-9
5	PV IMPACT: ANALYTICAL AND EXPERIMENTAL APPROACHES	5-1
5.1	FIELD DATA	5-1
5.2	MODELING AND SIMULATION	5-1
5.2.1	<i>Real-time and EMTP Simulation Tools</i>	<i>5-1</i>
5.2.2	<i>RTDS Modeling and Simulation Considerations</i>	<i>5-2</i>
5.2.3	<i>Modeling of the PV System</i>	<i>5-2</i>
5.3	HARDWARE-IN-THE-LOOP (HIL) SIMULATION	5-4
5.4	REDUCED MODEL APPROACH	5-5
5.5	LOAD MODELING.....	5-7
5.6	MODELING IN RTDS	5-8
5.7	MODEL VALIDATION.....	5-8
5.7.1	<i>Model Results Cross-Validation</i>	<i>5-8</i>
5.7.2	<i>Validation with Field Data</i>	<i>5-9</i>
5.7.3	<i>Sources of Error</i>	<i>5-10</i>
5.8	REFERENCES.....	5-12

6	STUDIES OF FLORIDA DISTRIBUTION CIRCUITS.....	6-1
6.1	OVERVIEW – FLORIDA FEEDERS STUDIED.....	6-1
6.2	FEEDER MODELS.....	6-3
6.3	VOLTAGE IMPACT.....	6-3
6.3.1	Feeder 1.....	6-3
6.3.2	Feeder 2.....	6-5
6.3.3	Feeder 3.....	6-7
6.3.4	Feeder 4.....	6-9
6.4	REFERENCES.....	6-11
7	DISTRIBUTION FEEDER REGULATION AND CONTROL.....	7-1
7.1	SIMULATION-ASSISTED VOLTAGE CONTROL STUDIES.....	7-1
7.1.1	Introduction and Current Practice.....	7-1
7.1.2	Future Trends.....	7-1
7.1.3	PV Inverter Voltage Regulation Methods.....	7-2
7.1.4	Voltage Regulation Studies with the Florida Feeders.....	7-2
7.1.5	Feeder 1.....	7-2
7.1.6	Feeder 2.....	7-7
7.1.7	Feeder 3.....	7-9
7.1.8	Feeder 4.....	7-11
7.2	PV SCADA.....	7-12
7.2.1	Solar PV Integration – Current and Historical Practice.....	7-12
7.2.2	Solar PV Integration – The Opportunity.....	7-12
7.2.3	Common Control Approaches in “Smart Inverters”.....	7-13
7.2.4	Testing Inverter Communications and Reactive Power Support in CAPS Lab.....	7-15
7.2.5	Strategies and Considerations for Utility-Controlled PV.....	7-16
7.2.6	Communications.....	7-17
7.2.7	Control.....	7-17
7.2.8	Towards RFP Model Language.....	7-17
7.3	REFERENCES.....	7-18
8	SUBSTATION PROTECTION.....	8-1
8.1	OVERVIEW.....	8-1
8.1.1	Traditional Distribution System Protection.....	8-1
8.1.2	Current Practices.....	8-1
8.1.3	Potential Impacts of PV integration.....	8-2
8.2	SUBSTATION 1.....	8-2
8.2.1	Substation Overview.....	8-2
8.2.2	Modeling.....	8-3
8.2.3	Simulation Setup.....	8-4
8.2.4	Results.....	8-4
8.3	SUBSTATION 2.....	8-7
8.3.1	Substation Overview.....	8-7
8.3.2	Modeling of Substation in RTDS.....	8-7
8.3.3	Modeling of PV system.....	8-8
8.3.4	High Penetration PV and protection studies.....	8-8
8.3.5	Sensitivity to Ground Fault Detection.....	8-9
8.4	CONCLUSIONS.....	8-12
8.5	REFERENCES.....	8-13
9	DISTRIBUTION FEEDER OPEN-USE DATASETS, MODELS, AND TOOLS.....	9-1
9.1	OPEN-USE SOLAR PV PLANT PRODUCTION DATA SETS.....	9-1
9.1.1	Approach – Data Synthesis Using Wavelets.....	9-1
9.1.2	Using baseline data.....	9-2
9.1.3	Comparison of Results from Simulations with Actual and Synthetic Profile Sets.....	9-2

9.1.4	<i>Future work</i>	9-3
9.2	REFERENCES.....	9-3
9.3	SOFTWARE TOOLS AND OPEN-USE MODELS.....	9-4
9.3.1	<i>Functions and Framework</i>	9-4
9.3.2	<i>Open-use Feeder Models in OpenDSS</i>	9-5
9.4	A MODEL REDUCTION TOOL FOR OPENDSS MODELS	9-10
9.4.1	<i>Introduction</i>	9-10
9.4.2	<i>Approach</i>	9-10
9.4.1	<i>Model Reduction Functions</i>	9-15
9.4.2	<i>Examples</i>	9-16
9.4.3	<i>Conclusion</i>	9-20
9.5	REFERENCES.....	9-22
10	SYSTEM IMPACT ASSESSMENT – A PARAMETRIC STUDY APPROACH	10-1
10.1	INTRODUCTION.....	10-1
10.2	APPROACH.....	10-2
10.2.1	<i>Process Description</i>	10-2
10.2.2	<i>PV and Load Profiles</i>	10-3
10.2.3	<i>Model Parameters</i>	10-4
10.2.4	<i>Response Quantities</i>	10-6
10.3	DESIGN AND ANALYSIS OF EXPERIMENTS	10-9
10.4	SELECTION OF REPRESENTATIVE SUBSETS OF PV AND LOAD PROFILES	10-9
10.5	EXAMPLES AND SELECTED RESULTS	10-10
10.6	CONCLUSION	10-14
10.7	REFERENCES.....	10-17
11	TRANSMISSION SYSTEM MODELING AND SIMULATION	11-1
11.1	MOTIVATION	11-1
11.2	APPROACH AND RESULTS	11-1
11.3	FUTURE WORK.....	11-2
12	CONCLUSIONS	12-1
12.1	KEY FINDINGS	12-1
12.2	FUTURE WORK.....	12-2
APPENDICES		
A.	APPENDIX – ACRONYMS	A-1
B.	APPENDIX – OPEN USE MODEL DOCUMENTATION	B-1
C.	APPENDIX – MODEL REDUCTION FUNCTIONS	C-1

(this page intentionally blank)

1 EXECUTIVE SUMMARY

Florida State University's Center for Advanced Power Systems and partners in the Sunshine State Solar Grid Initiative (SUNGRIN) have completed a five-year effort aimed at enabling effective integration of high penetration levels of grid-connected solar PV generation. SUNGRIN has made significant contributions in the development of simulation-assisted techniques, tools, insight and understanding associated with solar PV effects on electric power system (EPS) operation and the evaluation of mitigation options for maintaining reliable operation. An important element of the project was the partnership and participation of six major Florida utilities and the Florida Reliability Coordinating Council (FRCC). Utilities provided details and data associated with actual distribution circuits having high-penetration PV to use as case studies. The project also conducted some foundational work supporting future investigations of effects at the transmission / bulk power system level.

In the final phase of the project, four open-use models with built-in case studies were developed and released, along with synthetic solar PV data sets, and tools and techniques for model reduction and in-depth parametric studies of solar PV impact on distribution circuits. Along with models and data, at least 70 supporting MATLAB functions have been developed and made available, with complete documentation.

1.1 Impact of the Solar Resource in PV Integration

The solar resource itself is where study of high-penetration PV impact begins. This includes the temporal and spatial variability of the resource on different scales, including aggregation effects as overall installed plant capacity is considered. Realistic and appropriate solar PV plant output is also a necessary input for models used in studies.

In the first year, the SUNGRIN project established a data collection, historization and retrieval system to support the research, built on the OSI PI™ platform. Data from sites varied in location and size, both fixed and single-axis tracking, has been collected. This includes data from all locations where high penetration feeders were studied. Also included was data from a few sites outside of Florida, including the western U.S. and Hawaii.

With satellite and ground irradiance data, variability reduction of aggregate solar PV production was quantified and confirmed for scenarios within Florida. Also, variability indices for Florida were compared to California, Nevada, and Hawaii, with Florida variability patterns more similar to Hawaii and exhibiting greater overall variability than the Western U.S. If solar resource variability in Las Vegas, NV is taken to be representative of the desert southwest, then summertime variability in that region of the U.S. is around 50% *less* than what it is other times of the year, while in Florida, summertime variability is on the order of 50% to over 100% *more* than what it is other times of the year.

In support of solar PV integration research activities by the larger stakeholder community, a method for developing synthetic open-use PV data sets characterized based on actual data sets, was developed. The open-use data sets have been made available on the SUNGRIN portal.¹

¹ <http://www.caps.fsu.edu/sungrin.html>

1.2 Analytical Approaches

Methodical simulation-assisted approaches have been developed over the course of the project that are particularly suited to analyzing distribution feeders with sparse field measurement data and for employing electromagnetic transient program (EMTP) and hardware-in-the-loop (HIL) tools, as well as the open-source, open-use tool, OpenDSS.

The EMTP and HIL tools require reduction in the total number of nodes represented in a model. There are other benefits in reduced-model approaches as well, including speeding the model development and validation process, speeding model execution (particularly useful for multiple runs and parametric studies), reducing errors due to reduced model complexity, and easing maintenance and upkeep of models to be utilized over time or in the future. A methodical process for manually reducing models, employing several criteria geared towards high-penetration studies, was developed and used for reducing circuits for modeling in RTDS. An automated tool was developed for reducing models in OpenDSS, though tested and verified with IEEE test cases for limited circuit constructs.

Foundations for PV inverter testing with HIL and distribution circuit simulations were developed, and further built upon and demonstrated for several types of tests for utilities, inverter manufacturers, and NREL.

1.3 High Penetration PV Impacts, Florida Circuits

Extensive simulation-assisted studies of voltage impact and voltage regulation and mitigation on four actual high-penetration feeders in Florida have been completed over the course of the project. These show that whether voltage excursions will occur and under what conditions are very dependent on feeder design characteristics, operating conditions, including load characteristics and distribution, and PV location. Field data and simulation-assisted studies of four Florida feeders confirms that percent penetration is, by itself, a poor indicator of circuit hosting capacity, whether issues will arise on the utility circuit, and the types of issues that may arise. PV penetration levels range from around 25% to 600% of maximum daytime load. Voltage profile response to varying PV penetration, circuit loading, circuit X/R ratio, and PV location has been examined. Studies using selected one-hour simulation time periods were performed using RTDS and selected one-day time periods using OpenDSS

Simulation-assisted studies were also performed to examine potential impact on substation protection, including adjacent feeders. Two substations were examined in detail using information provided by utility partners. Simulations were performed in the RTDS environment, because, protection studies require EMTP simulation tools. A variety of scenarios were examined. There were no significant substation protection issues of concern revealed for the two utility partner substations examined.

1.4 Open-Use Models and Tools

OpenDSS models are provided for four utility feeders with high penetration PV. Each model is included with three cases that the user can run without any modification:

1. A “Normal” case based on the current configuration of the feeder, percent PV, and typical load profiles
2. An “Impact” case, where solar PV penetration has been increased to a level that produces voltages outside of ANSI limits on the feeder, and,
3. A “Mitigation” case, where regulation strategies are modified, usually to include some PV inverter participation in regulation.

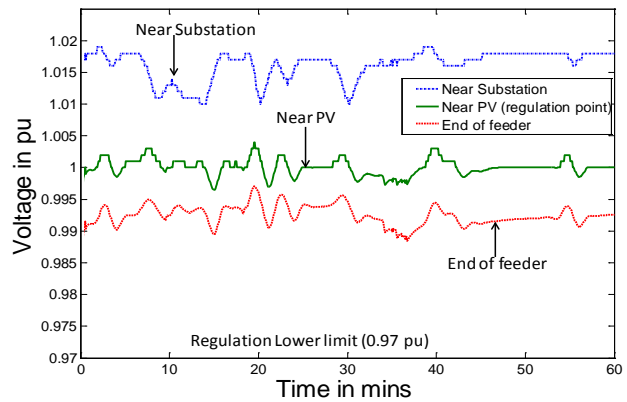
Additional cases can be constructed by the user by appropriate modifications to input files. The OpenDSS models are called from MATLAB and are accompanied by supporting MATLAB functions. Documentation with information on the feeder, the model and validation, and the three cases, is included with each feeder. A standalone version that does not require MATLAB is provided. It can be run from

the DOS command line or from a graphical user interface (GUI) that provides a flexible and intuitive means to run the cases provided or load new ones customized by the user.

1.5 Systematic Impact Assessment

A systematic approach to high-penetration PV impact studies was developed based on experimental design methods in factor screening and parametric studies. The approach utilizes the OpenDSS models and provides a powerful and flexible means to comprehensively study effects and interactions of multiple influencing factors against multiple metrics (“response quantities”) for a given circuit.

In developing the systematic impact assessment approach and tools, a number of new distribution circuit metrics have been formulated for use in the SUNGRIN analysis. These metrics were developed particularly for assessment of impact of high penetration solar PV on distribution circuits, where existing standard metrics were lacking or insufficient and could form the basis for expanding / updating existing standards. The metrics would generally apply to assessing impact of any distributed energy resources (DER). For example, two new metrics developed are similar to the familiar and widely used standard SAIDI and CAIFI metrics, but, rather than circuit interruption, are adapted to reflect voltage deviation magnitude and duration. The new metrics, as used on SUNGRIN, and proposed for broader use and adoption, are System Average Load Impact Index (SALII) and Customer Average Load Impact Index (CALII).



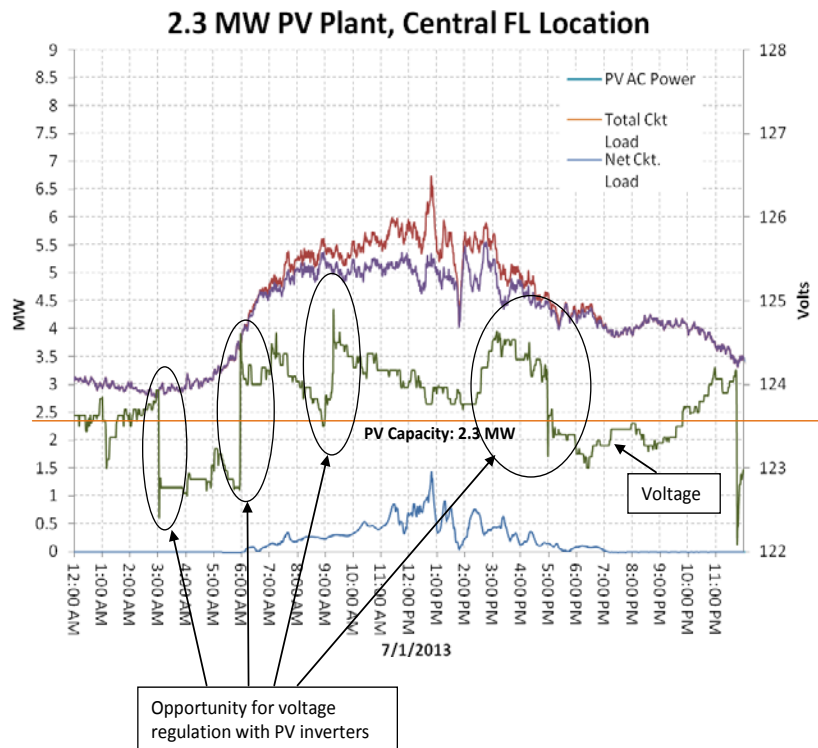
Feeder 1 voltage with PV regulating voltage during extreme load changes (simulation result)

1.6 Voltage Regulation

Studies show that modifications to control strategies on existing distribution voltage control devices and systems are often sufficient to mitigate voltage impacts on a circuit.

Multiple studies on different SUNGRIN utility partner high-penetration Feeders show that PV can provide very good voltage regulation on a circuit. Further, if existing regulation device control schemes are properly coordinated, device operations can be reduced, or, in some cases, the devices can be eliminated, providing lifecycle cost savings.

HIL testing combined with efficient reduced circuit models provide powerful capability to analyze and fully de-risk the more complete integration and control of PV.



(this page intentionally blank)

2 INTRODUCTION

2.1 Solar PV Integration Challenges and Opportunities

According to the Solar Energy Industries Association, installed solar PV capacity in the U.S. grew 30% from 2013 to 2014, 32% of all new electric generating capacity in the U.S. in 2014 came from solar, and, large amounts of residential solar are now being installed without any state incentives, as the price for solar has continued to decline [1]. With grid-connected solar expected to continue to experience steady growth, it is critically important that electric utilities, generation owners and end-users are equipped to successfully adapt to some of the unique system integration and operation considerations accompanying higher penetration levels of solar PV.

System impacts from high penetration levels of grid-connected solar PV generally arise for the following fundamental reasons:

- 1.) Solar PV is inherently intermittent – in a predictable diurnal pattern and less predictable intraday, day-to-day, seasonal, and yearly patterns.
- 2.) For solar PV connected at the electric distribution system level, most of the existing electric distribution system infrastructure was designed to serve loads and not connect generation.
- 3.) Solar PV inherently produces DC voltage and current, which must then be converted to AC voltage and current with solid state power electronics switching (inverters) devices. Unlike traditional synchronous generation, PV inverters do not produce pure sinusoidal wave forms, and, they do not have the highly damped stored energy that results from rotating inertia.

Large amounts of solar PV on a circuit have the potential to impact circuit behavior and operation in several areas, including voltage, power quality (PQ), fault detection and isolation (protection), and circuit restoration. Reverse power flow has been cited as a concern as well, but primarily for its impact on the preceding. Detection of islanded operation and behavior of solar PV in the event of formation of an island is also important and of interest.

2.1.1 Voltage

Real power injection on a circuit causes voltage rise at the point of coupling and voltage drop in the direction of power flow away from the point of coupling. And, when the real power injection goes away (sometimes rather quickly), the reverse occurs. Solar PV, therefore, always has some impact on circuit voltage, particularly when connected to the distribution system.

2.1.2 Power quality

In addition to voltage excursions, which are a specific type of PQ disturbance, there is also the possibility of PQ issues, such as flicker, due to rapid changes in solar PV system output due to solar irradiance variation and the much faster harmonic fluctuations due to the power electronics switching.

2.1.3 Protection

Protection system impacts may include fuse ratings and coordination along the distribution circuit, reclosers or other equipment along the circuit, settings and coordination of protective relaying and breakers at the solar PV plant(s), any other distributed generation (DG) or distributed energy resource (DER) locations, the substation, and adjacent circuits out of the same substation.

2.1.4 Reverse power flow

Radial distribution circuits are designed for power flow from the substation out to loads. DG on the circuit, including solar PV, may cause power flow (current) to go in the direction of the substation if the local generation exceeds the local and downstream load. This can impact protection, including breaker ratings and settings, and protection scheme design.

2.1.5 Island detection, anti-islanding, islanded operation

When a portion of the electric power system (EPS) containing one or more energy sources sufficient to sustain some load becomes electrically separated from the rest of the system, this is termed an electrical island, or “island” for short. Most often, electric utilities have mandated that solar PV disconnect within a prescribed timeframe following formation of an island, so as not to have it pose safety or operational issues. Island detection is accomplished with algorithms operating in the solar PV inverter that must reliably sense from the electrical characteristics of the circuit the presence of an islanded condition. Anti-islanding refers to the detection and disconnection of the solar PV plant from the EPS.

Having solar PV continue to generate when an island has formed may sometimes have benefits that outweigh risks and justify any additional associated cost or complexity. In this “islanded operation”, the circuit characteristics are quite different, and solar PV must continue to function reliably and safely if it remains connected.

2.2 The Sunshine State Solar Grid Initiative (SUNGRIN)

SUNGRIN is a five-phase high-penetration solar PV deployment project within the Systems Integration (SI) area of the Solar Energy Technologies (SETP) Program. Phase 1 was funded with ARRA funds. The fourth and final Phase of the project was completed February 28th, 2015.

The major goals and objectives of the SUNGRIN project were to gain significant insight into the effects of high-penetration levels of solar PV systems in the power grid, through analysis of solar PV and load data and modeling, simulation, and analysis of a technically varied and geographically dispersed set of real-world test cases within the Florida grid, where utility partners had circuits with recently or soon-to-be deployed solar PV at high penetration levels in-service over the five-year performance period. Project efforts included work to 1.) characterize and better understand the solar variation, 2.) develop simulation-assisted understanding of the impacts on the distribution grid of high penetration levels of PV, 3.) define possible solutions that enable successful integration of relatively high levels of PV, and 4.) disseminate information and facilitate the transfer of findings and results to partners and the stakeholder community and to advance the broader goals of the SunShot Program.

SUNGRIN electric utility partners include the Florida Municipal Power Agency (FMPA), Florida Power and Light (FPL), Gainesville Regional Utilities (GRU), Jacksonville Electric Authority (JEA), Lakeland Electric (LE), and the Orlando Utilities Commission (OUC). The Florida Reliability Coordinating Council (FRCC) has also participated as a project team member providing an additional linkage to electric utilities and emerging PV integration issues and as a linkage to the North American Electric Reliability Corporation (NERC) and bulk power system reliability and adequacy issues across the industry and North American power system.

Each phase of SUNGRIN built and expanded upon the efforts of the prior phases, including collection of field data, development of tools and approaches, development and validation of electric power system models for different utility partner circuits, and simulation assisted analysis of various potential system impacts and mitigation approaches. The examination and understanding of high-penetration solar PV issues included the solar resource itself, the electric power system, and the power conversion technologies and systems for integration with the grid.

While most of the work focused on the electric distribution system, some efforts were directed at advancing the tools and approaches for studying effects at the transmission system level, particularly in the area of modeling and simulation of the Florida bulk power system. Florida utility partners furnished for study information on actual distribution circuits with high penetration levels of solar PV to support development of impactful insight and solutions.

Considerations associated with integrating increasingly higher levels of solar PV into the electric grid include impacts on the actual electric system design, operation, and control, as well as regulatory and

market issues. The work of the SUNGRIN project and results presented herein are primarily concerned with the behavior, operation, and control of the electric power system and not the regulatory and market issues.

2.3 Tools and Data

The SUNGRIN project has made extensive use of simulation-assisted analysis. Several modeling and simulation tools have been used in conducting research and analysis over the course of this project, including:

- PSCAD/EMTDC – used in some preliminary investigations using standard IEEE distribution models, and, as a model cross-validation tool for some of the actual utility partner feeder circuit models
- MATLAB/Simulink – used for data processing and analysis and as the primary front-end and post-processing vehicle for OpenDSS
- RTDS – used for simulation of reduced models of utility distribution circuits for PV impact and PV voltage regulation, and, also for studying substation protection impact, primarily for shorter-term simulation runs
- PSSE (Siemens PTI) – used for developing a reduced model of the Florida transmission system, and, as a model cross-validation tool for some of the actual utility partner feeder circuit models
- SynerGEE (DNV-GL) – used for to provide utility circuit information and simulation results under various circuit loading conditions and as a check against other modeling and simulation tools used
- OpenDSS – used for open-use models of utility distribution circuits and for longer-term simulation runs

One of the objectives of the SUNGRIN project in the final phase, Phase 4, has been to produce open use tools to assist in understanding and analysis of PV integration impact and open use PV data sets. OpenDSS has been selected for the models delivered for open use, because, it is itself an open and freely available modeling tool, it is fairly mature (has been around over 15 years and was released as open source in 2008), and is supported by a reasonably large user community, periodic training and workshops by EPRI, and freely available documentation. Supporting functions including preprocessing of inputs and parameters, post-processing of results, and further analysis are accomplished with MATLAB, which calls OpenDSS through the COM interface.

In connection with some of the work described in this report, four models in OpenDSS, input data sets, supporting MATLAB scripts and functions, and standalone executables are available for download on the SUNGRIN website, <http://www.caps.fsu.edu/sungrin.html>. Unless otherwise specified, MATLAB functions were developed and tested in MATLAB version 2011a.

2.4 References

- [1] SEIA/GTM, "U.S. Solar Market Insight: 2014 Year-in-Review," Greentech Media / Solar Electric Industries Assoc., United States, March 2015.
- [2] D. Feldman, G.L. Barbose et al., "Photovoltaic (PV) Pricing Trends: Historical, Recent, and Near-Term Projections," National Renewable Energy Laboratory (NREL), Lawrence Berkeley National Laboratory (LBNL), 2012.

(this page intentionally blank)

3 GRID-CONNECTED SOLAR PV

3.1 PV Interconnection Practices

In 2010, as the SUNGRIN project was getting started, one of the most widely accepted practices employed by electric utilities in the U.S. for screening and approving connection of solar PV systems to the EPS was “the 15% rule”. This rule came about as a formally accepted screening practice in a 1999 revision of California Public Utilities Commission (CPUC) Rule 21 [1]. Essentially, it sets a threshold that allows fairly expeditious approval for interconnection of small generation on a line section when the total rated capacity of connected generation on a line section does not exceed 15% of the peak load for that section.

This 15% threshold then became part of the FERC Small Generator Interconnection Procedures (SGIP), which, in turn, became a model for many states regulators and utilities even for situations where interconnection was not under FERC jurisdiction.

Based on early results from the Dept. of Energy-funded High Penetration Solar PV Deployment projects, including SUNGRIN, and based on the cumulative prior field experience and observations with grid-connected solar PV up to that time, it became increasingly clear that the 15% rule was too conservative in many situations, and that supplemental studies triggered by generation exceeding 15% of peak load were often unnecessary. Nonetheless, this guideline remains somewhat entrenched, with 15% still used by some utilities as the threshold at which more costly and protracted studies may be required before PV can be interconnected to the EPS.

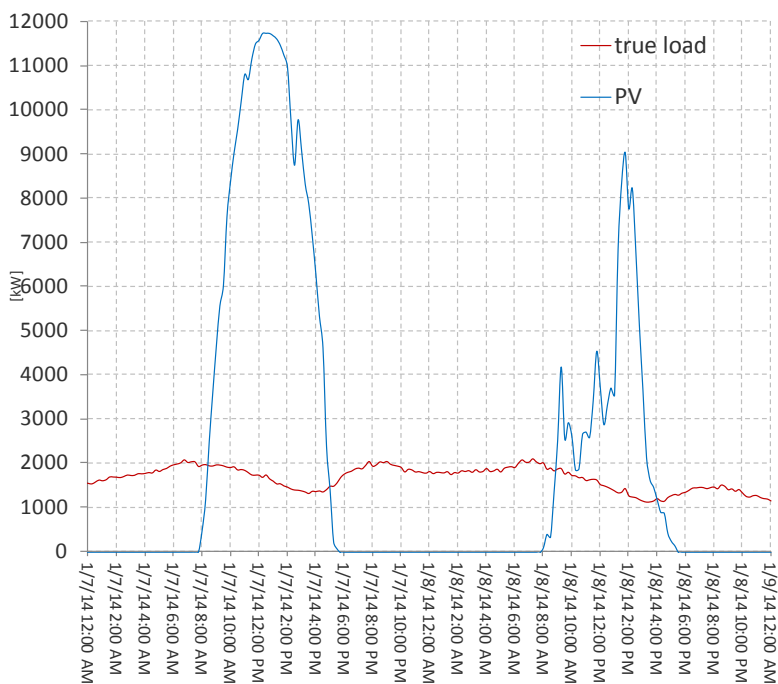


Figure 3-1. Load and PV, winter, very high PV penetration

In fact, in many cases, penetration levels far above 15% are possible with no significant impact on circuit operation or reliability.

Figure 3-1, from one of the Florida distribution feeders studied, shows load and PV production data representing a PV penetration of around 600% of peak, with routine reverse power flow back to the substation, and no significant issues with voltage regulation or protection.

3.2 PV Penetration and Load

The 15% threshold is aimed at keeping generation connected to the distribution system below the point where it might be supplying the entire load, that is, below the minimum load, or for solar PV, below the minimum daytime (DT) load. At the time the rule was made, the thinking was that peak load data was more readily available than minimum load, and, based on typical data, minimum load was usually about 30% of peak, so a conservative threshold would be half that, or 15% of peak.

Load profiles in Florida are often winter-peaking, with the widest range in load also occurring in winter months. Examining data for some of the Florida utility partner feeders studied on the SUNGRIN project,

typical minimum load during winter would be around 22% of peak and a typical minimum load in summer would be around 35% of peak.

Figure 3-1 shows Feeder 1 PV plant generation and circuit load for consecutive winter days, one sunny, followed by one with cloud activity for Feeder 1, both days exhibiting a load peak around 7 a.m.

Figure 3-2 provides an example of summertime load and PV production for Feeder 3, which is located in central Florida and includes a large 2.3 MW single-axis tracking solar PV plant near the end of the feeder. Because the load mix is largely commercial/industrial, there is generally good coincidence between PV production and load. Instantaneous PV penetration, as shown in the figure, reaches a maximum of about 39%, and, minimum daytime load is about 45% of peak for that day.

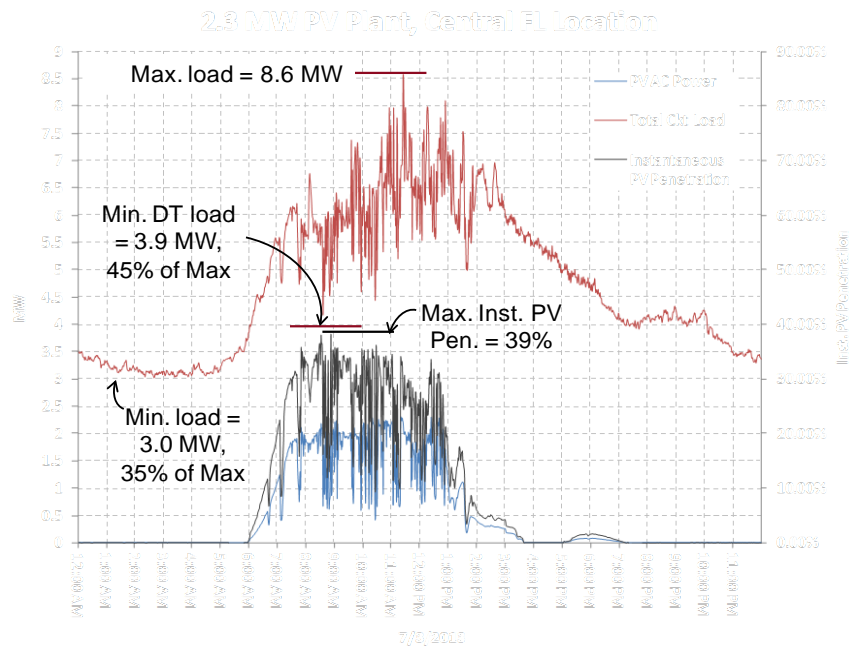


Figure 3-2. Typical summertime MW-scale solar PV plant output, circuit load, and PV penetration for a central Florida location (Feeder 3).

3.3 References

- [1] M. Coddington, B. Mather, B. Kroposki, K. Lynn, A. Razon, A. Ellis, R. Hill, T. Key, K. Nicole and J. Smith, "Updating Interconnection Screens for PV System Integration," National Renewable Energy Laboratory (NREL), Golden, CO, Feb. 2012.

4 UNDERSTANDING THE SOLAR RESOURCE

4.1 The Solar Resource from a System Integration Perspective

Studying the effects of high levels of grid-connected solar PV on the electric system necessitates an understanding of the variability of the resource. The range, temporal pattern, direction, and rates of change of power flow can be altered significantly from historical norms on any given distribution circuit as PV penetration increases.

While most prior studies of solar PV variation have focused on solar irradiance data, such as Global Horizontal Irradiance (GHI) [1], it is PV system AC output variation that is most of interest in studying grid integration effects. However, the dynamic responses of silicon-based PV cells and power electronics-based inverters switching well into the kHz range are both very fast relative to most phenomena of interest in studying effects of PV on the electric power system.

If the focus is not on the inverter behavior itself, and certain assumptions are made, such as maximum power point tracking (MPPT) assumed to operate close to optimally at all times, then irradiance, properly scaled based on the rating of the PV plant, can be used as a surrogate for either PV module(s)' DC output or the inverter(s)' AC output (while also applying any real and reactive power regulation rules or algorithms being considered).

4.2 Solar PV Measurements and Metrics

In the U.S., most efforts to collect and analyze solar resource data and study variability have focused on the Western U.S. Whereas, the SUNGRIN project has focused on the nature of the solar resource in Florida, using data collected from solar PV sites with installations rated at a few kilowatts up to 15 MW DC. The data has been used in the analysis of variability, ramp rates, PV penetration levels, and as inputs to models for simulation-assisted analysis of PV impact on the electric power system.

4.2.1 Data from Existing Field Instrumentation

Data has been collected and examined from geographically dispersed collection sites across the state of at sampling periods between 250 ms and 15 min., with most data collected at 1 min. intervals. An OSISoft PI system at FSU was used as the data repository (Figure 4-1). PI is a scalable enterprise-class high-performance real-time data collection, historian, and retrieval system used by many electric utilities, in various process industries and other applications. Solar PV plant data was collected local sources such as three 6 kW PV systems at FSU, from SUNGRIN project utility partner sites in the 500kW to 15 MW range, and a variety of other solar PV sites, mostly in Florida. In some cases, data is streamed directly into the PI system, and, in other cases, it is imported, usually monthly, from data files received from the electric utility or solar PV plant owner.

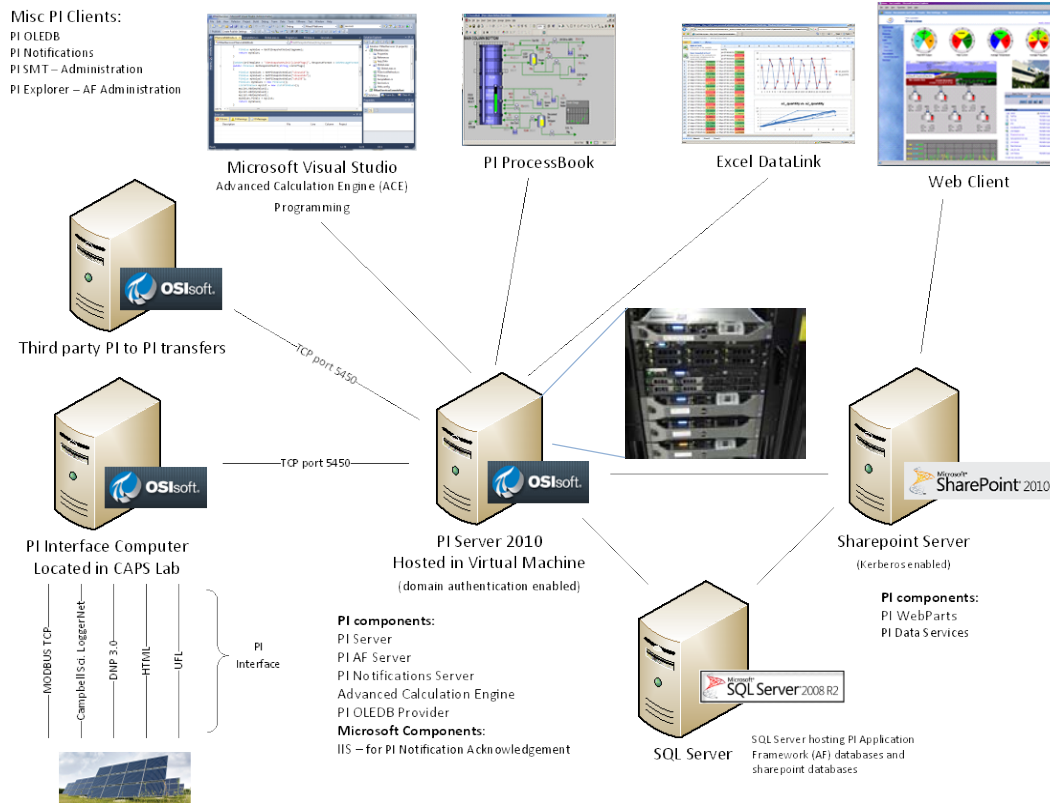


Figure 4-1. OSI PI data collection, historization, and retrieval system architecture at FSU

4.2.2 High-speed Data from SUNGRIN-installed Irradiance Sensor Network

To supplement data received from utility partners and solar PV plant owners with some temporally and spatially higher resolution data, an array of local irradiance sensors were installed at one of the larger PV sites connected to circuits studied by the project. The sensor network captures transients associated with cloud shadows of varying sizes and velocities traveling over the plant at a high enough resolution to characterize short-term output variability of a large central PV plant [17].

A wireless irradiance sensor network to acquire high-resolution solar irradiance measurements was designed, developed, and tested by SUNGRIN team members at the Florida Solar Energy Center (FSEC), in Cocoa Beach. The data acquisition system logs global horizontal irradiance (GHI) and wind speed at 1 second intervals, with the capability to transmit the data wirelessly or to download it locally. With the cooperation of the local electric



Figure 4-2. Irradiance high-speed field sensor array deployed at Lakeland Linder Airport PV site

utility and the PV plant owner, the data collection system was deployed around the periphery of two adjacent large PV plant sites together totaling over 5 MW in rated capacity (Figure 4-2). The sensor network consists of 8 sensors at the southern PV site and 6 GHI sensors at the northern PV site.

The wireless sensor network is comprised of a number of end units and a central coordinator that were assembled with commercially available products (Figure 4-3). A typical end unit includes a pyranometer,



Figure 4-3. Sensor components (left); autonomous sensor installation on fence (right)

an XBee2 transmitter (which performs the analog-digital conversion functions as well as transmitting the data), a small solar cell (5.5VDC, 170 mA), a lithium ion battery, and a charge controller. The coordinator contains an XBee2 receiver that communicates with the end units, an Arduino Mega 2560 processor board, a lithium ion battery, a charge controller, a micro SD storage device, and an SM5100B-D GPRS/GSM cellular engine. The coordinator and end units are solar-powered with battery backup.

4.2.3 Variability Metrics

4.2.3.1 Output Variability

The PV system output changes proportionally with irradiance over time in the plane of the array (POA). These changes in intensity of the solar resource over a given timescale are defined as PV output variability. Output variability is due to both the longer term deterministic changes associated with the diurnal solar cycle and seasonal changes, and more importantly in the context of predictability and forecasting, the short-term stochastic changes due primarily to clouds and other transient factors affecting the propagation of light through earth's atmosphere [8]. This output variability can be considered for a single PV system as well as an aggregate of multiple PV systems. The PV output variability is a calculated distribution of either irradiance or power step changes over a fixed time interval. The average PV output variability for a single system ($\sigma_{\Delta P_1}^\tau$) is defined in (1) as the standard deviation of the step changes over a different timescale period [9].

$$\sigma_{\Delta P_1}^\tau = \sqrt{\text{Var} \left[\frac{1}{\tau} \sum_{i=0}^{\tau-1} P_1(t+i) \right] - \left[\frac{1}{\tau} \sum_{i=-\tau}^{-1} P_1(t+i) \right]} \quad (1)$$

Where τ is the duration of the averaging interval and t is the time interval.

The variability of an aggregation of multiple PV systems, $\sigma_{\Delta P}^\tau$, is defined in (2) [9].

$$\sigma_{\Delta P}^\tau = \sqrt{\left[\sum_{i=1}^N \sum_{j=1}^N \text{Cov}(\Delta P_i^\tau, \Delta P_j^\tau) \right]} \quad (2)$$

Where N is the number of PV systems located across a balancing area or region.

4.2.3.2 Clearness Index

The *clearness index* (K) is a measure of how the actual irradiance for a given period of time deviates from the irradiance for a perfectly clear day. This provides a means of isolating the short-term stochastic changes in irradiance (i.e. the unpredictable changes) from the deterministic changes that can be determined analytically [10]. This provides a means of evaluating the predictability of the solar resource for individual sites as well as an aggregate of many sites. The equation for the clearness index is given by the following [8]:

$$K(t) = \frac{E_{GHI}(t)}{E_{ETR-GHI}(t)} \quad (3)$$

Where $E_{GHI}(t)$ is the global horizontal irradiance (GHI) at 0° tilt as a function of time, and $E_{ETR-GHI}(t)$ is the extraterrestrial GHI versus time. In this study, $E_{GHI}(t)$ was determined from the hourly SolarAnywhere data set and $E_{ETR-GHI}(t)$ was determined using a online tool created by NREL called the Solar Position and Intensity Calculator.

4.2.4 Spatial and Temporal Studies with Satellite-Derived Irradiance Data

4.2.4.1 Spatial Correlation

Research by others and by the SUNGRIN team has shown that aggregate variability of solar irradiance or solar PV plant output power is reduced as sites are more geographically dispersed (i.e. the so-called “smoothing effect”) [11]. Short-term localized variations average over larger geographical areas, resulting in ramp rates for aggregated systems normally less than those of the individual systems. The correlation of system variability for multiple sites as a function of the distance can therefore quantify this effect.

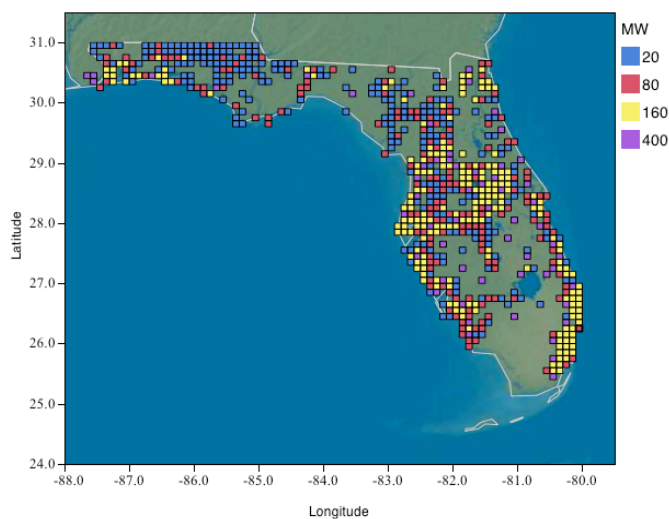


Figure 4-4. Scenario 3 model, with approximately 75GW of capacity distributed statewide.

Density	MW per square	Orientation Notes
Low-Density	20	20° slope, randomized orientation (90° - 270°)
Medium-Density	80	20° slope, randomized orientation (90° - 270°)
High-Density	160	20° slope, randomized orientation (90° - 270°)
Power Plants	400	50% of sites: 1-axis trackers 25% of sites: fixed at 20° slopes facing south 25% of sites: fixed at 20° slopes facing southwest

Table 4-1. Description of grid squares modeled in Scenario 3.

Pearson correlation coefficients were calculated for the clearness index of multiple sites. These coefficients give a quantitative measure of how effective multiple sites will be at mitigating variability for the group as a whole (i.e. well correlated output variability between multiple systems will do little mitigate variability). The ramp rates of the clearness index, $\Delta K(t)$, were used in this case, as opposed to GHI or modeled PV power output, to isolate the known correlation due to the aforementioned deterministic changes in irradiance due to the diurnal and seasonal solar cycle. In each case, this analysis was carried out over the 11 year period between 1998 and 2008. These correlation coefficients were investigated for sites distributed across Florida to assess the effect of distance between sites and variability correlation.

4.2.4.2 Scenarios

In order to obtain a good examination of PV output variability, PV systems with differing tilt and orientation were selected, along with appropriate solar irradiance information for respective locations across Florida. In this study, three high penetration scenarios were developed to investigate variability and high penetration PV across Florida. The developed PV simulation analysis tool was used for testing build-out scenarios and providing some perspective relative to high PV penetration planning in Florida. In scenario 1, the simulation consisted of a 1kW PV system in each 10x10km grid in Florida, with each array sloped at the site's latitude and at an orientation of true south (a 180° heading). In scenario 2, the orientation of each PV system was set to a different, random direction facing generally south and between 90° (east) and 270° (west). In scenario 3, a statewide grid was modeled with distributed generation roughly located with and proportional to population density, with large ground-mounted PV power plants modeled in open areas. Table 4 describes the layout for each simulated square, while Figure 5 shows the distribution of the squares throughout Florida. The total simulated capacity of approximately 75GW is within the technical potential for the state by 2020 [12].

4.2.4.3 Temporal Variability

A south-facing PV system in Florida operating during a clear, sunny day would be expected to produce power throughout the day from dawn to dusk with a power output peaking in the middle of the day (when the sun is at its most normal angle to the array), with smooth increases and decreases in power output as the sun passed overhead (Figure 4-5, top); However, this is rarely the case in summer months, where high variability is occurring almost daily (Figure 4-5, bottom).

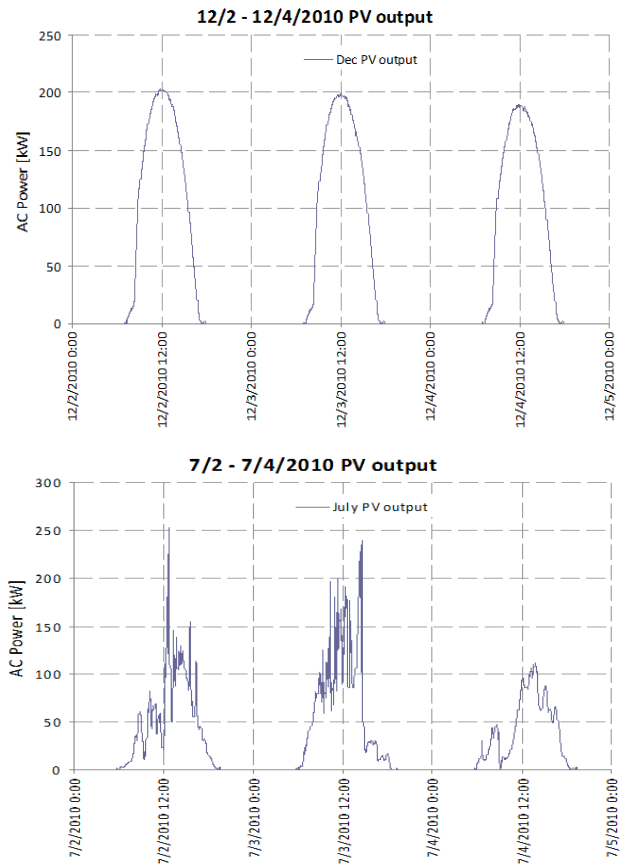


Figure 4-5. Typical daily PV plant output profiles, comparing winter and summer months, for a 250 kW central Florida plant.

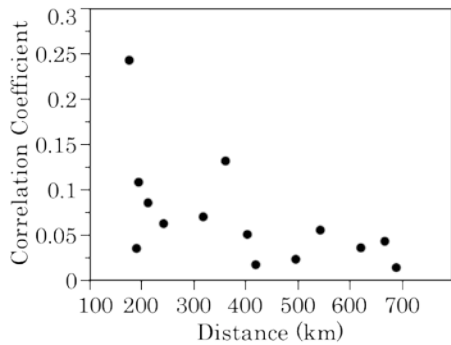


Figure 4-6. Correlation of $\Delta K(t)$ versus distance performed on six sites with respect to each other.

As described earlier, mitigating this short-term variability can be accomplished by dispersing PV over a large geographic area. Previous studies have shown that for N systems of equal size and with completely uncorrelated variability, the aggregated output variability can be reduced by the square root of N . The assumption of uncorrelated variability means the systems need to be sufficiently far apart. By calculating the correlation coefficients of six sites all across the state of Florida with respect to each other, a relationship between variability in the clearness index and distance emerged (Figure 4-6). Only those systems located within 400 km of one another show a correlation over 0.05.

When analyzing the statewide performance of these systems using the hourly data, the variability was consistent not only from hour to hour but also between months, as shown in Fig. 9 for the evenly-distributed statewide PV in Scenario 1. The figure depicts the average hourly changes in PV output as a changing percentage of the system's rated capacity.

Average hourly changes in PV output were generally consistent in magnitude and direction even across all scenarios.

4.2.5 Variability of Small and Large PV systems

For some perspective on the difference in variation between aggregated systems distributed across a wide geographic area and a single large system, Figure 4-8 below shows hourly power changes for approximately 75 GW of solar PV dispersed around Florida using Scenario 3, while Figure 4-10 shows hourly power changes over the first two years' operation of a 1MW PV system in Orlando, Florida (error bars are 1 standard deviation from the mean). As the system production is distributed over thousands of square feet rather than thousands of square miles, the variability of this system is larger than that of the three scenarios.

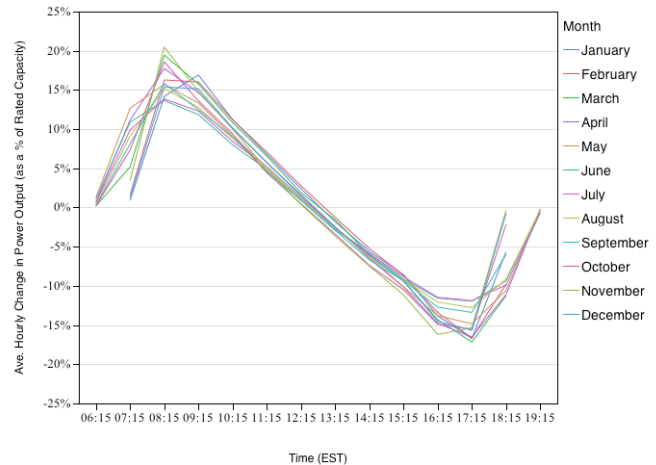


Figure 4-7. Scenario 1, showing average hourly changes in power output (by month) as a percentage of rated capacity.

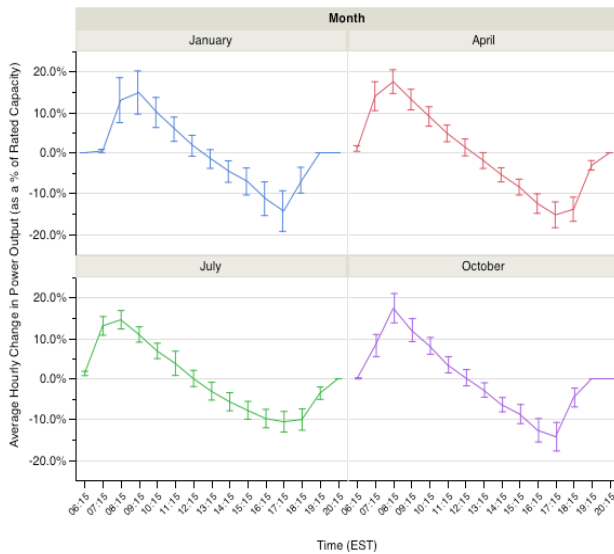


Figure 4-8. Average hourly changes in power output for approximately 75 GW of PV distributed across FL according to Scenario 3.

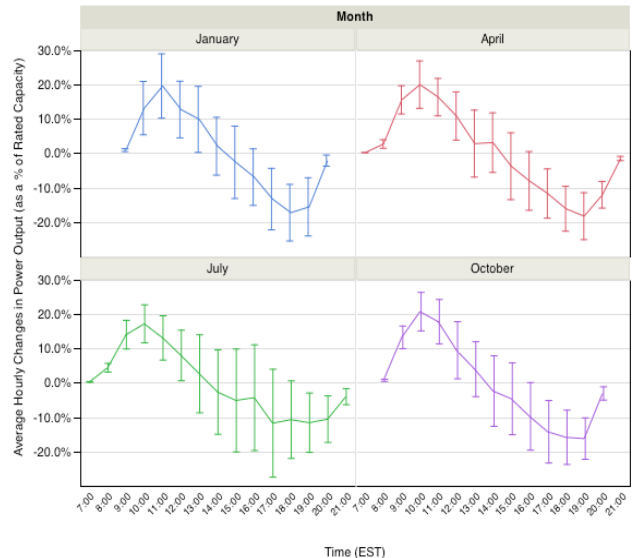


Figure 4-9. Hourly changes in power production for a 1MW (1016kW) PV system in Orlando, Florida.

Variability was also verified to be greater for smaller systems. Figure 4-10 depicts the different hourly ramp rates for a 3kW system in Cocoa, Florida during June 2011, compared with those for a 1016kW system in Orlando, Florida during the same period. The ramp rates for both systems fall generally between -35% to 25% when considering hour-to-hour changes, although as expected, the smaller system showed a much high probability of larger hour-to-hour ramps outside of this range, lacking the smoothing effects of a larger array area.

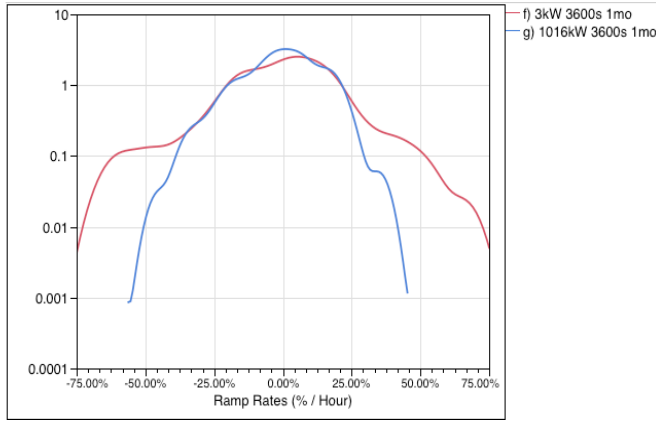


Figure 4-10. Differing variability of 3kW and 1016kW systems, sampled hourly, as a % change in rated output per hour

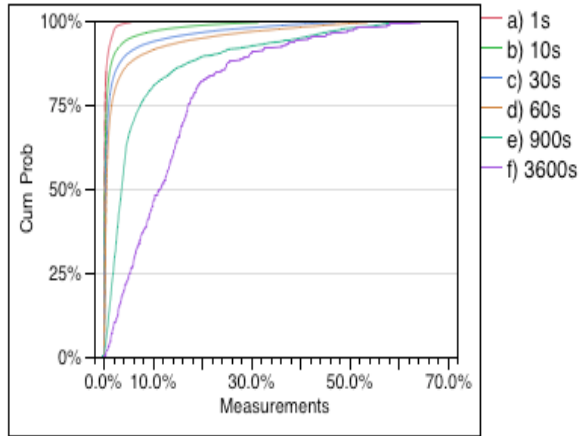


Figure 4-11. Cumulative distribution function showing the probability of ramp rate magnitudes.

Figure 4-11 shows a CDF of ramp rates for the 3kW system, during the month of June 2011 (a typical high-variability month in FL), when sampled at different time intervals. Being a small system, not benefitting from smoothing, and a high-variability time of year, this can be considered nearer the worst case end of the ramp rate ranges expected for Florida. On timescales of seconds, ramp rates are very small. It can be seen that probability of ramps greater than 5% in a second are nearly zero, while 30 second ramps of over 20%, while fairly low in probability, are observed and must be accommodated by the electric power system without adverse effects. Fortunately, the dynamic response of electric power circuits is much faster than these cloud-induced dynamics.

4.2.6 Ramp Rates for a 3 MW Central Florida Location

Daily ramp rates for a 3 MW PV plant in central Florida July and August 2013 (Figure 4-12) were examined. It can be seen that, during the summer, for a 3 MW plant (with single-axis tracking), multiple ramps per day of +/- 25-50% of plant capacity per minute are a common, almost daily occurrence.

4.2.7 Comparing Florida Variability to Western U.S. and Hawaii

The solar power variability in Cocoa, FL using the high resolution irradiance data (1 -sec) collected by the Florida Solar Energy Center was compared to the solar power variability in Lanai, HI, Las Vegas, NV and Arcata, CA using the high resolution solar irradiance data (1 -min) collected by the National Renewable Energy Laboratory (NREL)².

Lakeland 3MW % Ramp Rates August 2013

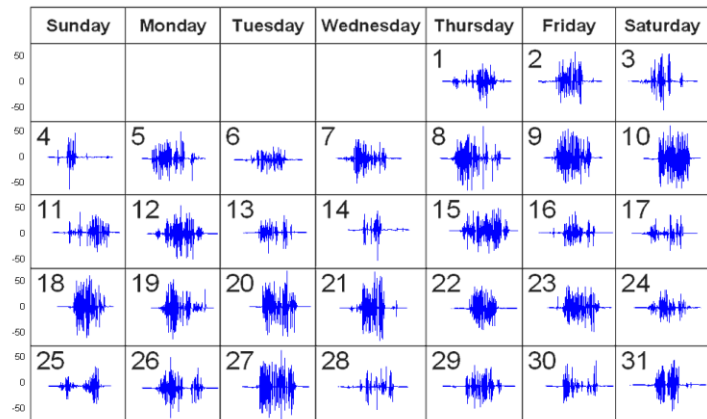


Figure 4-12. Daily ramp rates for a 3MW PV plant, August 2013 [% plant capacity / minute].

² <http://www.nrel.gov/midc>

To measure solar variability at each location, the Variability Index (VI), developed by Sandia National Laboratory, was used to classify the irradiance variability on a daily and monthly basis. VI is calculated as:

$$VI = \frac{\sum_{k=2}^n \sqrt{(GHI_k - GHI_{k-1})^2 + \Delta t^2}}{\sum_{k=2}^n \sqrt{(CSI_k - CSI_{k-1})^2 + \Delta t^2}}$$

where,

GHI is global horizontal irradiation, and,

CSI is clear sky irradiation averaged at the same time interval in minutes Δt [13].

An average value was calculated for each location, using 9AM-3PM EST data. Figure 4-13 is the average daily VI for each month of the year. Lanai experiences days of higher variability more than the other three locations. Lanai and Cocoa have a clear pattern of high variability in the summer and low variability in the winter.

Figure 4-14 shows daily clearness index and corresponding VI for each day of the year in each location. Lanai and Cocoa have most of the days with very high VI values; Las Vegas and Arcata have most of the days with low VI values and more clear days.

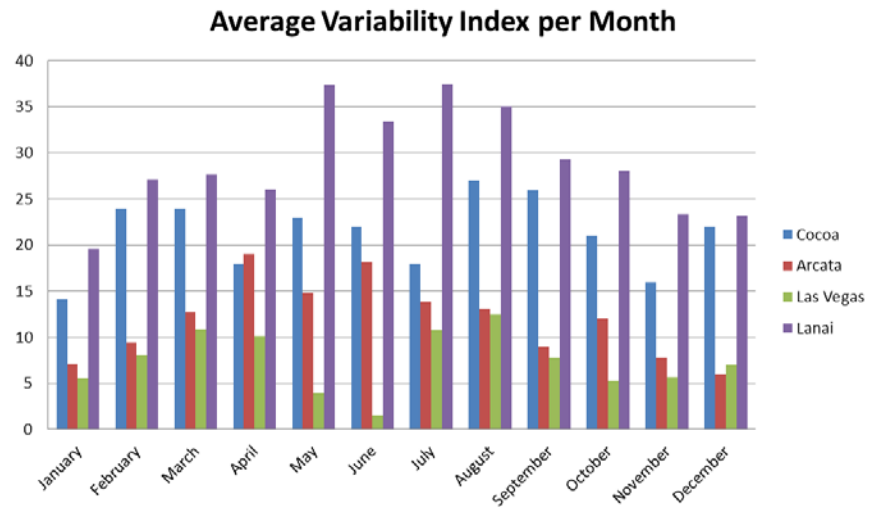


Figure 4-13. Average daily VI for each month

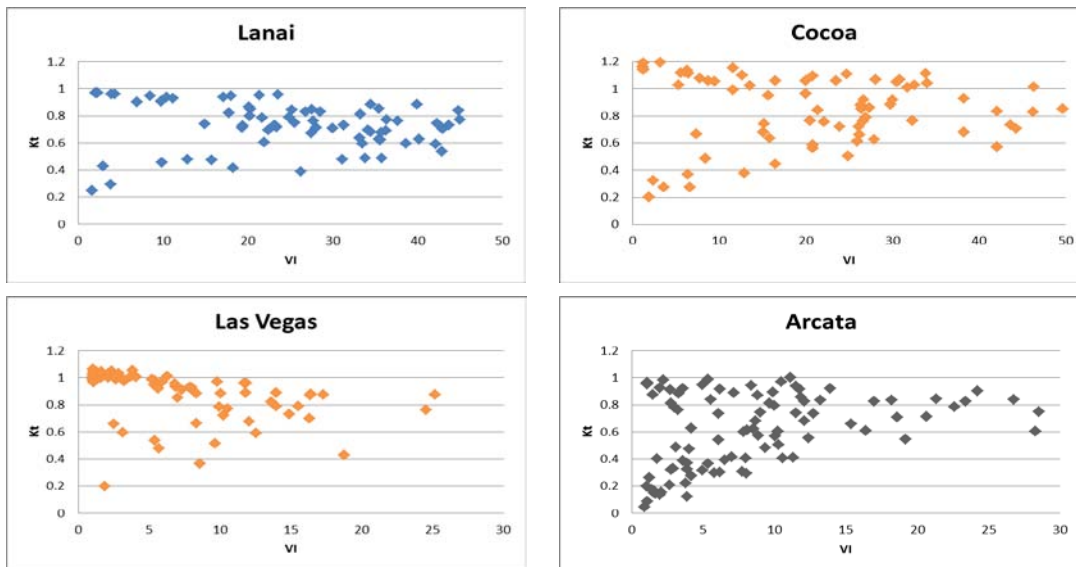


Figure 4-14. Clearness Index vs. VI

4.3 References

- [1] M. Lave and J. Kleissl, "Solar Variability of Four Sites Across the State of Colorado," *Renewable Energy*, vol. 35, pp. 2867-1873, 2010.
- [2] European Commission Joint Research Centre, "PV Status Report 2011", 2011.
- [3] Paula Mints, "The PV Industry 2009: In Search of Stability and Sustainability", *Renewable Energy World Magazine*, 2009.
- [4] US Department of Energy, Office of Integrated and International Energy Analysis, US Energy Information Administration. Annual Energy Outlook 2011. [Online]. Available: <http://www.eia.gov/forecasts/aeo/>
- [5] NERC Intermittent and Variable Generation Task Force (IGVTF), "Accommodating High Levels of Variable Generation", North American Electric Reliability Corp. (NERC), April 2009.
- [6] "FRCC 2011 Load and Resource Reliability Assessment Report", Florida Reliability Coordinating Council (FRCC), July 2011.
- [7] Clean Power Research, LLC. SolarAnywhere Web-Based Service that Provides Hourly, Satellite-Derived Solar Irradiance Data Forecasted 7 days Ahead and Archival Data back to January 1, 1998. www.SolarAnywhere.com.
- [8] A. Woyte, R. Belmans, J. Nijs, "Fluctuations in instantaneous clearness index: Analysis and statistics", *Solar Energy*, 81, p. 195-206, 2007.
- [9] Ernest Orlando Lawrence Berkeley National Laboratory, "Implications of Wide-Area Geographic Diversity for Short-Term Variability of Solar Power", September 2010.
- [10] M. Iqbal, "An Introduction to Solar Radiation", (Academic Press, Don Mills, Canada), 1983.
- [11] N. Kawasaki, T. Oozeki, K. Otani, K. Kurokawa, "An evaluation method of the fluctuation characteristics of photovoltaic systems by using frequency analysis", *Solar Energy Materials and Solar Cells*, 90, p. 3356–3363, 2006.
- [12] Navigant Consulting, Inc. Florida Renewable Energy Potential Assessment. [Online]. Available: http://www.floridapsc.com/utilities/electricgas/RenewableEnergy/FL_Final_Report_2008_12_29.pdf
- [13] J.Stein, C.Hansen, M.Reno, The Variability Index: A New and Novel Metric for Quantifying Irradiance and PV Output Variability, [Online], 2012.
- [14] R. Meeker, A. Domijan, M. Islam, A. Omole, A. Islam, A. Damjanovic, "Characterizing Solar PV Output Variability and Effects on the Electric System in Florida, Initial Results", Proceedings of the 5th International Conference on Energy Sustainability, ASME, Washington, DC, Aug. 2011.
- [15] H. Moaveni, D. Click, R. Meeker, R. Reedy, A. Pappalardo, "Quantifying Solar Power Variability for a Large Central PV Plant and Small Distributed PV Plant", Proceedings, 39th IEEE Photovoltaic Specialists Conference (PVSC), IEEE, Tampa, FL, June, 2013.
- [16] D. Click, H. Moaveni, K.Davis, R. Meeker, R. Reedy, C. Cromer, A. Pappalardo, R. Krueger, "Effects of Solar Resource Variability on the Future Florida Transmission and Distribution System", Proceedings, IEEE Power Engineering Society, Transmission and Distribution Conference and Exposition (T&D), IEEE, 2012.
- [17] Moaveni, H.; Click, D.K.; Pappalardo, A. "Development of an irradiance sensor network to model photovoltaic plant-average irradiance time series", Proceedings, 40th IEEE Photovoltaic Specialist Conference (PVSC), IEEE, 2014.

(this page intentionally blank)

5 PV IMPACT: ANALYTICAL AND EXPERIMENTAL APPROACHES

5.1 Field Data

Most electric distribution feeders are not heavily instrumented. Studies of solar PV impact require voltage, current, and real and reactive power measurements at multiple points along a feeder. Normally, voltage and current are available at the substation, at reclosers (if there are any), and, at larger solar PV locations. It is also helpful to have time-stamped data on the operation of regulation devices that may exist. These may include switched capacitor banks (SCB's), step voltage regulators (SVR's), and on-load tap-changers (OLTC's). Utilities that have SCB's under control of a volt/VAR management system usually have historical data available for SCB operation. Historical records of SVR operation is more difficult to obtain, as the operation of these devices tends to be completely local, according to the settings in the regulator. Records of OLTC operation also tend to be difficult to come by, presumably for the same reason.

In any case, field data can only be used to examine solar PV impact on a circuit for conditions that have actually occurred. A simulation-assisted approach provides for much more thorough investigation of possible impacts over many different scenarios. Field data, then, is important in the validation of models developed for simulation-assisted studies.

There are several important challenges and consideration involving obtaining adequate field data for distribution circuit studies and model validation. The first is simply the lack of data. Without installing additional instrumentation above and beyond the norm, with attendant costs and schedule delay, it is often the case, as mentioned, that only two-three measurements along a main feeder circuit will be available.

Field data typically provided consisted of real and reactive power, voltage, and current at the substation and the PV plant, and at a recloser if one was present.

Besides the lack of data, the time resolution and accuracy of the measurements must be considered, as well as the dependability and data quality (e.g. spurious missing or erroneous data). For high-penetration solar PV impact studies, temporal conditions and spatial conditions, along the length of the feeder, are of interest. This often means data is coming from field instrumentation that may be completely independent, and, importantly, not time-synchronized.

5.2 Modeling and Simulation

5.2.1 *Real-time and EMTP Simulation Tools*

Electromagnetic-transient Program (EMTP) based simulation tools are useful for full 3-phase simulations that can accurately capture dynamic and transient behavior in electrical circuits. For high-penetration solar PV studies, these types of modeling tools are useful for studying voltage regulation, PV inverter interactions, power quality effects, fault response and system protection. The SUNGRIN project utilized two types of EMTP-based tools – PSCAD/EMTDC and RTDS.

PSCAD/EMTDC is a commercially available PC-based EMTP tool with a computer-aided-drafting (CAD)-like drag and drop user interface, along with a library of common power system elements and components, to speed model development. Because it is a PC-based tool performing high-fidelity, small-time-step simulation, execution times can become a significant consideration in performing multiple simulation runs, as they rise significantly with increasing model complexity.

RTDS is a commercially available real-time digital simulation system that, similar to PSCAD/EMTDC, includes a well-developed user interface and library to speed model development. Simulations can be run in real-time at time-steps down to less than 2 μ s for portions of the model and less than 50 μ s for entire systems. The real-time performance is achieved with custom-designed hardware and software optimized for the purpose. The size of the electrical system that can be modeled is limited by the hardware, consisting or racks of processor cards, and input/output (I/O) cards, and other supporting cards. The

electrical state at any node in the simulation can be brought out to real I/O to interface with actual hardware, including controllers or power equipment, providing the means to conduct hardware-in-the-loop (HIL) experiments.

FSU CAPS has a 14-rack RTDS system. Feeder models developed for the SUNGRIN project took between 1 and 3 racks each. One-rack versions of each of the four feeder models were relied upon for most of the work.

5.2.2 RTDS Modeling and Simulation Considerations

There are some particular technical considerations that must be addressed in modeling electric distribution feeders in the RTDS. The RTDS is designed to handle large scale models of power systems, typically at the transmission system level. Models can span over several racks which are interconnected through a fast back plane. Signal transfer from one rack to another takes 1 time step. A typical time step used for simulation is 50 μ s.

Since RTDS uses a travelling wave algorithm to model transmission lines, the length of a line should correspond to a time step. Thus a 50 μ s time step corresponds to a 15 km line length (line length = time step * speed of light [$LL=50 \mu s * 3*10^8$]). If a 50 μ s time-step is used, to model systems using 2 racks, a transmission line of at least 15km length has to be there in the model. An alternative to using transmission lines is using cross-rack transformer models. But they introduce unnecessary inductance in the system.

Distribution feeders seldom are 15 km long. Most distribution feeders are 3-7 miles long. Even if they are, they cannot be split into two racks since splitting a line would not be long enough. Thus distribution feeders have to be modeled in one rack if they have to run in a real-time environment.

For this reason, single-rack versions of all of the four feeder models were developed for the RTDS. Most of system modeling was done using the vast library of power system components provided by RTDS. User written models were used where RTDS did not have a specific model to represent the equipment. Power system components used in the models included AC source, breakers, RL branches, relays, PI sections, transformers, current source injection model, constant power load, induction motor load, capacitor banks, capacitors, and resistors. Several control blocks available in RTDS libraries like tap changer controller, signal processing, signal generators, comparators, mathematical blocks were also used.

5.2.3 Modeling of the PV System

Figure 5-1 shows the typical PV system setup used in RTDS simulation studies of the feeders. The PV array is connected to a capacitor which acts as DC bus for the inverter. The inverter is connected to DC bus and is connected on the AC side to the grid through a dedicated transformer.

PV arrays are usually characterized by plotting the array's output voltage, V versus current, I which is known as the V-I characteristic curve. Solar irradiation and temperature both impact the output of PV panels and the array output changes as a function of these two variables.

Since input power at inverter source end will be intermittent due to changes in solar irradiation on the panels, it is important to maintain an appropriate 'DC link' voltage so that a good quality power with minimal ripple can be supplied to grid and energy transfer from the PV system can be maximized according to the V-I curve. The 'DC link' voltage is maintained by making use of maximum power point tracking algorithm (MPPT). The MPPT technique used is the incremental conductance method.

The PV array component model in RTDS is used to model the PV strings. The model has the option to input the number of panels in series and parallel. The panels are modeled using single diode theory. The panel also has options to input data which is typically available from PV panel manufacturers like short circuit current (I_{sc}), current at maximum power (I_m), open-circuit voltage (V_{oc}), voltage at maximum power (V_m), diode ideality factor (n), temperature dependency factor.

For the study, an average model of the inverter is used since the case studies conducted do not require a switching model. Also, use of a switching model requires running inverter models in the small time step environment ($2 \mu\text{s}$) in the RTDS, which consumes a large amount of processing power.

The inverter controls are modeled using the direct-quadrature (DQ) reference frame method. The purpose of using DQ method is to simplify the system which reduces three AC quantities to two DC quantities. The ‘d-axis’ controls the real power of inverter while ‘q-axis’ controls reactive power component. Figure 5-2 shows the control of real and reactive power of the inverter. The inverter is current limited to 1.2 p.u.

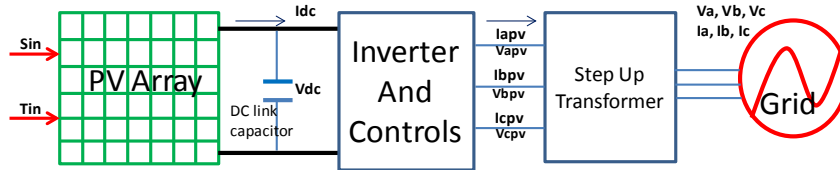


Figure 5-1. Block diagram of PV system modeled

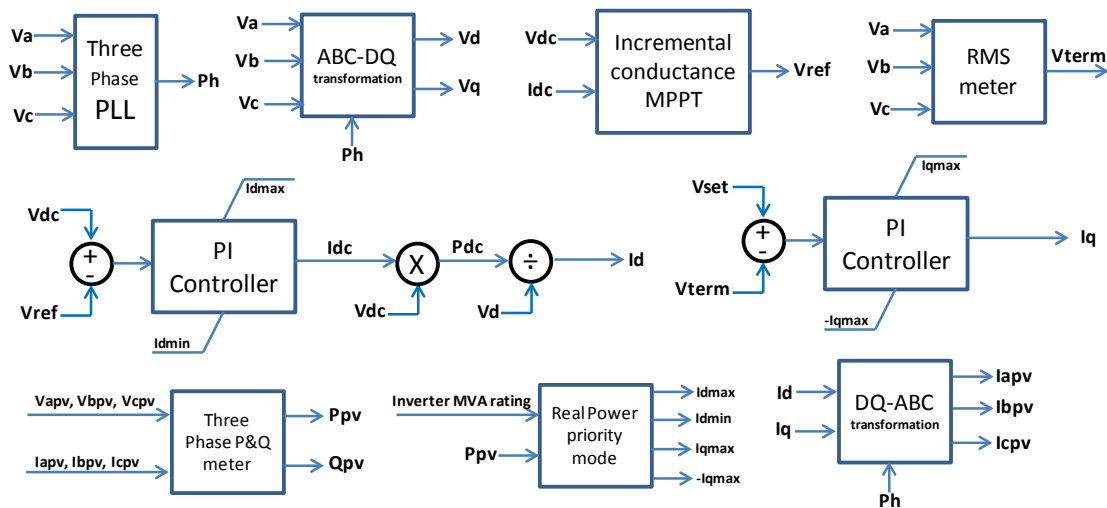


Figure 5-2. Control of real and reactive power of PV inverter

Figure also shows the control and operation of inverter and PV system. A solar irradiation, S_{in} and air temperature, T_{in} is given as inputs to PV panels. The PV panels generate a voltage, V_{dc} and current I_{dc} from module. A three phase ‘Phase Locked Loop’ (PLL) module is used to lock phase of PV system to the grid side. The terminal voltages at the PCC are run through an ABC-DQ transformation block to obtain the reference voltages V_d and V_q in DQ reference frame. To maximize the power output from PV panels, the incremental conductance MPPT method is used. The MPPT outputs a reference DC voltage V_{ref} to maintain a constant voltage at capacitor. This V_{dc} is compared with actual dc link voltage which is input to a PI controller which determines the PV panel current output at inverter I_{dc} . This I_{dc} is used to generate a ‘d-axis’ current reference, I_d which is the real power part of inverter.

Since inverters are often required to operate with unity power i.e. generating ‘zero’ reactive power, the current ‘ I_q ’ which determines the reactive current of inverter can be set to zero. But for the studies going beyond the norms of the legacy IEEE 1547 standards, the inverters are allowed to regulate voltage at its

terminals. This allows for various methods of control of reactive power from inverter. For example, with the set point voltage control method, the measured voltage at the inverter's PCC, V_{term} is compared with a set point voltage V_{set} which is then integrated using a PI controller to generate a 'q-axis' current reference, I_q which is the reactive power part of inverter. The inverter reference currents I_d and I_q are converted to 3 phase currents I_{apv} , I_{bpv} and I_{cpv} using a DQ-ABC transformation block.

5.3 Hardware-in-the-loop (HIL) Simulation

For assessing PV integration, including participation in voltage regulation, voltage and frequency ride-through, curtailment or ramp-limiting, island-detection and anti-islanding, islanded operation, and standards compliance test methods, a hardware-in-the-loop (HIL) test bed and associated methods have been developed, commissioned and tested. The high-penetration PV simulation-assisted analysis approaches based on RTDS models developed and utilized in prior phases provide the means for realistic HIL testing and evaluation. This has been leveraged on the SUNGRIN project to examine an improved integrated voltage regulation and island-detection method and on related projects to evaluate inverter performance under realistic conditions prior to deployment to the field.

A PV hardware-in-the-loop (HIL) testbed including a 17kVA inverter and a 25kW power electronics converter high-performance interface to the RTDS was developed for realistic evaluation of effectiveness

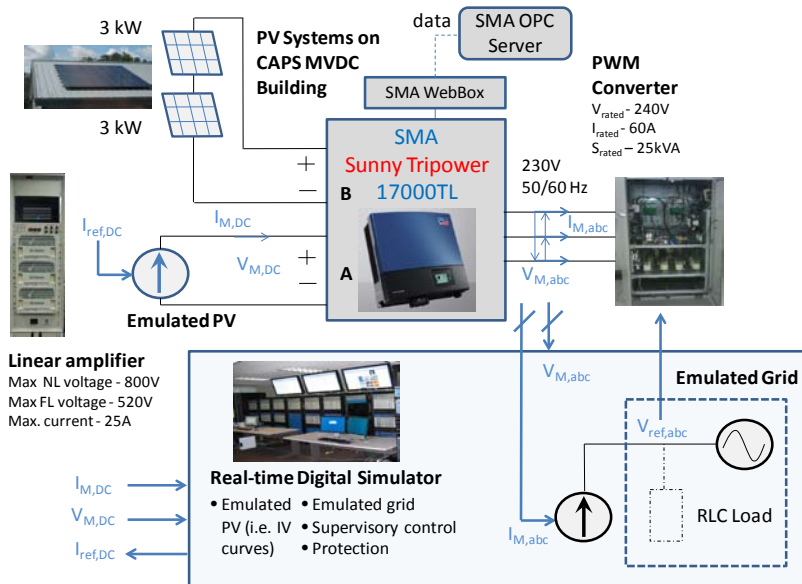


Figure 5-3. PV Inverter low-power HIL lab arrangement

supply. The DC amplifier's maximum power capability of about 14 kW was established, and together with the solar PV array available at CAPS, the PV converter's full power range of 17 kW was successfully tested.

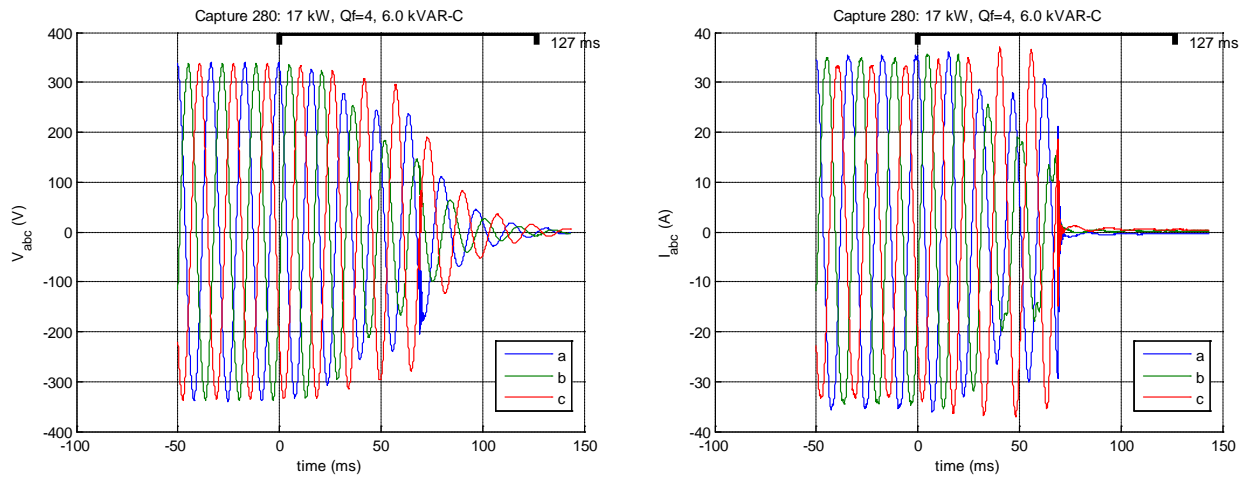
Interface techniques and algorithms for the DC side of inverter HIL testing were developed, tested in simulation, and prepared for use the low-power testbed of Figure 5-3 and the MW-scale testbed.

Once the laboratory facility was established and operation confirmed, the first project in cooperation with the National Renewable Energy Laboratory (NREL) was used to test the PHIL arrangement. The objective was to analyze if the results based on tests with a dedicated RLC load bank can be reproduced with a model of the RLC load bank simulated in real time and interfaced with the solar PV converter through power amplifiers. Complete results can be found in the relevant NREL reports.

complete system performance including hardware and high-fidelity circuit simulations.

The Solar PV Inverter test facility established within the SUNGRIN project was successfully used to record the anti-islanding behavior of the installed 17 kW unit (SMA Sunny TriPower 17000TL). The project provided foundational capability in support of more extensive testing activity in collaboration with NREL that included PHIL testing of anti-islanding for other inverters and a range of scenarios.

An overview of the setup is shown Figure 5-3. This test setup was used to evaluate the facilities operation while connected to the AC grid



3-phase voltages

Phase current

Figure 5-4. Testing the PV laboratory facility: Anti-Islanding test at converter's rated power (17 kW) and quality factor of 4 (inverters typically detect island and disconnect in 50-150 ms)

5.4 Reduced Model Approach

For distribution planning, most utilities model distribution feeders in great detail with commercially available distribution system simulation tools such as SynerGEE, CYMDIST, WindMil, etc. These models usually represent every single lateral and transformer installed on feeder. However, it is advantageous, sometimes essential, to reduce the level of detail in the model before running simulations. The advantages in working with a reduced model include reduced places for error in model development, improved manageability and maintainability, faster execution times (especially useful for EMTP studies and detailed studies requiring multiple simulation runs), and ability to run the model on real-time simulation platforms. Further, in cases where the number of locations for which field data is available for validation, an overly detailed model may not be verifiable, and, for many types of studies, may be unnecessary.

Four utility partner feeders were modeled on the SUNGRIN project with reduced models developed based on circuit information and field data provided by the utility. The process was refined and improved with each feeder model. Circuit topology and conductor and equipment information is provided in various forms by the utility, including drawings, notes, and, in most cases, a SynerGEE database. The process for arriving at a reduced distribution feeder model in the RTDS includes applying a set of criteria for how much to reduce the model and what details to retain, along with some engineering judgment.

The criteria and how they were applied on the SUNGRIN project are shown in Table 5-1³:

³ An automated reduction tool with a more detailed and sophisticated set of criteria was developed in Phase 4 for reduction of OpenDSS models (discussed in the Model Reduction Tool section).

Table 5-1. Model Reduction Criteria

Criteria	As applied to SUNGRIN feeders
Type and scope of study (e.g. load flow, voltage regulation, anti-islanding, harmonics, transient behavior, protection response, etc.)	Load flow and voltage regulation studies on all feeders Protection studies on Feeders 1 & 2 (with detailed substation models)
Feeder bus limit – the maximum number of busses the final model will contain	The goal was to have at least one version of a reduced model for each feeder that was 24 busses or less, to be able to simulate on a single RTDS rack
Bus retention criteria – e.g. retain busses with major PV plants, voltage regulation devices, and key measurements	Retained busses with PV plants, voltage regulation devices, reclosers, and key measurements (aids in model validation)
Area of interest – the entire feeder or a particular portion?	For all of the feeders studied on SUNGRIN, the entire feeder was of interest.
Simulation tool used – e.g. phasor based or EMTP solver; off-line or real-time	EMTP real-time simulation in RTDS Phasor-based solution with OpenDSS in final project phase

Typically, modeling a distribution feeder with 6-20 line sections with lumped load at each section is sufficient. Long laterals can be retained in the system while short laterals can be lumped together.

Consider Feeder 3 as an example. This feeder is 4.5 miles long and mostly radial in layout. Based on utility data provided, the actual feeder circuit consisted of approximately 100 line sections (Figure 5-5(a)). Applying the criteria, and retaining the length of feeder, a 22 bus reduced model was obtained, having 7 line sections and 6 lumped loads (Figure 5-5(b)). The single-line diagram for the reduced model is shown in Figure 5-6.

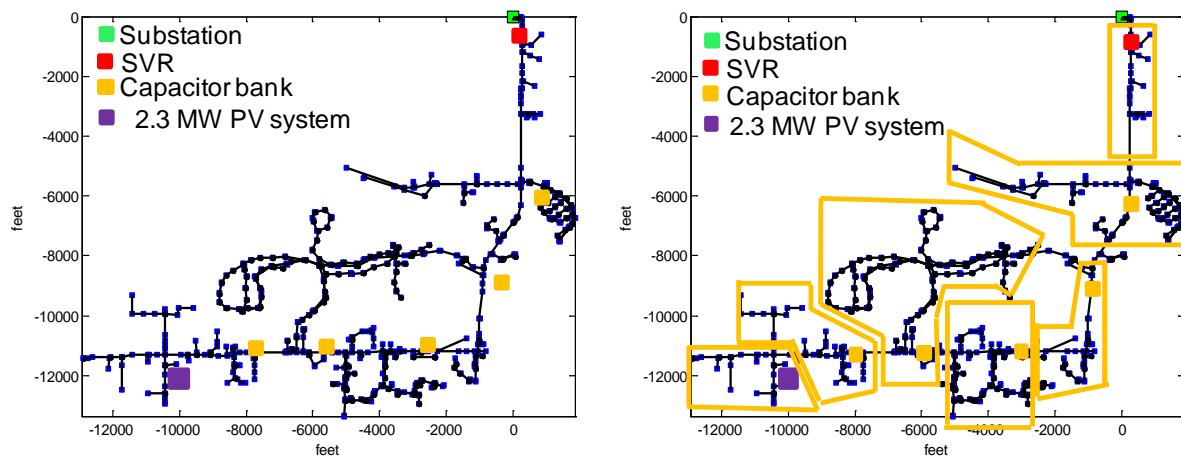


Figure 5-5. (a), left, Feeder 3 layout, (b), right, Feeder 3 sectioning for model reduction.

The reduced model of the utility feeder under study is intended to be used for primarily for voltage profile analysis, voltage regulation of feeder and PV participation in voltage regulations analysis. For these types of studies, detailed modeling of each PV system and inverter is not required. This PV system is represented using an average (mathematical) model, with appropriate regulation and control strategies included as needed.

5.5 Load modeling

In distribution feeder modeling, load allocation is perhaps the most difficult issue. Typically information regarding installed transformer kVA is available to use as a guide for load distribution along the feeder, though exact loading on the transformers may not be available. Loads on feeders are usually a mixture of constant power load, constant current load and constant impedance load. If exact mix of load types are not known for a feeder, typical mixes of constant power and constant impedance loads depending on the type of feeder (e.g. residential-commercial, urban, industrial) can be found in the reference literature. For studies pertaining to voltage drop analysis, modeling loads as constant power is a conservative approach. Power factor for loads are usually fixed equal to the power factor measured at substation if information for power factor at the loads are along the feeder is not known..

Figure 5-6. Single line diagram of reduced feeder

Again, as an example, Feeder 3 data provided by the utility had information regarding type of load and load power factor. The utility also provided estimates on loading at various locations on feeder. This data was used for setting load characteristics at each location. Loads were modeled as a mixture of constant power, constant impedance and constant current using available load models in RTDS.

Table 5-2 shows load distribution per phase for 500 A total loading for Feeder 3 for each of the 6 lumped loads. The load on the feeder varies from 100A to 500A on the circuit. To model the load distribution, five (5) different loadings (100A, 200A, 300A, 400A, 500A) were used, with a load distribution determined at each load level (loads are actual load served, as if no PV).

Table 5-2. Feeder 3 load distribution per phase, per location, at five load levels

Load	load distribution[kVA] at 100A, 2.15 MW			load distribution [kVA] at 200A, 4.32 MW			load distribution [kVA] at 300A, 6.48 MW			load distribution [kVA] at 400A, 8.64 MW			load distribution [kVA] at 500A, 10.8 MW		
	Phase A	Phase B	Phase C	Phase A	Phase B	Phase C	Phase A	Phase B	Phase C	Phase A	Phase B	Phase C	Phase A	Phase B	Phase C
1	52.4	36.8	32.8	66.6	53.5	46.7	118.7	112.6	97.8	188.6	184.5	155.2	343.4	174.5	165.5
2	189.8	225.6	195.9	379.2	507.3	449.2	559.9	759.3	693.6	746.5	1004.5	889.8	1041.9	1048.1	806.4
3	66	54.8	44.3	137.5	124.7	106.7	203.1	189.1	164.1	236.9	220.7	180.1	364.9	256.9	193.6
4	190.8	189.8	188.8	360.3	397.5	410.6	537.8	598.5	636.9	727.7	804.7	830.8	1005.4	884.1	790.9
5	150.4	146.3	155.8	257.4	285.7	321	402.3	445.5	514.2	556.3	606.9	679.3	784	681.5	653
6	90.9	76.2	67.2	205.4	185.9	170.5	284	261.5	244.8	369.3	339.1	309.8	479.6	359.7	284.7

Figure 5-7 shows plot of how load varies at each location as total loading on the feeder changes. It can be seen that loads do not vary linearly at each location. This load data was used to model load distribution in

RTDS. A non-linear graph block was used which determines the load at each location for given total load at substation.

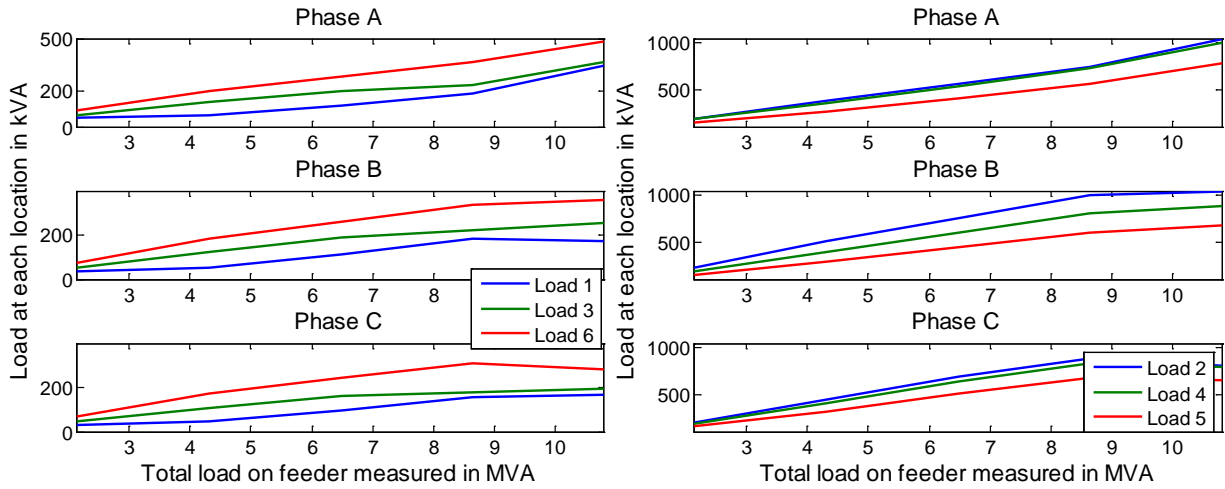


Figure 5-7. Per phase load at each aggregated load location.

5.6 Modeling in RTDS

Reduced models for each of four feeders were produced having no more than 24 busses, allowing simulations to execute in one RTDS rack. Line sections for the reduced models were modeled using ‘PI’ circuit models. Table 5-3 shows impedance data for 7 line sections of the model for Feeder 3. The SVR located at the substation operates based on voltage with a 30 sec time delay (included in the model). The Five capacitor banks located on different busses switch to maintain at least 0.98 power factor on feeder. This control mechanism was also modeled in RTDS. The 2.3 MW PV system was modeled using an average model of PV with a DQ-axis control scheme.

Table 5-3. Impedance data for 7 line sections

Line section	R+ in Ω	X+ in Ω	R0 in Ω	X0 in Ω
1	0.273305	0.797679	0.819915	2.393037
2	0.203153	0.541333	0.609458	1.623999
3	0.166145	0.486696	0.498435	1.460088
4	0.102677	0.30079	0.308032	0.90237
5	0.114954	0.33674	0.344862	1.010221
6	0.087545	0.256452	0.262636	0.769356
7	0.114988	0.361437	0.344965	1.084311

5.7 Model Validation

5.7.1 Model Results Cross-Validation

In the earliest stages of SUNGRIN, in the modeling of Feeder 1, initial checking of the model was performed by building the model, based on utility supplied information on the circuit, in two different EMTP modeling tools (PSCAD/EMTDC and RTDS) and cross-checking the results, which were in nearly perfect agreement. This provided some basic level of error-checking while awaiting more complete field data.

For Feeder 2, the utility’s SynerGEE model had been previously validated against short circuit field data by the utility. Taking SynerGEE then, to be the “truth” model, in that case, short circuit data from SynerGEE was then used to also validate the feeder model developed in the RTDS. As shown Table 5-4, model errors based on the short circuit validation are around 1%.

5.7.2 Validation with Field Data

All four feeder models were validated against field data, usually at the substation, the PV plant and, when possible, a recloser location out on the circuit. The Feeder 1 RTDS model was validated at points across nearly the entire range of PV production is shown in Table 5-5.

RTDS models were developed for all four feeders, followed later by OpenDSS models.

Numerous validation scenarios were run for each Feeder to ensure models performed reasonably well over a range of conditions. As a practical matter, validation of the RTDS models was based on selected one-hour time periods. Periods were selected that were considerably different in load level and PV production.

Table 5-4. Short circuit validation data for FEEDER 2

Location	3-Phase fault current (A)		Fault current error (%)
	SynerGEE	RTDS	
Near Substation	5182	5250	1.3
At Recloser	2994	3034	1.3
At PV site	2428	2451	0.9
Location	L-G fault current (A)		Fault current error (%)
	SynerGEE	RTDS	
Near Substation	3790	3823	0.8
At Recloser	1841	1862	1
At PV site	1469	1484	1

Table 5-5. Feeder 1 model validation – power flow validation against field measurements

Time Stamp	PV (MW)	Breaker Power		Breaker Voltage in kV			PV voltage (primary at recloser) in kV			Breaker Current in A		
		MW	MVar	Meas.	RTDS	Error (%)	Meas.	RTDS	Error (%)	Meas.	RTDS	Error (%)
07/01/12 2:00 AM	0	1.047	0.265	23.849	23.344	1.97	23.814	23.516	1.25	26.67	25.54	4.23
07/05/2012 06:30 PM	3.2	1.454	0.467	23.740	23.241	2.10	23.714	23.377	1.42	37.94	36.71	3.24
07/03/2012 10:00 AM	6.34	-5.28	0.546	23.593	23.111	2.04	23.710	23.385	1.37	130.18	125.15	3.86
07/08/2012 01:15 PM	11.83	-10.14	1.554	23.719	23.194	2.21	23.686	23.316	1.56	254.34	241.82	4.92

Consider a specific validation case for Feeder 2, for the period 4.00-5.00 P.M on May 14th, 2012. The average loading on feeder for simulation was 6 MW at substation. One-minute data provided by the utility was linearly interpolated to 5 sec data and used as input to model. Validation was conducted by matching feeder model real power at substation to measured real power data at substation and observing the errors between voltage and currents at substation and recloser. Loads were linearly varied to achieve measured power at substation. Figure 5-9 compares measured and simulated currents at the substation for one of the Feeder 2 RTDS model validation runs. Model real power was in agreement with field data, with an average error of 1.5 %.

For both RTDS and OpenDSS model validation for all feeders, field measurements for current and voltage on each phase at multiple locations along the feeder and real and reactive power flow were compared to simulation results. Generally, simulated voltages agreed with field values within about 2% error, while currents, being more sensitive to the particular behavior and variation of load, had average

errors for each case varying from around 0.6% to 5%, with maximum errors as high as 16% in some (usually low-load) cases.

5.7.3 Sources of Error

When pursuing a simulation-assisted approach to EPS analysis, there are a number of possible sources of error that can arise in the course of model development. Sources of error include:

- Inaccurate information on the circuit topology and equipment
- Errors in formulation and construction of the model
- Insufficient field data (locations, time periods, resolution, time synchronization)
- Inaccurate representation of protection and control systems
- Load variability

5.7.3.1 Inaccurate information on circuit

Utility drawings, documentation, databases, and models, along with the institutional knowledge residing with experienced personnel are the source of information needed to construct a model. There is always the possibility that information the utility has in the form of documentation, databases, and models, contains errors. Diligence and review by knowledgeable and experienced personnel can help mitigate these kinds of errors.

The types of information required and the level of detail depend upon the modeling tool being used and the types of studies to be performed. A modeling information request form was developed on the SUNGRIN project to facilitate gathering the information required to construct the models in RTDS.

5.7.3.2 Errors in formulation and construction

Human error can come into play in construction of the model to run in the tool of choice. Chances of this type of error increase with model detail and complexity, reinforcing the case for a reduced (simplified) model approach. On occasion, though not often with current modeling tools available, model data can be ported between modeling tools, reducing some opportunity for data entry error. Cross-checking model results across different modeling tools can help catch and reduce some of these types of errors.

5.7.3.3 Insufficient field data

Distribution circuits often have few measurements available. For solar PV impact studies, it is desirable to have RMS current and voltage, as well as real and reactive power data, for multiple locations along a feeder at sample-time resolutions of 1-min. or better. Based on the feeders examined on SUNGRIN, data is usually only available for three locations – the substation, the PV plant, and a recloser. It usually can be obtained at 1-min. resolution, but, obtaining resolutions finer than that often require installation of special instrumentation such as digital fault recorders (DFR's) or power quality (PQ) meters configured to capture and store at high speed, or modifications to data collection configuration in the SCADA, DMS, or real-time process information systems.

Smart meters can provide load data at the load service entry points, but, these would typically be many more points than are needed or even practical in some cases (on the order of thousands) and are usually only available at 15-min. resolution, at best, and sometimes only 1-hour resolution.

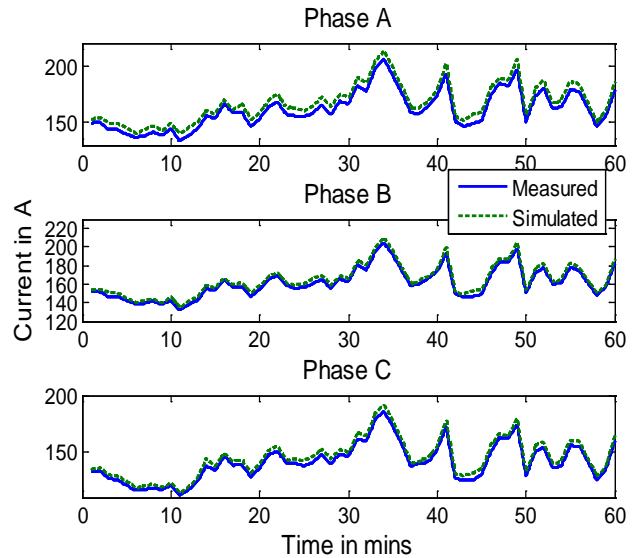


Figure 5-9. Current at Feeder 3 substation breaker

A fairly common issue encountered, when conducting analysis and validating models using data from multiple locations along a feeder, is field measurement time synchronization. Often field measurements on distribution circuits originate from different instrumentation or different pieces of equipment that are not time synchronized. Some of the errors observed in SUNGRIN feeder validation were attributable to this. A study was performed on Feeder 2 to provide some idea of the sensitivity of this error by deliberately lagging and leading the timestamp of a measurement from the PV plant location relative to a measurement from the substation location. The result of the lag case is shown in Table 5-6.

Table 5-6. Time synch. error tabulation for lag case

Delayed measurement of PV	Phase A		Phase B		Phase C	
	Avg. %	Max. %	Avg. %	Max. %	Avg. %	Max. %
10 second	0.42	2.51	0.39	2.33	0.36	2.14
30 second	1.15	5.07	1.07	4.71	0.98	4.31
1 minute	2.20	9.16	2.04	8.51	1.88	7.74
2 minute	4.06	15.90	3.79	14.91	3.46	13.67
3 minute	5.65	20.21	5.28	19.02	4.82	17.52

5.7.3.4 Inaccurate representation of protection and control systems

Since voltage is one of the most common impacts expected and, therefore examined, associated with high-penetration PV, it is important to have correct information on the voltage regulation devices present, their ratings, and the settings and control strategies governing their operation. For protection studies, accurate information on sizing and settings of protection devices is important, including, fuses, breakers, relays, and sensing devices such as current transformers (CT's) and potential transformers (PT's).

The most common voltage regulation equipment on Florida distribution feeders are distribution substation transformer on-load tap changers (OLTC's), step voltage regulators (SVR's), and switched capacitor banks (SCB's). There may also be fixed capacitor banks that are always connected and manually switched capacitor banks that are switched remotely from the SCADA system or locally in the field.

Voltage regulation control schemes often reside in separate systems dedicated to that purpose. Often these systems were configured and installed by a third party and there may not be extensive institutional knowledge within the utility as to the configuration or rationale for some of the control settings and strategies. This can be exacerbated by personnel turnover and retirements.

Reactive power flows in SUNGRIN models for circuits with regulation devices sometimes didn't compare as well as expected with field data. This was usually attributable to the actual operation of voltage regulation devices in the field, especially SCB's, not matching simulation, where control details and settings for devices were modeled on the utility's best understanding of how they were set up to function. Whether regulation devices are switching or not is readily apparent by observing times-series reactive power flows (field data compared to simulation). This inconsistent operation or mismatch is due to 1.) control settings or strategies not implemented exactly as described or understood, 2.) manual overrides of the control by operations, and, 3.), malfunctioning or failed equipment in the field.

5.7.3.5 Load variability

Due to limited data on load and the stochastic and nonlinear nature of load variation, this is one of the most pervasive challenges in modeling distribution feeders. With limited measurement points and sample resolution, load variability cannot be captured entirely. Certain loads may turn completely on or off at various points in time which can introduce substantial error during those simulation periods if accounted for. The load distribution may change daily on each phase but modeling is done in such a way that distribution is fixed so as to achieve similar power at substation and recloser. Despite these challenges, acceptable agreement was achieved with the four feeder models using the reduced model approach with aggregated loads.

5.8 References

- [1] P. McLaren, O. Nayak, J. Langston, M. Steurer, M. Sloderbeck, R. Meeker, X. Lin, M. Yu, P. Forsyth, “Testing the ‘smarts’ in the smart T&D grid”, IEEE Power Engineering Society (PES) Power Systems Conference and Exposition (PSCE), IEEE, 2011.
- [2] M. Steurer, R. Meeker, K. Schoder, P. McLaren, “Power Hardware-in-the-Loop: A Value Proposition for Early Stage Prototype Testing”, 37th Annual Conference on IEEE Industrial Electronics Society (IECON), 2011.
- [3] Kersting, W. H., “Distribution System Modeling and Analysis”, 3rd Ed., CRC Press, 2012.

6 STUDIES OF FLORIDA DISTRIBUTION CIRCUITS

6.1 Overview – Florida Feeders Studied

The SUNGRIN project has identified, and systematically modeled and studied, four distribution feeders in Florida electric utility partner service areas. The circuits were selected because all have relatively high penetration levels of solar PV on them, 26% up to over 500% of maximum load.

The feeder circuits studied differ considerably in design and solar PV penetration. Characteristics of the four circuits examined, including range of PV penetration, are summarized in Table 6-1.

Table 6-1. Penetration levels and other selected characteristics for circuits examined.

FEEDER:	1	2	3	4
Amount of PV installed [MW AC], (tracking)	12.6 (fixed)	2.6 (fixed)	2.3 (1-axis)	5.3 (1-axis)
Feeder Loading (Min./Max.) [MW]	0.4 / 2.1	3.8 / 8.1	2.5 / 9.0	0.4 / 1
% PV penetration vs Min. / Peak Load	3150 % / 600%	68 % / 32%	92% / 26%	1375% / 550%
Nature of PV Penetration	Single large plant	Concentrated in two locations	Single large plant	Single large plant
Length of feeder	9 miles	4.4 miles	4.5 miles	7.1 miles
Location of PV	4.8 miles	4.2	4.3 miles	3.4 miles
Load mix (Residential / Commercial+Industrial)	85 / 15 %	40 / 60%	35 / 65%	100%
Feeder topology	Radial, primarily one single main circuit	Radial, with two major laterals	Radial with small laterals	Radial, primarily one single main circuit, with two small laterals midway, one to the PV plant
Reverse power flow	Yes (routinely)	No	No	Yes (routinely)
Voltage regulation equipment	None	SVR (near sub.) and SCB's along feeder	SVR (near sub.) and SCB's along feeder	None
Switched capacitor bank (SCB) control method	n/a	VAR flow at substation breaker	PF at substation breaker (≥ 0.98)	n/a
Further PV penetration possible?	Yes	Yes, with changes to SVR and cap. bank operation	Yes	Yes, but, requires mitigation /regulation

Topological representations of the four feeders are shown in Figure 6-1.

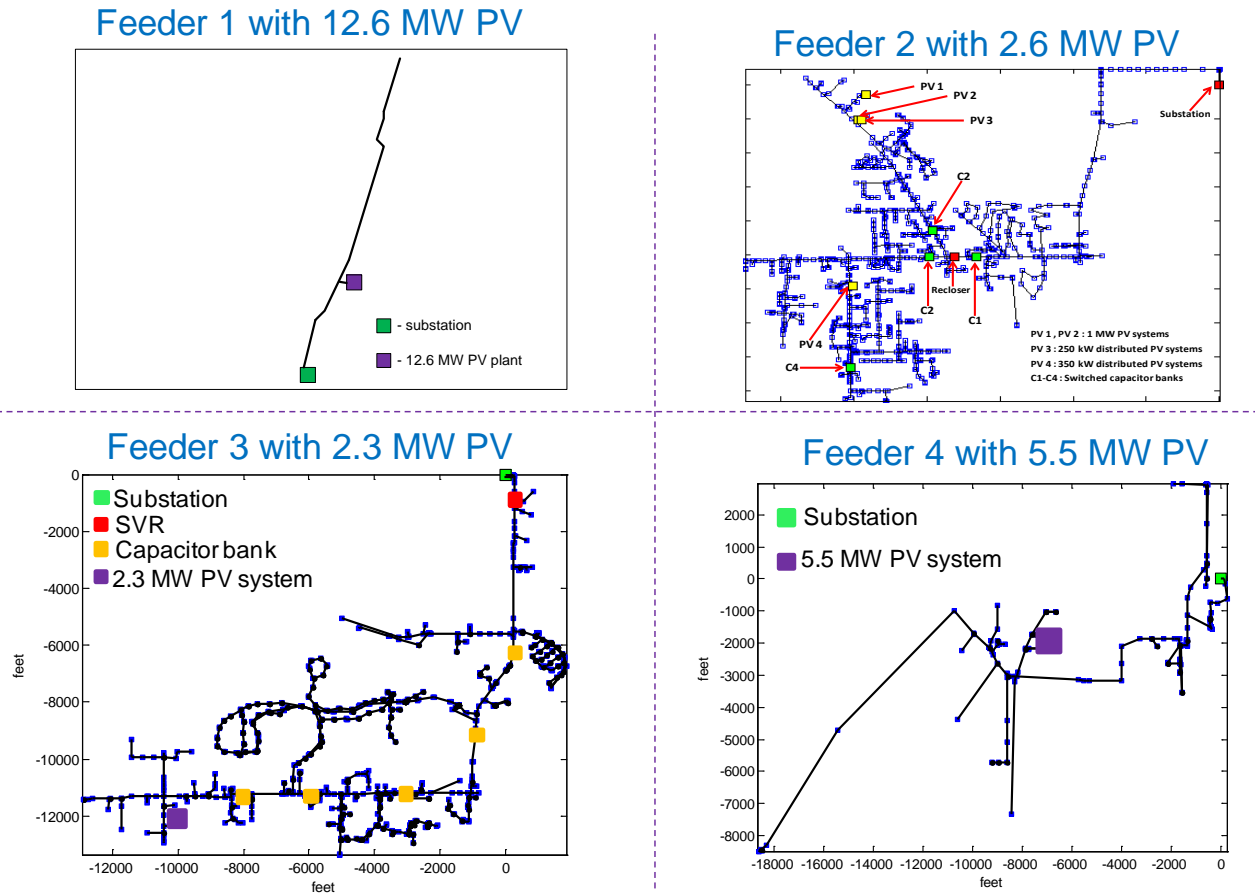


Figure 6-1. Four (4) utility distribution feeders modeled and studied under the SUNGRIN project.

Feeders were studied sequentially, with some overlap, and with substantial refinements to the modeling and simulation methodology as the project progressed. Field data itself was examined, and provided some insight as to PV impact on the circuits, but far more could be ascertained from simulation-assisted studies where wide-ranging conditions could be specified and carefully controlled.

The process required obtaining engineering and design information necessary to model the feeder circuits, and obtaining field data and utility simulation runs (from utility’s “truth” model) to validate the SUNGRIN project models. An important aspect of the refined modeling process was obtaining simulation results from the utilities’ distribution models for multiple cases, covering minimum, average, and high loading periods, and compiled to correspond to the combined line sections and aggregated loads of the reduced models.

Voltage impact studies were completed first, followed by voltage regulation and mitigation studies, followed by, for Feeders 1 and 2, detailed substation protection studies. In the final phase of the project, some of the voltage profile and voltage regulation and mitigation studies were repeated in OpenDSS to examine response over longer time periods and to perform more thorough and methodical screening for impact relationships (see Section 10 on Parametric Studies).

6.2 Feeder Models

Simulation-assisted studies allow exploration of a wide range of scenarios to gain a more thorough understanding of high-penetration PV impact and mitigation, even with a relatively few number of feeder circuits. The four distribution feeders studied were modeled first in RTDS and, then, in OpenDSS. The approach to developing and validating the models was described in Section 5.

Some feeders were also modeled in other tools, including PSCAD/EMTDC, MATLAB/Simulink, and PSSE. This facilitated cross-validation of models and also certain specific types of studies. For example, some studies over longer time periods, but, requiring less detail, were performed in MATLAB/Simulink.

Single-line diagrams of the reduced versions of the four feeders, as modeled in RTDS and OpenDSS are shown in Figure 6-2.

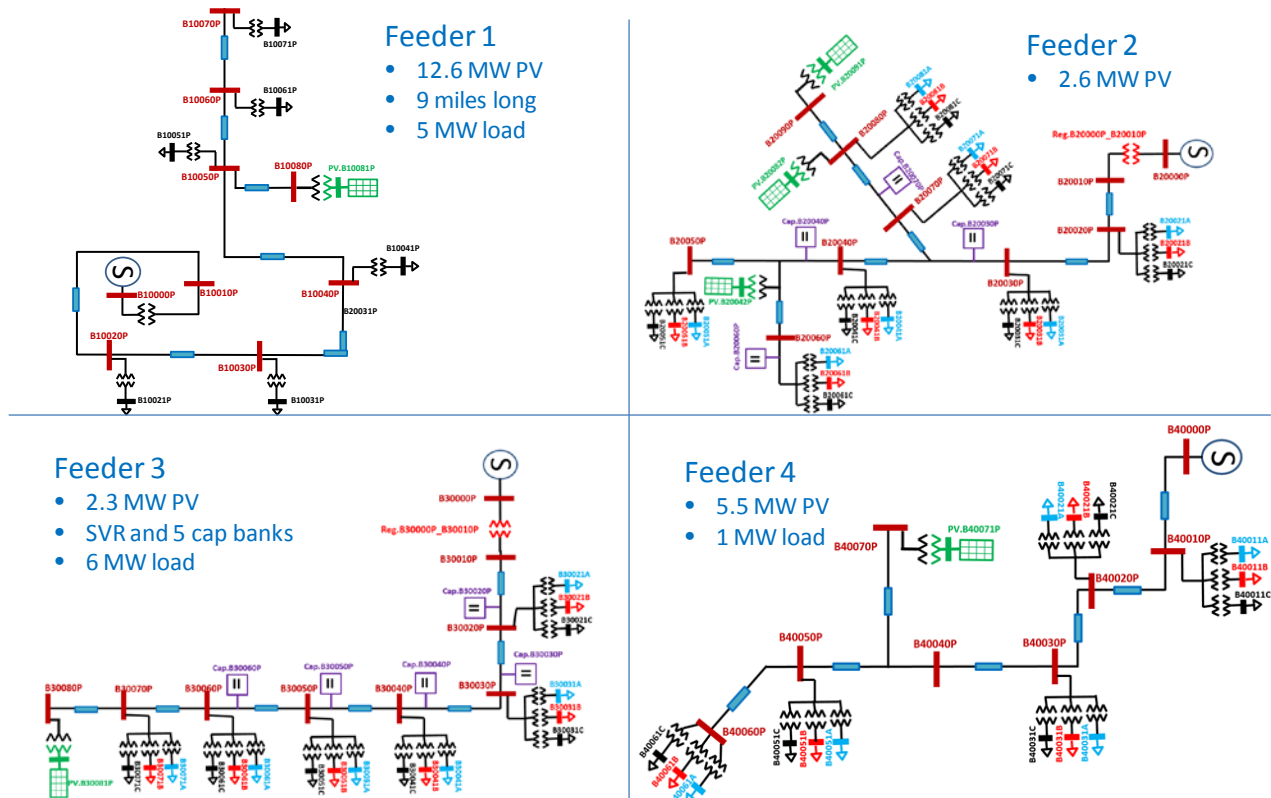


Figure 6-2. Single-line diagrams of the reduced circuit models for the four (4) utility feeders

6.3 Voltage Impact

The most certain impact that large amounts of PV will have on a circuit is voltage. This is particularly true if the PV plant is maximizing real power production and is not configured to mitigate voltage issues or participate in regulation. Voltage profile on all four feeders was examined carefully with RTDS and OpenDSS simulations. Selected results for each feeder follow.

6.3.1 Feeder 1

Feeder 1 is a 24kV circuit with a 12.6 MW-AC PV plant located at roughly 3/4 the length of the circuit. The circuit has no voltage regulation equipment. This feeder circuit hosts the largest PV plant among the utility feeders studied.

Figure 6-3 shows voltage profile range of operation for Feeder 1 over 30 days, as simulated in OpenDSS using actual load and PV data actual load and PV variations. These results are from simulation with the OpenDSS reduced circuit model for Feeder 1. At low loads, the voltage can approach the ANSI limit⁴ [ref], but, even with 600% penetration, it operates within limits the entire period.

A series of power flow simulation cases were run with the RTDS models to examine voltage profile along the circuit in response to varying the total load and PV levels, X/R ratio, and power factor (Figures 6-4, 6-5). Essentially, for increasing load or having more inductive (lagging PF) loads, the presence of PV is a benefit, as these tend to lower the voltage on the circuit, which PV helps to mitigate. As for X/R ratio, smaller conductor, lower X/R, creates more potential voltage rise issues.

Varying the load, X/R, or power factor to extremes beyond the normal operating range can cause low voltage violation of ANSI limits in simulation, but, the impact of the solar PV plant is a benefit in all of these cases, as it tends to raise the voltage out on the circuit.

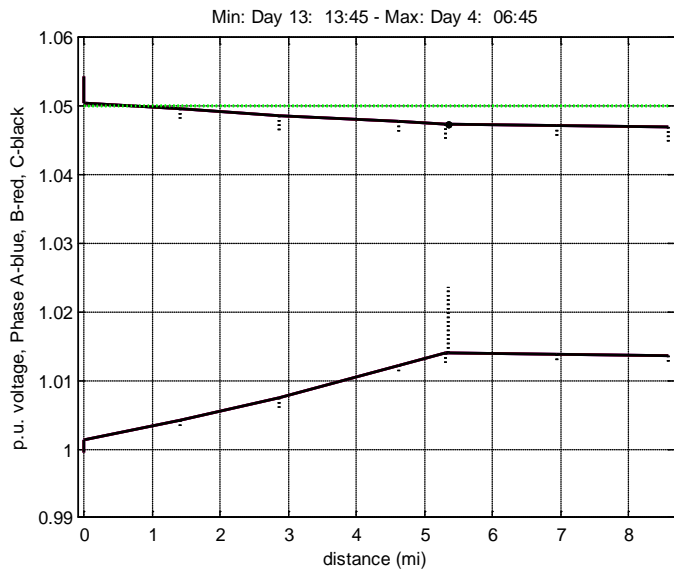


Figure 6-3. Voltage profile range over 30-day period for Feeder 1

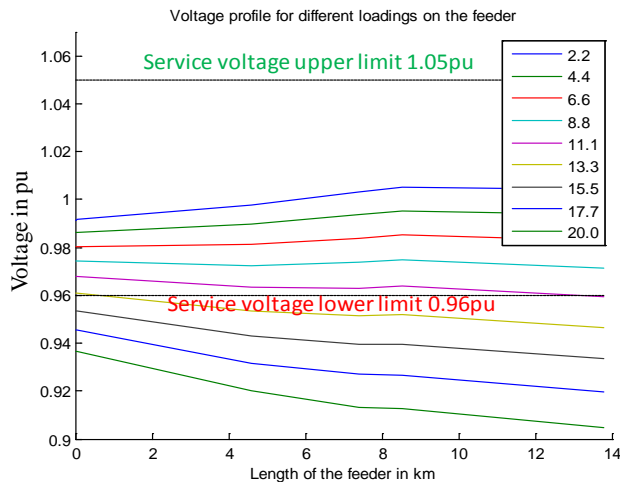


Figure 6-4. Voltage profile for load variation with PV power = 12MW

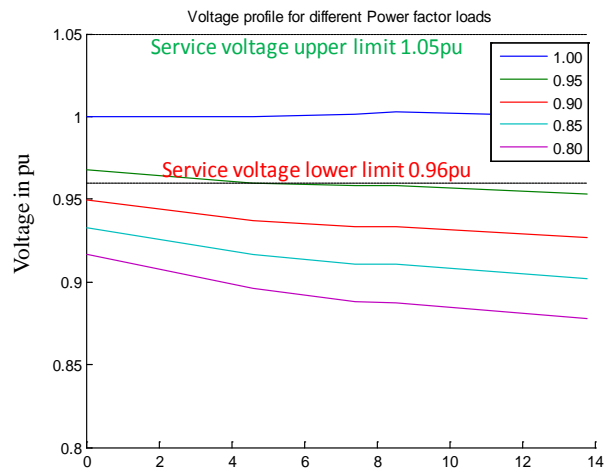


Figure 6-5. PF variation. PV power=12 MW

Scenarios were created by varying the load size, power factors of the load, and PV power output. The results were mapped with PQ meter data obtained at PV plant and cross-examined to select valid scenarios for simulation. For the load variation studies, loads along the feeder were varied from 2.2 MVA

⁴ ANSI C84.1 specifies *service* and *utilization* voltage limits. Solid traces on voltage profile plots are actual main feeder voltages, so, it is not always strictly the case that *exceeding* the limit on the feeder will result in the limit being exceeded at the service entrance or utilization point, nor that being *in* limits on the feeder will guarantee service and utilization voltages are in limits.

to 20 MVA, intentionally overloading it beyond the normal range. Loads were equally distributed with 0.9 power factor. PV plant power output was kept constant at either 12 MW, which is close to peak PV power, or 3 MW which is the average PV output of the plant for a year.

6.3.2 Feeder 2

Feeder 2 is a 12.47 kV urban/sub-urban feeder as shown in Figure 6-7. The substation feed is 138 kV. The feeder splits into two main laterals each extending to around 4 miles from substation. The feeder has 2.6MW of distributed PV. There are two 1-MW ground mount systems and smaller roof top units totaling 250 kW on one lateral and another single 350kW roof top unit on other lateral. The feeder has a step voltage regulator around 0.4 miles from substation. The step voltage regulator (SVR) has $\pm 10\%$ regulation with 32 steps with a 2 minute operation time. The feeder also has 4 switched capacitor banks (3- 900 kVAR and 1- 600kVar) installed, totaling to 3.3 MVAR. The capacitor banks operate based on MVAR flow at substation. If MVAR flow into feeder is greater than 600 kVar, based on priority, a capacitor bank is turned ON and if VAR flow is greater than 300 kVAR to substation, a capacitor bank is turned OFF. Feeder 2 mainly has residential and commercial type loads. A recloser is located at 2.2 miles from substation. Voltage, current, and power measurements are collected from meters at the substation and recloser. Data from the meters was provided at a 1 min. resolution. The average feeder load is around 5MW.

6.3.2.1 Modeling of Distribution Feeder

Two versions of the Feeder 2 model were built in the RTDS. A detailed model utilizing 3 racks on the RTDS was built as an intermediate step in reducing feeder nodes. The model has 22 line sections with load on each section. 4 PV models were built – 2x1MW PV systems, a 250 kW system, and a 350 kW

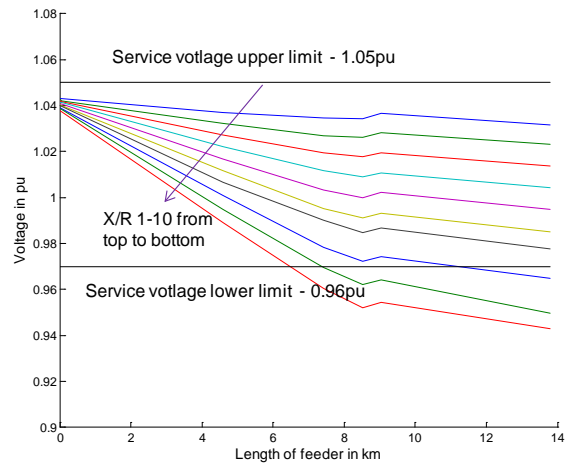


Figure 6-6. Feeder 1 voltage prof. vs.X/R ratio

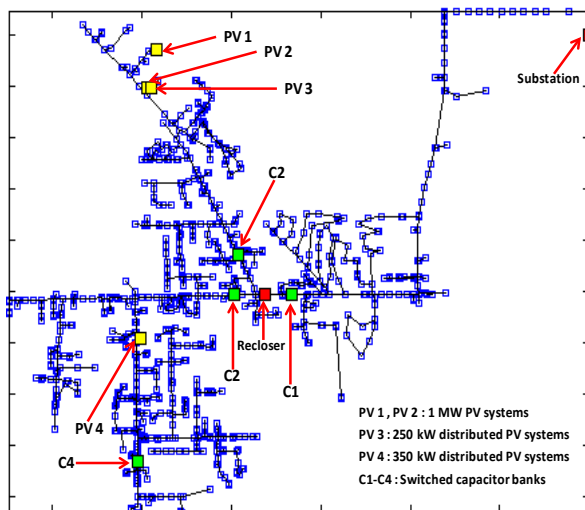


Figure 6-7. Feeder 2 topology

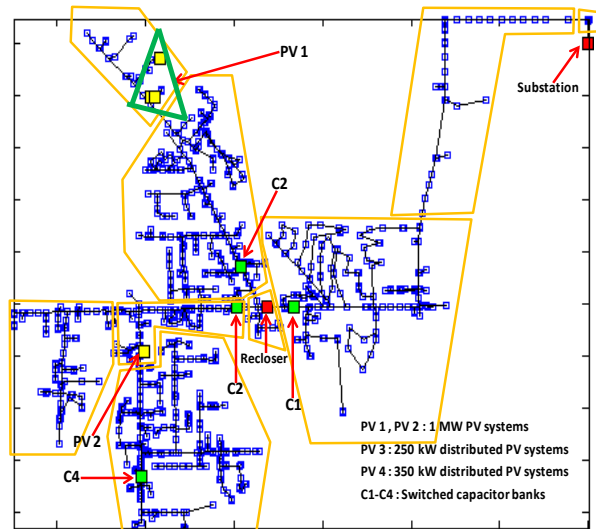


Figure 6-8. Feeder 2 circuit reduction and load aggregation

system. But, to make use of RTDS real-time capability, a second one-rack model was built. The circuit reduction and load aggregation for the final one-rack model is shown in Figure 6-8.

6.3.2.2 Accommodating High Penetration PV

Figure 6-9 shows the measured voltage at the recloser for 8 days of 1 min data. Voltage on the circuit is found to routinely exceed the ANSI C84.1 high voltage limit at the recloser location, with the current PV penetration and existing method of operation of SVR and SCB's. The average voltage for 8 days was 1.038 p.u. Any further significant increase in PV penetration would likely require some kind of voltage regulation mitigation. Figure 6-10 shows voltage profile range (min. and max.) for feeder for 8 days. It also shows the locations of capacitor banks (C1-C4), the voltage regulator, and two 1-MW PV sites. It is observed that the minimum voltage measured on the feeder end is 1.02 p.u.

To observe the impact on voltage with additional PV penetration on the feeder, the PV penetration was increased in simulation from the current level (2.6 MW) to 10 MW in increments of 2 MW by increasing it at the 2x1MW ground-mount site. This was performed at loadings of 9 MVA and 4 MVA resulting in voltages along the feeder as shown in Tables 6-2, 6-3. At approximately double the current level of PV penetration, at low load, the voltage would exceed the ANSI limit everywhere on the feeder.

The reason the voltage exceeds the limits is due primarily to the current method of operation of the SCB's and SVR. The SVR is set to operate if the voltage is outside the range of 1.01-1.06 p.u., but it never reaches that limit. Also, the SCB's operate based on VAR flow from the substation. With PV penetration increasing, there is a rise in voltage, which is not accounted for by either the

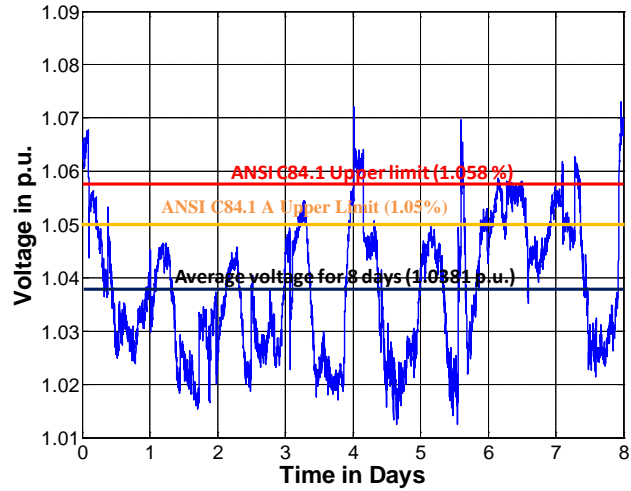


Figure 6-9. Feeder 2 recloser voltage field measurement

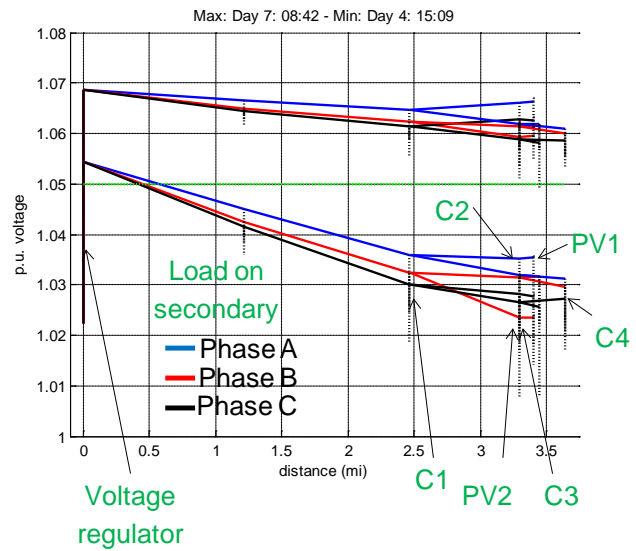


Figure 6-10. Feeder 2 min. and max. voltage profiles, per phase, over 8 day period

Table 6-2. Voltage Profile, High Loading (9 MVA)

PV penetration [MW]	Voltage at Breaker [p.u.]	Voltage at Recloser [p.u.]	Voltage at PV site [p.u.]	Voltage at other end of feeder [p.u.]	No. of cap banks ON
0	1.046	1.02	1.015	1.017	4
2.6	1.045	1.027	1.027	1.025	4
4	1.046	1.031	1.034	1.029	4
6	1.046	1.036	1.042	1.033	4
8	1.045	1.039	1.049	1.036	4
10	1.047	1.043	1.056	1.041	4

Table 6-3. Voltage Profile, Low Loading (4 MVA)

PV penetration [MW]	Voltage at Breaker [p.u.]	Voltage at Recloser [p.u.]	Voltage at PV site [p.u.]	Voltage at other end of feeder [p.u.]	No. of cap banks ON
0	1.051	1.046	1.044	1.044	3
2.6	1.048	1.045	1.049	1.043	3
4	1.048	1.048	1.054	1.046	3
6	1.051	1.059	1.069	1.058	3
8	1.05	1.061	1.074	1.06	3
10	1.048	1.062	1.078	1.061	3

SVR or the SCB's. Three SCB's were ON for all levels of PV penetration.

To accommodate higher penetrations of PV, changes are required to the existing method of operation for the SCB's and SVR. One such operational change was conceived and tested on the feeder in simulation utilizing the RTDS model. For this scenario, the basis for operation of the SCB's was changed from VAR flow-only to MW and MVAR flow, configured as follows: If reactive power (Q)

into the feeder is greater than 1 MVAR, turn ON an SCB; If real power (P) (reverse flow due to PV) into the substation is greater than 2 MW, turn OFF an SCB for every 2MW increase. This new method of operation was tested in simulation for low loading (4 MVA) on the feeder.

Table 6-4 shows the voltage profile with the new method of operation of the capacitor banks. It can be observed that even with 10MW of PV penetration, voltages at various locations stay within limits. Also with an increase in reverse power flow at the substation, capacitor banks are turned OFF, which offsets the rise in voltage due to reverse power flow.

6.3.2.3 Hosting and Mitigation

The simulation assisted analysis for Feeder 2 reveals that increasing the penetration of PV on this feeder would require modification to existing voltage regulation schemes and settings. Legacy voltage control schemes and settings may not be adequate on distribution circuits experiencing increasing levels of PV.

Of the four feeders studied, Feeder 2 probably most typifies urban-suburban type radial feeders in terms of length, topology, voltage, types of loads, and types of regulation equipment employed. For these types of feeders, it is likely it will often be the case that leveraging the flexibility inherent in automated volt-VAR control systems will allow higher PV penetration levels to be accommodated, with careful and informed modification of control settings or strategies.

6.3.3 *Feeder 3*

Feeder 3 is a suburban and rural feeder operating at 12.47 kV. The feeder is 4.5 miles long. The load varies from 100A to 500A, with a residential / commercial load mix of 25% / 75%. There is one 2.3 MW solar PV system located near the end of feeder. Regulation equipment on feeder 3 includes a step voltage regulator (SVR) located near substation with $\pm 10\%$ regulation with 32 steps and capacitor banks installed along the circuit (4x600 kVAR and 1x300 kVAR). The capacitor banks turn on based on power factor on feeder. Capacitor banks switch ON to maintain at least 0.98 power factor.

6.3.3.1 Accommodating High Penetration PV

Figures 6-10 and 6-11 show daily profiles for power flow at the substation and PV plant power generation for an 8 day period, Figure n for the low-variability days, and Figure m for the high-variability days. As was evident in Figure 3-2, because the high PV penetration comes from a single large single-axis tracking ground-mount PV plant and there is a fairly high percentage of commercial-industrial load on the feeder, it is apparent that the PV is offsetting quite a bit of the normal daytime load.

Figure 6-12 shows OpenDSS simulation results for the voltage profile ranges on Feeder 3, per phase, for the 8-day period for which the model was validated (Feb. 1 – Feb. 8, 2013). It can be seen that, for this Feeder, with around 26% PV penetration, voltage mostly remains in ANSI limits, except for one phase which exhibits a tendency to experience high voltage from the middle to the end of the feeder.

Table 6-4. Voltage Profile with new cap control bank technique

PV penetration [MW]	Voltage at Breaker [p.u]	Voltage at Recloser [p.u]	Voltage at PV site [p.u]	Voltage at other end of feeder [p.u]	No. of cap banks ON
0	1.048	1.038	1.037	1.036	2
2.6	1.048	1.045	1.049	1.042	2
4	1.048	1.049	1.055	1.046	2
6	1.043	1.040	1.047	1.038	1
8	1.037	1.03	1.040	1.028	0

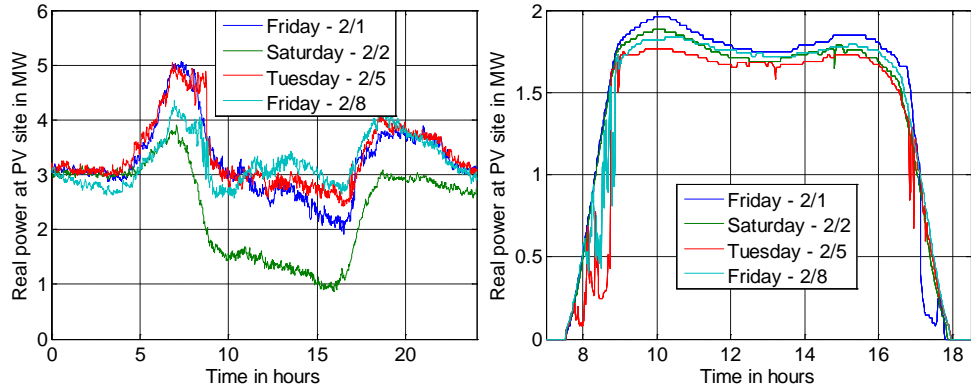


Figure 6-10. Feeder 3, substation real power and PV real power for low variability days

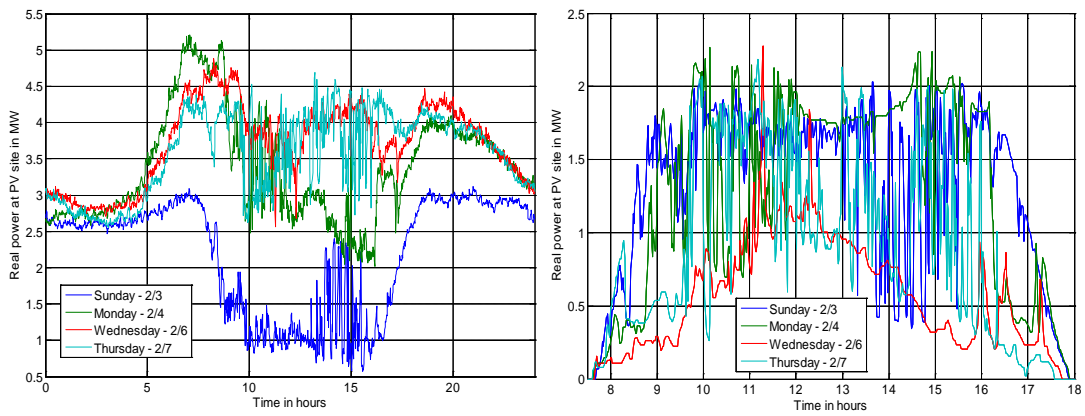


Figure 6-11. Feeder 3, substation real power and PV real power for high variability days

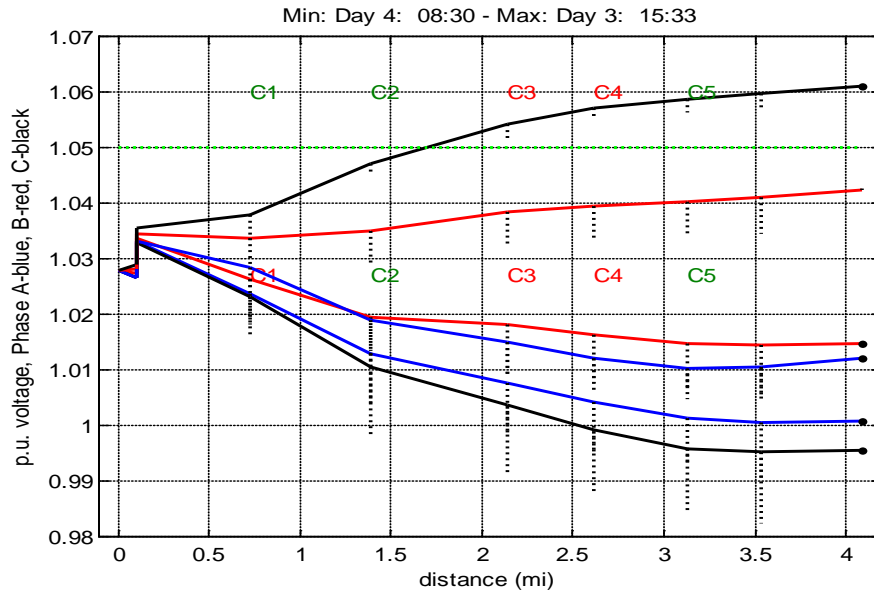


Figure 6-12. Feeder 3 min. & max. voltage profiles, per phase

To examine voltage profile on the system and assess hosting capacity from a voltage regulation point of view, PV penetration on the feeder was varied from 0-10 MW. Three different loading scenarios were used, low load (2.3 MVA), average load (5.7 MVA) and high load (10.97 MVA). For all cases, the PV system was set to inject real power only. Figures 6-13 to 6-15 show voltage profile on the feeder for three different loading scenarios for various level of PV penetration. The large PV plant is located at the end of the feeder.

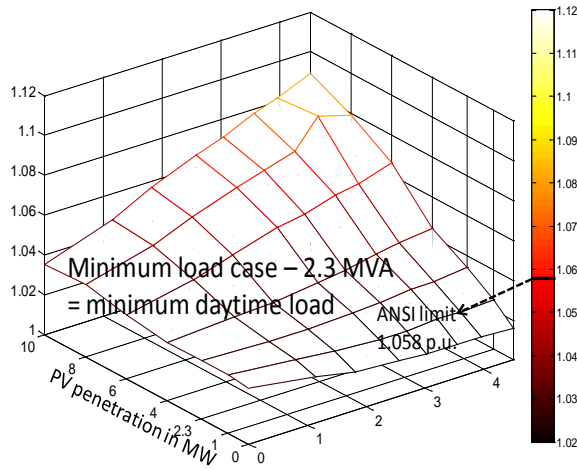


Figure 6-13. Feeder 3 voltage profile vs. installed PV generation, at low load

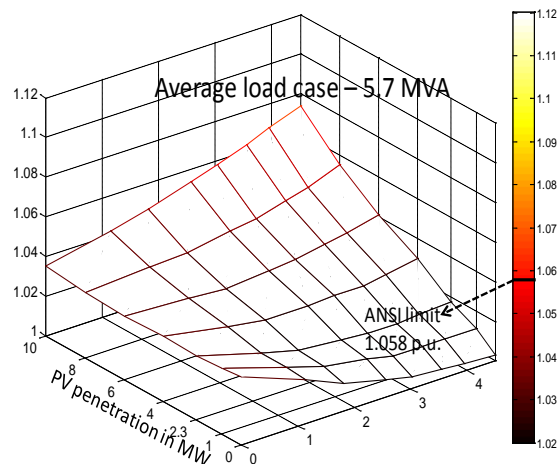


Figure 6-14. Feeder 3 voltage profile vs. installed PV generation, at average load

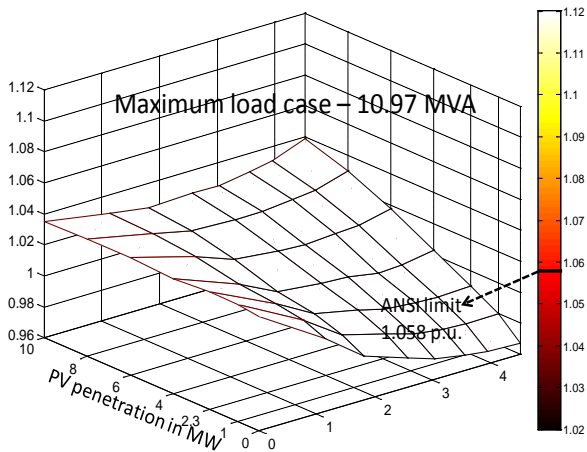


Figure 6-15. Feeder 3 voltage profile vs. installed PV generation, at high load

These results suggest, based only on average voltage profile, that the PV capacity at the current site could possibly be increased to about 4 or 5 MW. This only considers voltage and, also, is not examining each phase, recalling the OpenDSS model (Figure 6-12) showed a tendency for high voltage on C phase, so more investigation would be warranted if the penetration were to be increased much further. A more thorough assessment of hosting capacity would also consider PV location as well as other factors. The profiles on the 3-D plots suggest locating additional PV towards the middle of the circuit would allow more additional PV than adding it at the end.

6.3.4 Feeder 4

Feeder 4 serves almost entirely small industrial loads. It is 7.2 miles long and operates at 12.47 kV. Feeder loading ranges from about 500kW to 1.1 MW. The feeder has a single 5.5 MW solar PV plant located approximately midway along the feeder on a lateral. The feeder has no voltage regulation equipment installed.

6.3.4.1 Modeling

As with the other feeders, validated models of Feeder 4 were developed in both RTDS and OpenDSS, with a one-rack reduced model in RTDS. The feeder was split into 8 line sections and 5 lumped loads at the first six sections. The 5.5 MW PV plant is located 3.42 miles from substation. Being essentially 100% industrial, the loads could be considered all constant power for modeling purposes.

6.3.4.2 Voltage profile analysis

The minimum and maximum voltage profiles on Feeder 4 from a one-week OpenDSS simulation are shown in Figure 6-16. Voltages exceeding the ANSI limit are observed in the vicinity of the PV plant PCC about 1/3 of the way down the circuit.

To observe and analyze voltage profile on the system for various amounts of PV penetration, PV penetration on the feeder was varied from 0-10 MW. Three different loading scenarios were used, low load (0.5 MVA), average load (1 MVA) and high load (1.5 MVA). For all cases, PV system was set to inject real power only.

Figures 6-17 and 6-18 show voltage profiles on the feeder for low and high loading scenarios for various levels of PV penetration. Since the load is industrial and does not vary much relative to the amount of PV on this feeder, the slightly high voltage in the vicinity of the PV plant is present at all load levels.

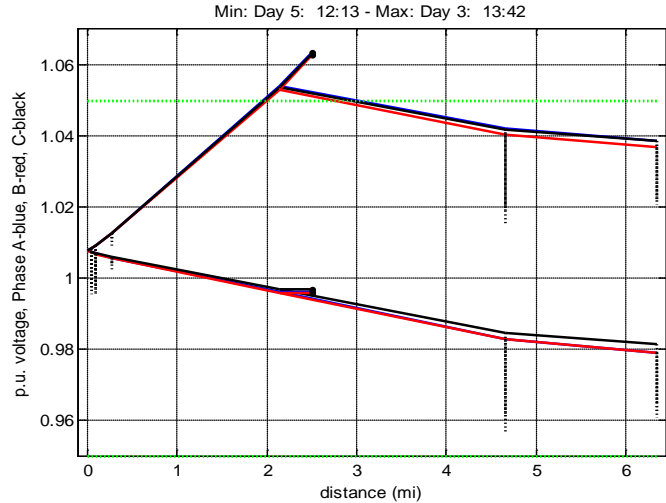


Figure 6-16. Feeder 4 min, max voltage profiles, 1 week

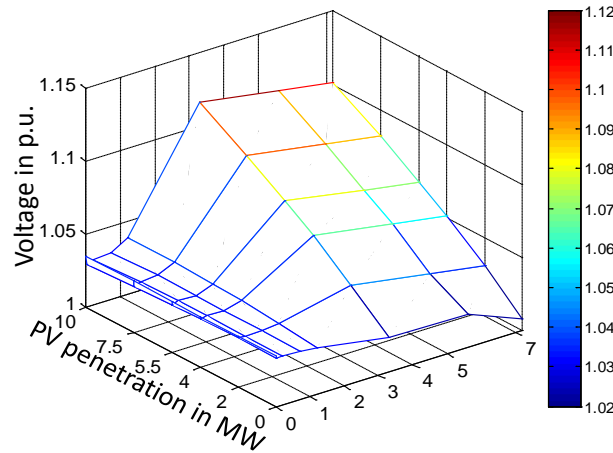


Figure 6-17. Feeder 4 voltage profiles vs. PV penetration, low loading.

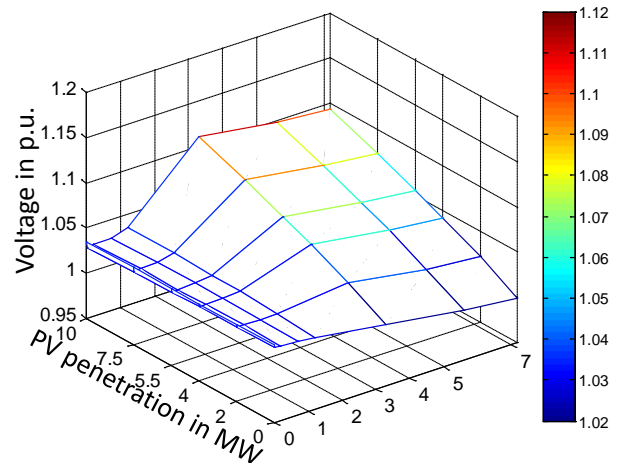


Figure 6-18. Feeder 4 voltage profiles vs. PV penetration, high loading.

6.4 References

- [1] R. Meeker, "Understanding and Addressing High-Penetration PV Issues Through Analysis of PV Integration in Florida Utility Circuits," in DOE, EPRI, SNL, NREL Workshop: Achieving High Penetrations of PV: Streamlining Interconnection and Managing Variability in a Utility Distribution System, Solar Power International 2012, Orlando, FL, 2012.
- [2] "Simulation Tool – OpenDSS", <http://smartgrid.epri.com/SimulationTool.aspx>

7 DISTRIBUTION FEEDER REGULATION AND CONTROL

7.1 Simulation-Assisted Voltage Control Studies

7.1.1 Introduction and Current Practice

Factors that influence the feeder voltage include size and location of PV plants and the loads, intermittency of the PV power injection, feeder characteristics including conductor sizing, substation source impedance, presence, location, and configuration of conventional voltage regulation devices, and voltage control technologies used in the inverters for PV interconnection.

ANSI C84.1 defines voltage limits at the point of service connection to the customer premise and at the point of utilization. Two ranges are provided (Table 7-1). Range A limits are where voltage should normally be maintained. Voltage excursions within Range B limits are allowed for short periods of time while regulation and control actions are taken to bring voltage back into Range A. Suppliers of utilization equipment, then, must ensure equipment works properly for voltages within Range B.

Table 7-1. 120V limits according to ANSIC84.1-1995

120V Level	Service Voltage		Utilization Voltage	
	Min.	Max.	Min.	Max.
Range A	114 (-5%)	126(+5%)	110(-8.3%)	125(+4.2%)
Range B	110(-8.3%)	127(+5.8%)	106(-11.7%)	127(+5.8%)

In general, a distribution network's voltage regulation devices adjust the primary voltage of the feeder and thus maintain the voltage within acceptable limits. Current voltage regulation techniques typically employ On-Load Tap-Changing transformers (OLTC), Step Voltage Regulators (SVR), and Switched Capacitor Banks (SCB) to control the voltage [8]. The usual practice is to use OLTC in the first step of voltage regulation at a substation bus and then use SVR and/or SCBs as needed. Most distribution networks are radial systems designed for unidirectional power flows, and, the current regulating equipment is sufficient to control the voltage. However, as Distributed Generators (DG), such as PV plants, inject power into the system, bidirectional power flows may arise in distribution feeders. This warrants a re-evaluation of voltage regulation devices, settings, and control schemes for these circumstances.

Following is a brief description of these common distribution system voltage regulation devices:

- 1) On-Load Tap Changing Transformer (OLTC)- An OLTC is a distribution power transformer which is capable of changing its output voltage by changing its tap position. It is usually installed at distribution substation. Typical regulation limits are in the range of $\pm 10\%$. It can operate usually in three modes, i.e., Type L (linear), Type R (change over selector), and Type D (fine switching). OLTCs are available with different operating time characteristics.
- 2) Step Voltage Regulator (SVR) - SVRs are usually autotransformers with adjusting taps. Commonly available SVR's have a regulation limit of $\pm 10\%$ in 32 steps. SVR's are used on feeders on which a large voltage drop is expected or on laterals with commercial/industrial loads and on long feeders serving remote loads [9].
- 3) Switched Capacitor Bank (SCB) – SCBs are arrays of capacitor banks, used for supplying leading VAR to boost the voltage in undervoltage situations. Capacitor banks are installed at the substation bus or along the feeder or at a utilization end close to a large inductive load. Various control modes like voltage, time, temperature, power factor correction or a combination of modes, are used.

7.1.2 Future Trends

Relevant standards, including IEEE 1547 and California Rule 21 are being updated to permit solar PV participation in voltage regulation. An amendment to IEEE 1547 has been approved that allows PV participation in regulation in coordination and cooperation with the utility. California Rule 21 is currently in the process of being updated to prescribe the range of capabilities expected in smart inverters and

addressed in considerable detail an integrated approach to solar PV, considering overall integration with system for real and reactive power needs (voltage control).

7.1.3 PV Inverter Voltage Regulation Methods

Various methods exist for PV inverter voltage regulation, including constant power factor, constant reactive power, voltage set point, volt-var curve, volt-pf curve, and German voltage standard curve. Figure 7-1 shows the curves along with some reasonable limits a few of the “curve” methods. The limits may often be configurable in practice.

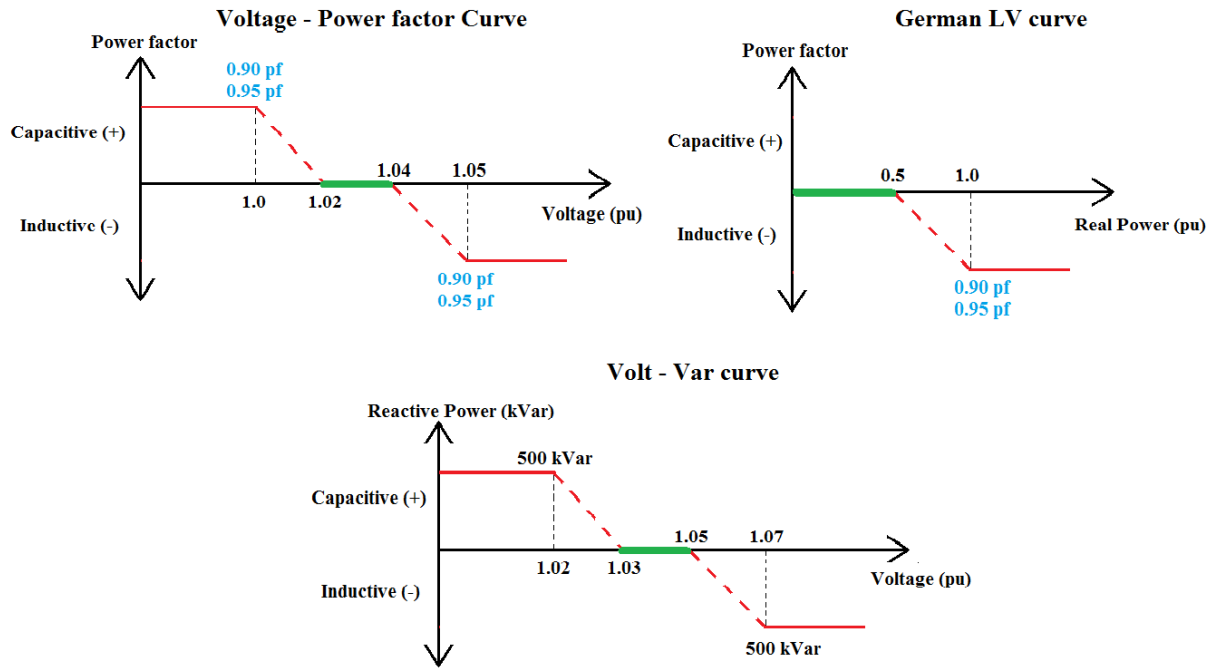


Figure 1 Voltage regulation curve limits

7.1.4 Voltage Regulation Studies with the Florida Feeders

Simulation-assisted studies have been performed for all four feeders, both with the RTDS models and the OpenDSS models to examine impact of PV on traditional regulation devices and benefits of PV participating in regulation.

7.1.5 Feeder 1

Feeder 1 has no regulation devices and voltage remains in limits at current loads and very high PV penetration. To examine regulation on this circuit, modifications were made to the RTDS and OpenDSS models to include regulation and loading beyond the norm.

In the RTDS model, an OLTC and an SCB were added.

An OLTC was added to the distribution transformer and was set to operate in fine switching mode with a regulation limit of $\pm 10\%$ with 32 steps with each step having a regulation of 0.00625 pu of voltage, and with a 30 sec. on-delay timer upon limits being exceeded and a 1 sec. delays between successive tap changes.. The OLTC was set to regulate the voltage near the PV plant, which is approximately 4.8 miles from the substation, with an operation upper limit of 1.03 pu and lower limit of 0.97 pu.

A capacitor bank was added to the feeder at the same location as the PV plant, configured to operate in 8 equal steps with an overall rating of 6 MVA. It operates in voltage control mode and a linear switching

method was used with voltage setpoints of 1.03 pu and 0.97 pu. Each step change is followed by a 5 s delay before additional decisions are made.

For purposes of the study, an arbitrary load profile was produced with a peak load of 15.5 MVA (far in excess of normal peak loads on the circuit, but within the actual transformer rating, so, not entirely infeasible). Each section of the reduced feeder model has load modeled as a mixture of constant impedance (50%), constant power (25%), and induction motors (25%). Around 60% of load is distributed between the substation and PV plant and the rest is between the PV plant and end of the feeder.

The solar PV plant is modeled through controllable voltage sources with proportional-integral controls for magnitude and relative phase angle [14]. The controls have been tuned to achieve short settling times using the full-circuit model with varying loading and solar power injection levels and steps. The 3-phase voltage sources inject balanced voltages and do not include switching-level details.

For studies where PV is allowed to participate in regulation, the PV system can be either set to operate in real power priority mode (P-priority) or reactive power priority mode (Q-priority). For P-priority mode, the model injects all the real power generated by the PV and depending on the inverter rating, the remaining capacity is used for reactive power injection. Similarly, in reactive power priority mode, reactive power from the PV gets the preference over real power. For our case studies, the real power priority was used. Voltage regulation can be set to operate on droop control mode, voltage mode, power factor correction mode, and reactive power supply mode. Voltage control mode is used in this case, based on controlling to a voltage set point at the PV plant PCC location.

7.1.5.1 RTDS Simulation Cases

Two separate cases (large concentrated PV and distributed PV) were built to analyze the interactions of voltage regulation equipment. The first case has the single 12.6 MW PV plant about 4.8 miles from the substation, as exists on the actual feeder. The second case has the PV plant split equally into six (6) 2.15 MW PV plants located at the six (6) load points. For the distributed case, the PV power profile is shifted by 3 min for each consecutive PV plant to provide some simple representation of the effect of moving clouds.

For both cases a common load profile and PV power profile were used as inputs. 1-minute data from another Florida PV plant, scaled to the Feeder 1 PV plant capacity, was used for the PV output profile (only 15-minute data was available for the actual Feeder 1 PV plant). Figure 7-2 shows the scaled PV power profile for a one hour period from July 1 2010, and Figure 7-3 shows the load profile, with an intentionally large load swing to aid in comparing regulation effectiveness and impact.

For each case, several simulation scenarios were performed to see the interaction of voltage regulation equipment operation. The base simulation case is designed to observe feeder voltage with PV plant active and no voltage regulation equipment present. The subsequent cases focus on the independent operation of OLTC, capacitor bank and PV reactive power

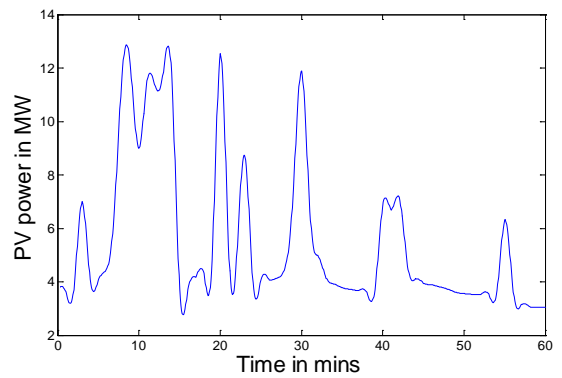


Figure 7-2. PV profile

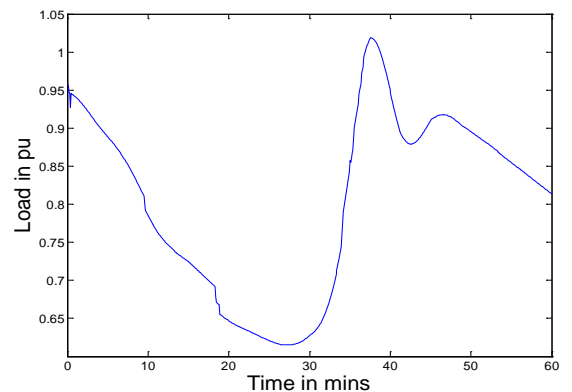


Figure 7-3. Load profile

support scenarios for the same PV profile and load profile. A final scenario focuses on the employment of all three voltage regulation approaches at the same time.

7.1.5.1.1 Case 1-Large PV plant

For the assumed PV power input and load profile show in Figures 7-2 and 7-3, the feeder voltage profile without any regulation is shown in Figure 7-4. The extreme load swing causes voltage to dip below the service limit of 0.95pu about 38 sec. into the simulation.

As shown in Figure 7-5, if an OLTC is added in the simulation run, operating based on voltage in the vicinity of the PV plant, it is cable of raising the voltage back in range (only requiring one tap change operation, which happens to occur at the beginning of the simulation run due to the initial voltage and the load trajectory). If regulation is achieved with the SCB instead of an OLTC, it is similarly effective, with two SCB operations occurring during the 60 min.'s. the mid-point of the feeder (4.8 miles from the substation) goes out of the range (1.03pu and 0.97pu).

Figure 7-6 shows the result if the PV plant is given the task of regulating voltage. For this simulation run, the PV plant was the only regulation equipment. It was set to operate in voltage control mode (1 pu at the PCC) by supplying reactive power as required, with real power priority and the aggregate rating of all the plant inverters set to 13MVA. With real power priority mode, real power is given first priority and the remaining capacity is used for reactive power support. It can be seen the substantially improved voltage regulation possible with the PV plant participating.

In this particular case, if the OLTC and SCB are also activated in the simulation, while PV is allowed to regulate, there are no OLTC or SCB operations, because, the PV never allows the voltage to reach the limits at which the OLTC or SCB would activate. So, the response would be identical to Figure n.

7.1.5.1.2 Case 2-Distributed PV plant

For the distributed PV case, the results for regulation with an OLTC and an SCB are similar to the central PV case, only with a few more

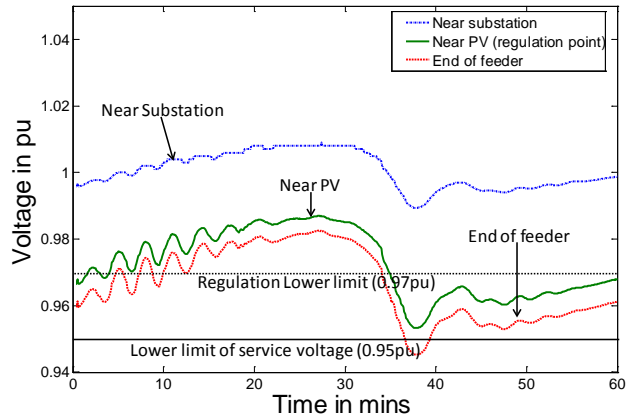


Figure 7-4. Feeder 1 simulated voltage profile, extreme load, no regulation

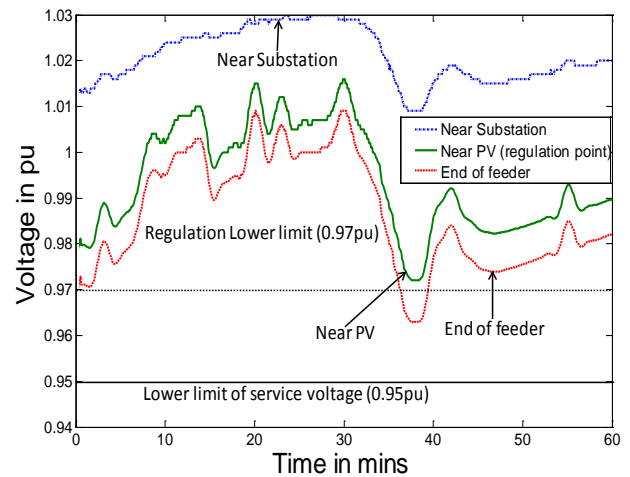


Figure 7-5. Feeder 1 simulated voltage profile, with OLTC regulation

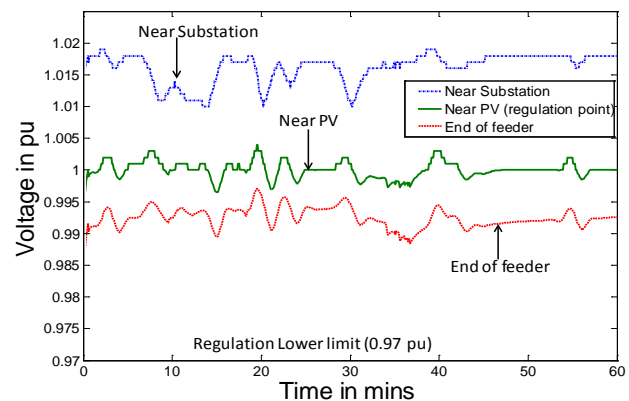


Figure 7-6. Feeder 1 simulated voltage profile, extreme load, PV regulation of voltage

operations of the OLTC or SCB. When PV is allowed to regulate, in the distributed case, based on voltage on the secondary of the transformer at the PCC, there is more of a tendency for oscillation due to interaction and voltage drifting high due to the inverters operating in real power priority mode.

Figure 7-7 shows regulation with PV only in this case, where voltage lingers towards the high limit, with some oscillation, due to the reactive power limits and real power priority. Real power injection was very close to the inverter maximum rating which brought down the reactive power injection capability close to zero.

Figure 7-8 shows PV regulation in combination with an OLTC and SCB. In this case there is interaction between the PV and the OLTC, because voltage does drift high enough repeatedly to cause a tap change until the tap changer reaches its low limit (Figure q). PV will perform better at raising voltage, i.e. as the voltage stays well below the limit, e.g. for the higher load, and, the OLTC may stay at its low limit for a protracted period of time.

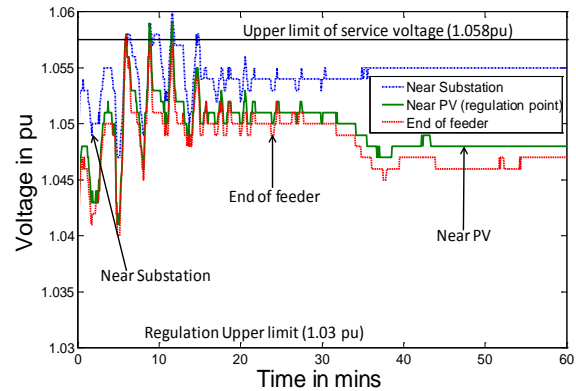


Figure 7-7. Voltage profile on the primary with PV controlling the voltage

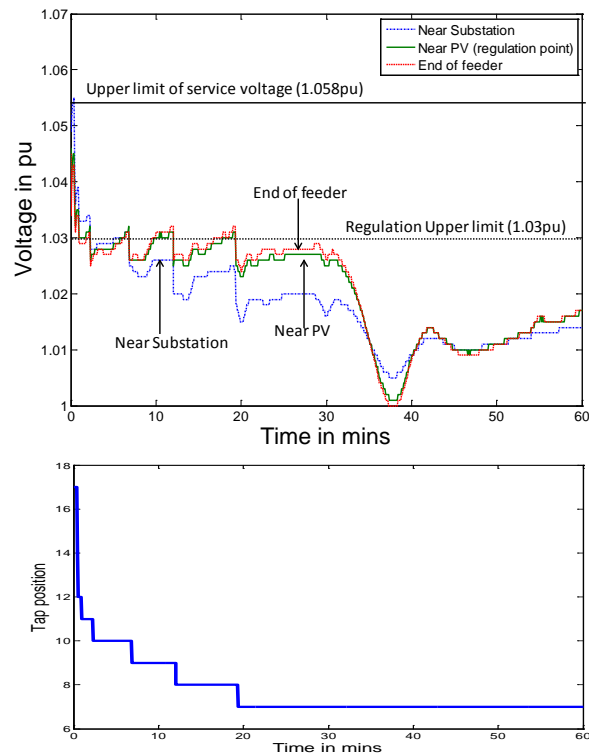


Figure 7-8. Voltage profile and OLTC tap positions when PV, OLTC, and SCB are allowed to control voltage.

Thus to minimize the over-voltage on some locations of the feeder, a coordinated voltage control method was simulated, where voltage setpoints on the PV plants are staggered, within the acceptable range of operation, depending on location. The plant nearest to the substation may be controlled for 1.0 pu voltage and gradually the reference voltage will be smaller with the increase of distance from the substation. To investigate this concept, the following regulation scheme was set: the first 2 PV systems are set to regulate voltage to 0.98 pu, the next two to 0.9775 pu and the last two systems to 0.975 pu. There was still oscillation, possible interaction between PV plants in this case, but, voltage did not go high. Oversizing the inverters (in simulation) to allow more reactive power capacity was found to smooth the oscillations. More thorough and methodical investigation into the system dynamics, particularly with multiple inverters, is needed.

For this particular case, for a single large PV plant, the number of operations of the OLTC might be reduced, however, for distributed PV plants with voltage control features enabled, frequent operation of the OLTC could be observed if inverters are allowed to operate at their maximum rating. Allowing them to operate at a slightly lower value could minimize the number of operations of other

conventional regulators including OLTC. Operation of voltage regulating equipment for a large PV plant may be different from that of distributed PV plants. A coordinated voltage control approach may be appropriate where the setpoints are staggered across distributed PV plants.

Since many possible control strategies are possible if the PV inverter is allowed to participate in regulation, it is useful to utilize feeder simulations to compare the performance of various methods. For Feeder 1, this was done using the three (3) scenarios from within a 60-minute PV and load profile time series as shown in Figure 7-9 (same load profile as used in the preceding simulation runs).

Figure 7-10 shows how a number of different methods compare for scenario 1. Perhaps more instructive is to examine the total apparent power requirement of the inverters for each method and the impact on the operation of existing regulation devices. As can be seen in Table 7-2, there are considerable differences in the inverter capacity consumed for each method. As shown in Table 7-3,

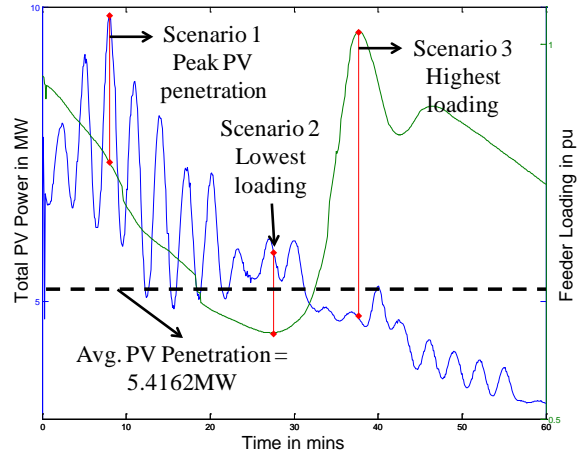


Figure 7-9. Feeder 1 PV and load profile for comparing PV regulation methods

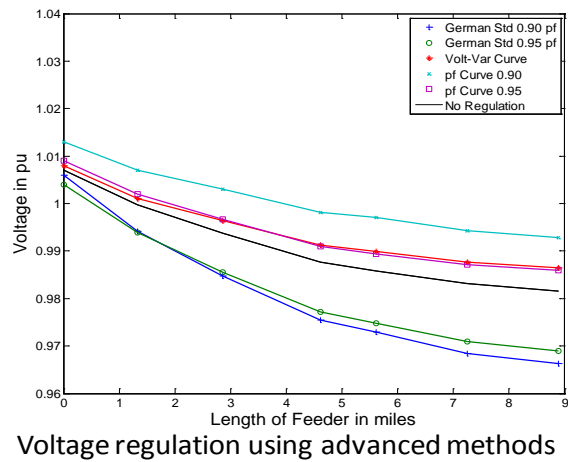
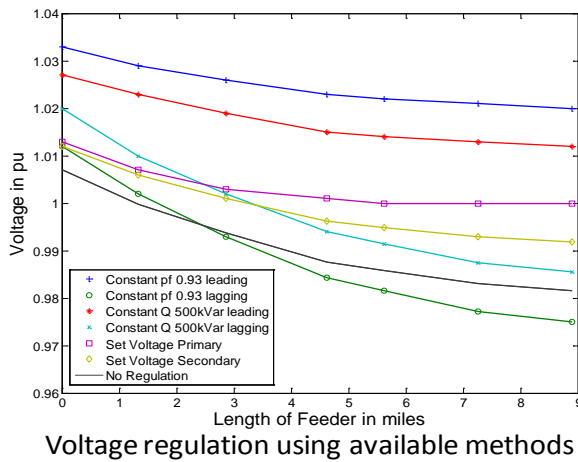


Figure 7-10. Feeder 1 simulated voltage profiles for different PV inverter voltage control schemes.

there are also significant differences in the numbers of OLTC and SCB operations. In this particular case, it is shown that either the volt-VAR curve or PF curve method would appear to be most economical.

Table 7-2. Feeder Inverter loading for different PV regulation methods

Voltage Regulation Mode	S of Inverter (% of 2.15MVA)						Avg. Change
	Inv 1	Inv 2	Inv 3	Inv 4	Inv 5	Inv 6	
No Regulation	45.37	44.94	44.19	41.96	39.22	36.37	
Constant pf - 0.93 Leading	48.78	48.32	47.51	45.12	42.17	39.11	3.16%
Constant pf - 0.93 Lagging	48.77	48.36	47.50	45.12	42.11	39.08	3.15%
Constant Q - 500kVar Leading	50.97	50.58	49.95	48.00	45.54	43.19	6.03%
Constant Q - 500kVar Lagging	50.96	50.60	49.94	48.02	45.57	43.21	6.04%
1 pu Set Voltage – Primary	96.57	95.69	52.54	72.21	77.70	78.34	36.83%
1 pu Set Voltage – Secondary	48.25	45.21	45.18	43.85	43.15	41.92	2.59%
German std - 0.90 pf	45.99	45.57	44.80	42.43	39.43	36.51	0.45%
German std - 0.95 pf	45.67	45.24	44.49	42.18	39.27	36.41	0.2%
Volt – Var Curve	45.40	44.96	44.37	42.29	39.80	37.33	0.35%
pf curve - 0.90	45.49	44.94	44.19	41.95	39.23	36.48	0.04%
Pf curve - 0.95	45.38	45.00	44.32	42.20	39.53	36.70	0.18%

Table 7-3. Feeder 1 simulated OLTC, SCB operation for different PV regulation methods

Voltage Regulation Mode	OLTC Operation	SCB Operation
No Regulation	NO	YES - 2
Constant pf - 0.93 Leading	NO	NO
Constant pf - 0.93 Lagging	NO	YES - 1
Constant Q - 500kVar Leading	NO	NO
Constant Q - 500kVar Lagging	YES - 5	YES - 1
1 pu Set Voltage – Primary	YES - 1	NO
1 pu Set Voltage – Secondary	YES - 5	NO
German std - 0.90 pf	YES - 2	NO
German std - 0.95 pf	YES - 2	NO
Volt – Var Curve	NO	NO
pf curve - 0.90	NO	NO
Pf curve - 0.95	NO	NO

7.1.6 Feeder 2

Recalling from Section 6, Feeder 2 actually has periods of high voltage under current conditions. Several one hour cases were simulated with PV systems regulating voltage to observe the interactions between devices.

Figure 7-11 shows Feeder 2 voltage profiles for various PV penetration levels at low load. Figure 7-12 shows voltage profiles if the current SCB control strategy, based on reactive power flow at the substation is changed to operate, instead, on a combination of real and reactive power flow. By merely modifying

the control strategy for the existing regulation devices, it is likely more PV can be accommodated on the Feeder 2 circuit, at least, based on voltage control alone.

As was done for Feeder 1, it is useful to examine PV participation in voltage regulation. For the simulations performed, all PV systems were aggregated to one unit. The loading on the feeder occurred on 5/14/2012 from 4.00 P.M. to 5.00 P.M. The cap banks (3 – 900 kVar, 1 – 600 kVar) are set based to operate on MVar flow from substation as indicated by the utility. If MVAR flow into feeder is greater than 600 kVar, based on priority, a capacitor bank is turned ON and if VAR flow is greater than 300 kVar to substation, a capacitor bank is turned OFF. The SVR is set to operate with a regulation of $\pm 10\%$ regulation with 32 steps with a 2 minute operation time. The regulator operates with a lower limit of 1.02 p.u. and an upper limit of 1.066 p.u. Actual load and PV data for the selected one-hour period are used.

Table 7-4 shows the average reactive power of PV inverters for different methods of voltage regulation. It can be seen that almost every method of voltage regulation required at least 10% of the inverter's capacity. The worst case regulation mode was the set point voltage regulation mode regulating on the secondary which required the most reactive power since the voltage on the feeder was high and a lot of inductive reactive power was required to bring down the voltage to 1 p.u.

Table 7-5 shows the interactions between SCB, SVR and PV inverter. It can be seen that the no regulation case required 2 cap bank operation and 1 regulator operation on phase B. Most voltage regulation modes required either the operation of capacitor banks or the step voltage regulator.

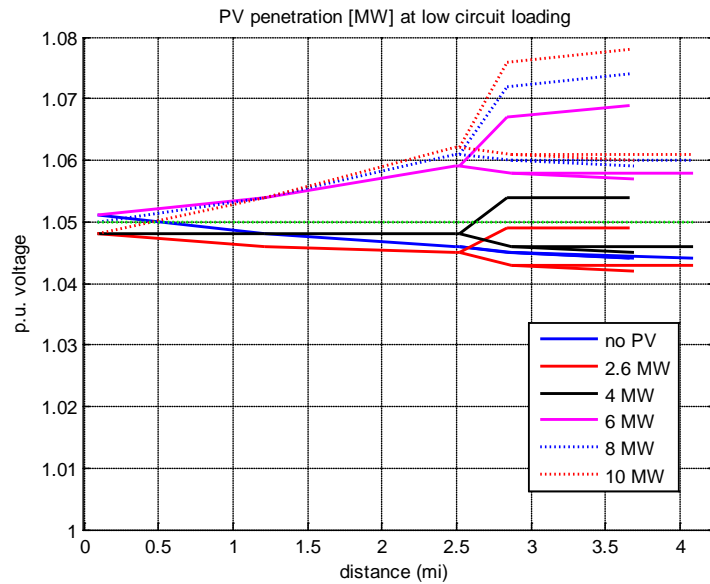


Figure 7-11. Feeder 2 voltage profile vs. PV penetration, low loading, existing SCB control

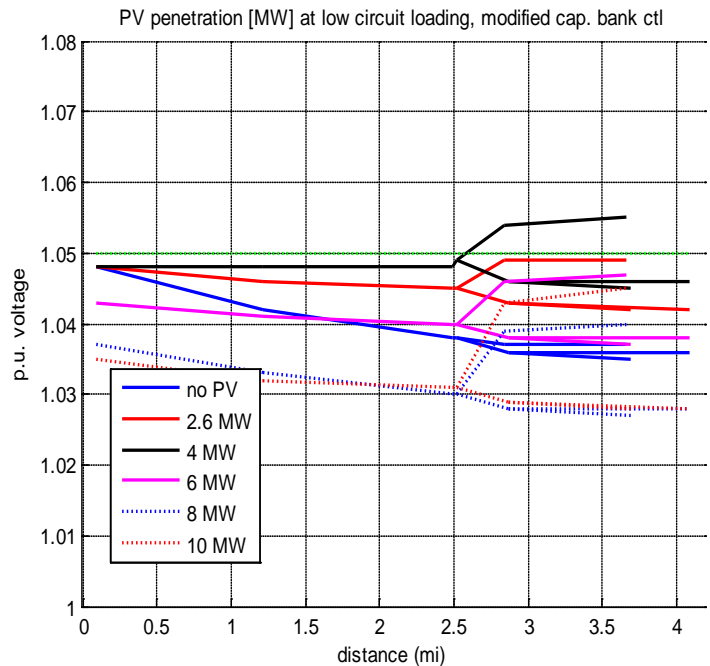


Figure 7-12. Feeder 2 voltage profile vs. PV penetration, low loading, modified SCB control

Table 7-4. Feeder 2, inverter capacity used for different PV regulation methods

Voltage Regulation Mode	Reactive power output (Mvar)	Average Inverter loading (% of 2.6 MVA)	Average change in Inverter loading (%)
No Regulation	0.0	75.82	
Constant pf - 0.93 Leading	0.7189	91.63	15.81
Constant pf - 0.93 Lagging	0.7189	91.65	15.83
Constant Q - 400kVar Leading	0.3996	87.42	11.6
Constant Q - 400kVar Lagging	0.400	87.37	11.55
1 pu Set Voltage – Primary	0.4389	87.75	11.93
1 pu Set Voltage – Secondary	1.2794	100.0	24.18
German std - 0.90 pf	0.6083	90.24	14.42
German std - 0.95 pf	0.4354	87.87	12.05
Volt – Var Curve	0.1907	86.27	10.45
pf curve - 0.90	0.2767	86.01	10.19
Pf curve - 0.95	0.2282	85.77	9.95

Table 7-5. Operation of OLTC and SCB for various PV voltage regulation methods for Feeder 2

Voltage Regulation Mode	No. of Capacitor Banks ON	SVR Operation		
		Ph A	Ph B	Ph C
No Regulation	2	0	1	0
Constant pf - 0.93 Leading	1	0	1	0
Constant pf - 0.93 Lagging	3	0	0	0
Constant Q - 400kVar Leading	2	0	1	0
Constant Q - 400kVar Lagging	3	0	0	0
1 pu Set Voltage – Primary	3	0	1	0
1 pu Set Voltage – Secondary	4	1	1	1
German std - 0.90 pf	3	0	1	0
German std - 0.95 pf	2	0	1	0
Volt – Var Curve	2	0	1	0
pf curve - 0.90	2	0	1	0
Pf curve - 0.95	2	0	1	0

7.1.7 Feeder 3

Adding very high penetration to Feeder 3 provides an additional look at the interplay and trade-offs between PV participation in regulation and traditional regulation devices. In this case, the Feeder 3 PV plant in the RTDS model is increased in capacity from 2.3 MW to 10 MW, with a high variability profile (selected from actual data) over a one hour simulation time. This intentionally causes a high voltage condition along the last mile and a half of the feeder, to the highest voltage out where the PV plant is located.

The base case (Figure 7-13) is with the feeder's existing regulation strategy, using SCB's switched based on power factor at the substation. In this case, the SCB's do not operate and voltage exceeds the limits multiple times during the course of the hour along the last mile or so of the feeder. In the second case, Figure 7-14, the SCB control strategy is modified to be based on voltage at the PV site. In this case, feeder voltage remains in limits, while the SCB's switch 8 times during the hour. In the third case, Figure 7-15, PV is allowed to participate in voltage regulation using the volt-VAR curve method, and SCB control is left as it currently is (in the base case). This results in very good voltage regulation, but 4 SCB operations. Finally, in the fourth case, Figure 7-16, SCB's are disabled, and PV controls voltage using the volt-VAR curve. Regulation is still good, and there are no SCB operations. A longer term study would help determine if the SCB's could be eliminated altogether by allowing PV participation in regulation.

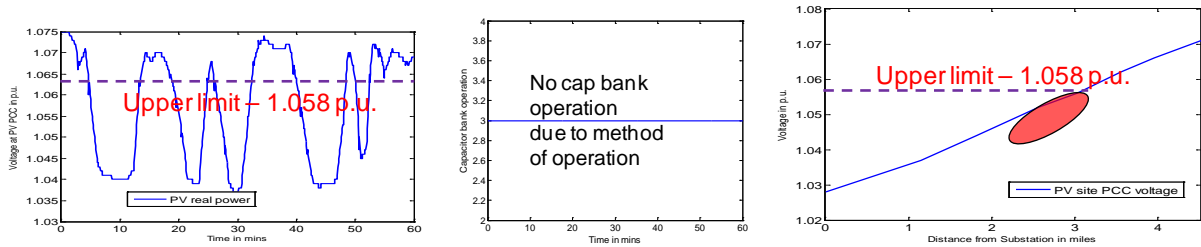


Figure 7-13. Feeder 3 voltage regulation, base case – current SCB control strategy

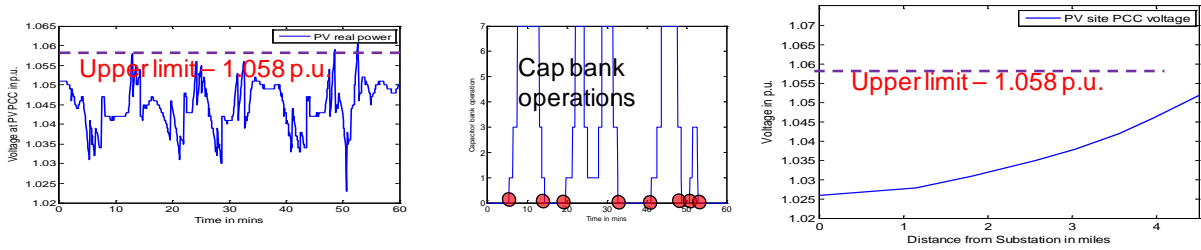


Figure 7-14. Feeder 3 voltage regulation, modified SCB control strategy

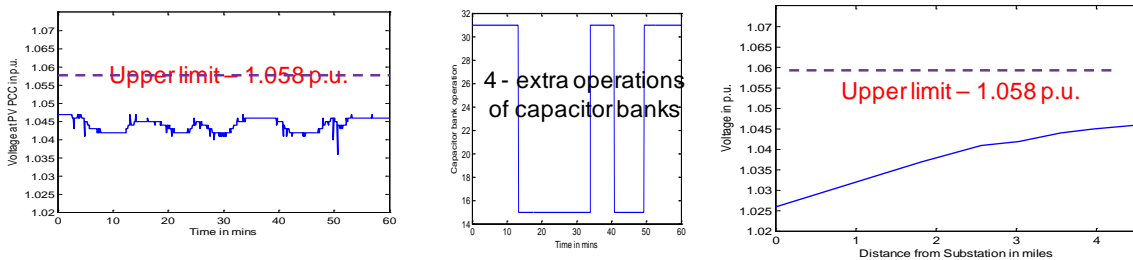


Figure 7-15. Feeder 3 voltage regulation, PV volt-VAR curve regulation and SCB base case control strategy

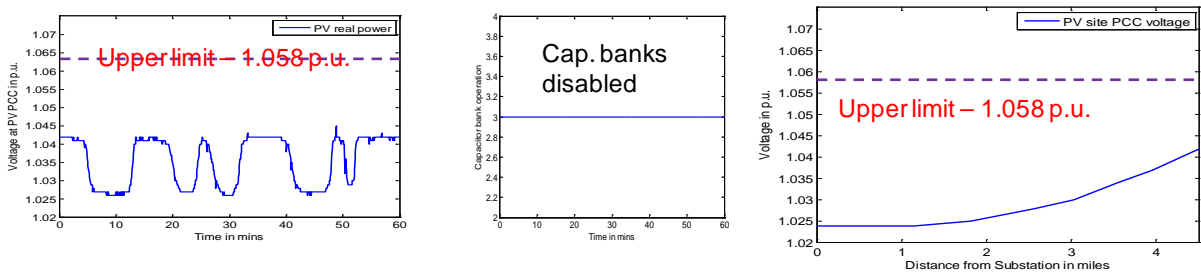


Figure 7-16. Feeder 3 voltage regulation, PV volt-VAR curve regulation only – SCB's disabled

7.1.8 Feeder 4

Using the RTDS model and actual PV and load profiles, several cases were examined for Feeder 4 with different PV voltage regulation techniques. Like Feeder 1, there are no existing voltage regulation devices on the feeder. In this case, we consider just the case of PV inverter participation in regulation, comparing a variety of methods under different instantaneous PV penetration and circuit loading conditions for a cloudy day and a sunny day.

Figures 7-17 and 7-18 show voltage profiles using various control methods for the high and low loading conditions, respectively, on the cloudy day. Comparing to the studies for the other feeders, it is apparent that the best choice depends upon the circuit, but, it is also evident that the best choice also depends on the particular conditions – high loading, low loading, cloudy day, sunny day. Also, it is apparent that for some methods, no regulation is actually better.

Table 7-6 compares the impact of the different PV regulation methods on inverter capacity, for Feeder 4. By this measure, the volt-VAR curve method is most economical.

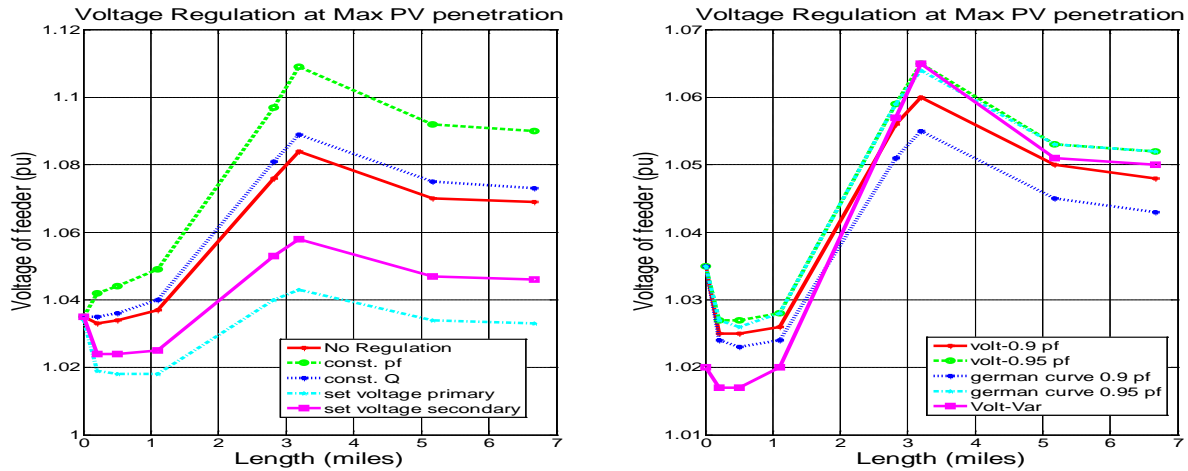


Figure 7-17. Voltage profile of feeder for scenario 1 at highest PV penetration

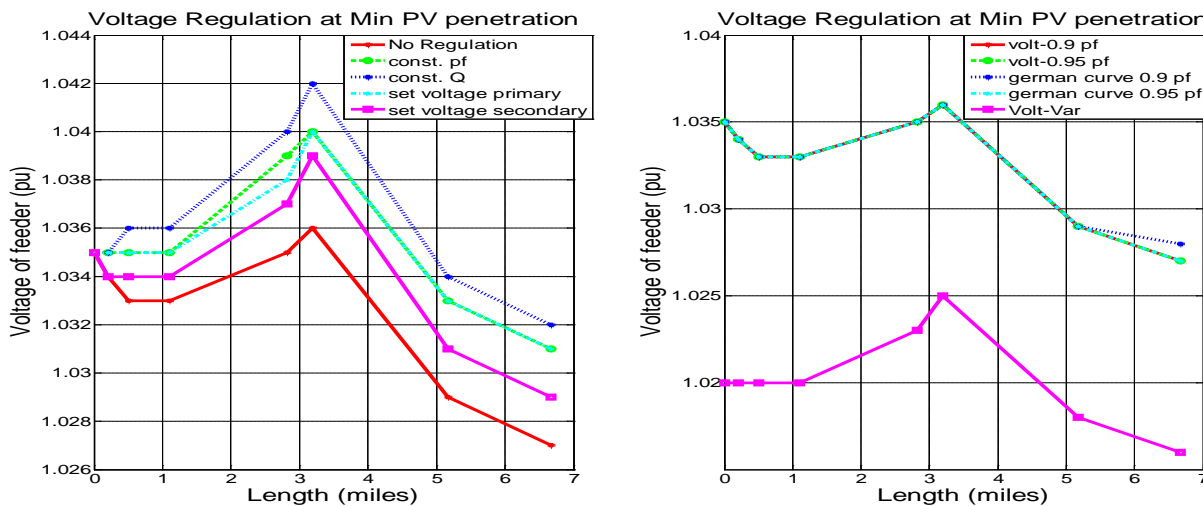


Figure 7-18.2 Voltage profile of feeder for scenario 2 at lowest loading

Table 7-6. Change in inverter output for various PV voltage regulation methods

Method of Regulation	Min. PV Inverter Loading (%)	Max. PV Inverter Loading (%)	Average PV Inverter Loading (%)	Change in avg. Inverter loading (%)
No regulation	13.34	87.29	49.55	0
Constant power factor leading	12.02	80.96	46.08	3.47
Constant reactive power leading	11.8	86.73	48.78	0.77
Set voltage on primary	12.27	75.73	43.76	5.79
Set voltage on secondary	12.7	81.6	47.08	2.53
German std. 0.9	13.15	80.55	47.74	1.82
German std. 0.95	13.07	83.82	48.64	0.91
Volt - 0.9 pf curve	12.96	82.65	47.9	1.66
Volt - 0.95 pf curve	13.23	84.06	48.39	1.16
Volt- Var	12.69	86.91	49.39	0.16

7.2 PV SCADA

7.2.1 Solar PV Integration – Current and Historical Practice

Solar PV has been connected to the EPS primarily to offset local load and export excess energy to the EPS (“Net Metering”) or to export the majority of the energy production to the EPS. When solar PV not owned by the electric utility is installed for the purpose of providing the majority of the energy production to the grid, it is normally under a power purchase agreement (PPA) or a feed-in tariff (FIT) program. In these cases, real power production is maximized, with the PV plant usually operating at a power factor of 1. And, in all of these cases, the integration policies employed by the utilities have been a “do no harm” approach that requires solar PV to trip offline on any grid disturbance (such as low voltage) or on detection of a possible EPS island.

Current utility practices for SCADA at the distribution system level vary considerably depending on the size of the utility. Municipal and cooperative utilities often do not have separate distribution management systems (DMS) and energy management systems (EMS), yet, often, completely separate systems are used for volt/VAR management. Communications capabilities are limited, and, where they exist, they often exhibit high latencies due to bandwidth on the types of carriers (e.g. radio or cellular) and signal transmission delays over the long distances associated with electrical circuits.

7.2.2 Solar PV Integration – The Opportunity

DC current and voltage produced by Solar PV is converted for connection to the EPS by power electronics (PE) inverters. The high-speed switching that produces essentially a synthesized AC waveform at the grid connection side of the inverter also inherently provides the capability for very fast, highly-granular control of the AC waveform characteristics, including power factor and frequency. These are fundamental capabilities of solid-state power-electronics switching technology. The extent to which these fundamental capabilities are exploited and reflected in the specifications and capabilities delivered in any particular solar PV inverter is most often governed by economic rather than technical considerations.

Solar PV capacity factors vary between about 11% and 32%, with a typical or average expected value around 25%^{5,6}. Using 25%, then, on an energy basis, 75% of the inverter capacity over time is not utilized. Yet, inverters have the capability to continue to operate to fundamentally alter the waveform at the AC point of connection, whether there is power being produced on the DC side or not. This is, by design, the fundamental capability in Flexible AC Transmission System (FACTS) power electronics devices employed at the transmission system level, along with similar purpose-specific devices, such as distribution-Static VAR Compensators (dSVC's), employed at the distribution system level. So, while solar irradiance is not at the maximum for a given site at any particular time, or, perhaps, even zero, such as at night, a sophisticated piece of equipment is installed and available for grid support, though, currently rarely utilized for that purpose.

Figure 7-19, from a 2.3 MW plant in central Florida, shows a day when PV production is well below capacity for the entire day due to clouds, with multiple regulation device operations occurring (as evidenced by voltage, second trace from the bottom). This is a clear opportunity for PV to participate in regulation.

In fact, there are a range of capabilities being increasingly offered in modern “smart” inverters, including the ability to “ride through” system faults or disturbances (such as voltage or frequency), curtail real power production, connect/disconnect from the system, and, as mentioned, participate in volt/VAR support. When a “smart” inverter becomes part of a “smart” grid, then overall system performance and reliability can potentially be enhanced. This systems-approach is enabled by PV Supervisory Controls and Data Acquisitions (PV-SCADA) systems functionality.

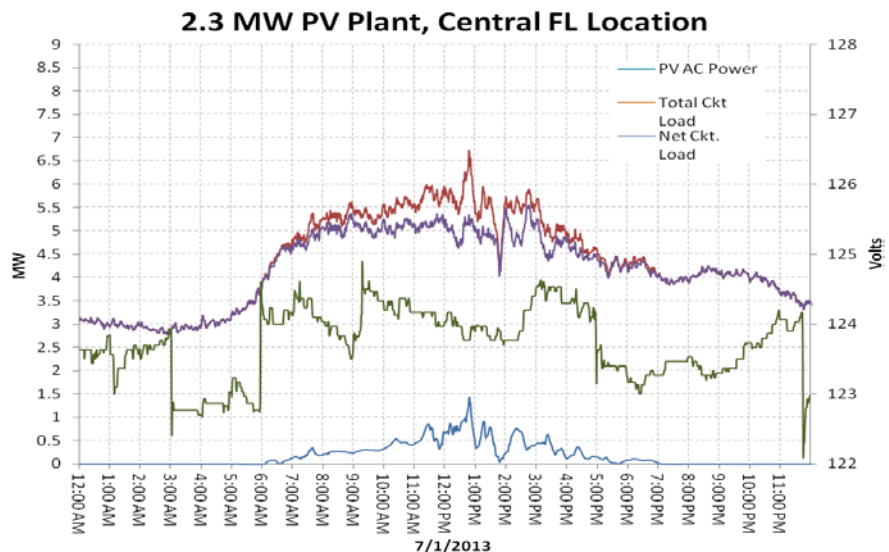


Figure 7-19. Single line diagram of reduced feeder model

7.2.3 Common Control Approaches in “Smart Inverters”

Voltage regulation via distributed inverters has been a topic of analysis and regulatory integration for some time [16]. Although still without tariff support (at least in the US), prescient inverter manufacturers have begun to include standard control methodologies for inverters even in the low kW class. The recognition and expectation of this future capability is also shown by its inclusion in the SunSpec Alliance specifications [17].

PV inverters have inherent capability to supply reactive power and regulate voltage on feeder. This method of regulation is extremely fast (3-5 cycles) compared to traditional distribution system voltage regulation devices like OLTC, SCB and SVR. Some of the methods of voltage regulation that are currently available by various inverter manufactures are as follows:

⁵ http://www.eia.gov/electricity/monthly/epm_table_grapher.cfm?t=epmt_6_07_b

⁶ http://www.eia.gov/forecasts/aeo/pdf/electricity_generation.pdf

7.2.3.1 Constant reactive power mode:

The inverter can be set to supply fixed reactive power. The reactive power can be capacitive or inductive. The inverter operates with real power priority mode in which first priority is given to real power and remaining capacity of the inverter is allotted to reactive power support.

7.2.3.2 Constant power factor mode:

The inverter can be set to maintain a fixed power factor value. The power factor setting can be leading or lagging based on desired voltage profile to be maintained. The inverter operates with real power priority mode in which first priority is given to real power and remaining capacity of the inverter is allotted to reactive power support. The inverter supplies appropriate reactive power so as to maintain requested power factor. But real power curtailment is used to maintain power factor if necessary.

7.2.3.3 Voltage – Reactive Power Curve

A Volt-VAR curve shown in Figure 7-20. Voltage sampling rate can be set as required (10Hz-1000Hz). The reactive power output of inverter is based on a ‘Z’ style curve. There are five distinct regions of operation for the curve. If voltage at point of measurement is less than set point V1 (region 1), it indicates that voltage is well below desired value. Hence, to boost voltage, a fixed leading (capacitive) reactive power is supplied by the inverter.

If voltage lies between set points V1 and V2 (region 2), reactive power generated depends on the slope of the line. . If voltage at point of measurement between set points V2 and V3 (region 3), it denotes that feeder voltage is in desired range of operation and hence no reactive power is required to be generated. Unity power factor will be maintained by inverter when operating in region 3. If voltage at point of measurement between set points V3 and V4 (region 4), it denotes that feeder voltage is slightly above desired range of operation. A lagging (inductive) reactive power based on slope is supplied by the inverter to bring down the voltage. If voltage at point of measurement is beyond set point V4 (region 5), it denotes that feeder voltage is excessively high and a fixed lagging (inductive) reactive power is to be supplied by the inverter. The maximum limits of inverter reactive power can be set based on sizing of inverter and inverter’s capability. The voltage set points can be selected based on an initial assessment of feeder.

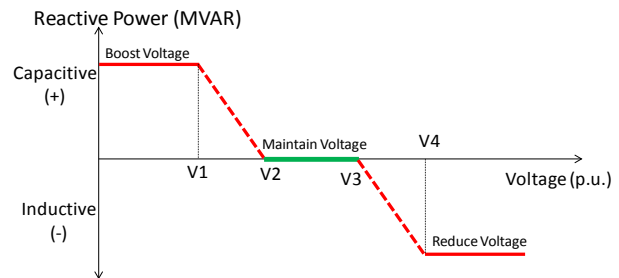


Figure 7-20. Volt-VAR curve

7.2.3.4 Voltage – Power Factor Curve

The Volt-pf curve method of operation is very similar to Volt-VAR curve. Instead of supplying fixed reactive power based on the curve, a fixed power factor is maintained by the inverter. The volt-pf curve is shown in Figure 7-21. Voltage sampling rate can be set as required (10Hz-1000Hz). The reactive power output of inverter is based on a ‘Z’ style curve. There are five distinct regions of operation for the curve. If voltage at point of measurement is less than set point V1 (region 1), it indicates that voltage is well below desired value. Hence, to boost voltage, a leading (capacitive) power factor is to be maintained by the inverter. If voltage lies between set points V1 and V2 (region 2), power factor to be maintained depends on the slope of the line. If voltage at point of measurement between set points V2 and V3 (region 3), it

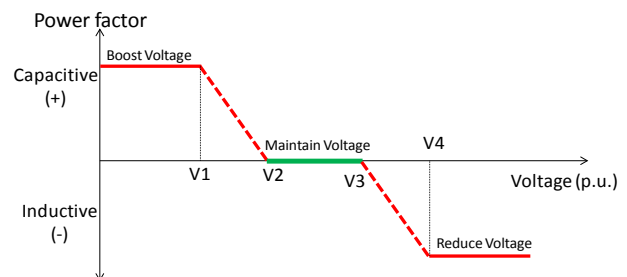


Figure 7-21. Voltage-PF curve

denotes that feeder voltage is in desired range of operation and hence no reactive power is required to be generated. Unity power factor will be maintained by inverter when operating in region 3. If voltage at point of measurement between set points V3 and V4 (region 4), it denotes that feeder voltage is slightly above desired range of operation. A lagging (inductive) power factor based on slope is to be maintained by the inverter to bring down the voltage. If voltage at point of measurement is beyond set point V4 (region 4), it denotes that feeder voltage is excessively high and a fixed lagging (inductive) power factor is to be supplied by the inverter. The power factor limits can be selected based on sizing of inverter and inverter's capability. The voltage set points can be selected based on an initial assessment of feeder.

7.2.3.5 Power-Power Factor Curve

An alternative to voltage-PF offered by inverter manufacturers is a power-PF curve, as shown in Figure 7-22. With this method, the inverter adjusts its power factor dynamically based on per unit power. The way this curve operates is similar to that described for the voltage-PF curve, except the set points are real power not voltage.

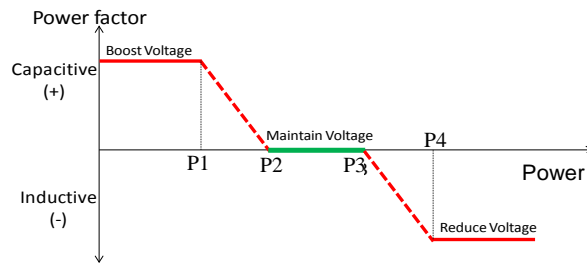


Figure 7-22. Power-PF curve

7.2.3.6 Set point Voltage control mode:

The inverter can be set to maintain the voltage to a fixed value. The inverter can regulate its reactive power output to maintain the fixed voltage.

7.2.3.7 3.5.1 German Low-Voltage Std. Curve

The German low voltage interconnection standard (10 kV – 240 V) requires PV system at point of common coupling to supply reactive power. PV systems are required to generate lagging (inductive) reactive power to account for rise in voltage due to injection of real power. The amount of reactive power required to be supplied is based on a curve shown in Figure 7-23. As long as the inverter real power output is less than 0.5 p.u., power factor is to be maintained at 1 p.u. If the PV real power exceeds 0.5 p.u., a lagging power factor based on the slope is to be maintained. The maximum power factor setting can be either 0.90 or 0.95 p.u. lagging.

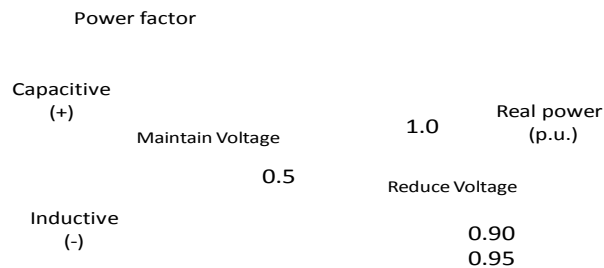


Figure 7-23. German LV Interconnection Std. curve

7.2.4 Testing Inverter Communications and Reactive Power Support in CAPS Lab

Mid-size and larger 3-phase inverters currently on the market have communications capabilities and some built-in regulation options. In the process of HIL testing inverters from 17kAV up to 500 kW in the CAPS lab, there have been opportunities to test and gain experience with communications and inverter feature-sets and functionality.

This capability was tested at the Center for Advanced Power Systems as part of a power-hardware-in-the-loop (PHIL) simulation, using the AC/DC Variable Voltage Source (VVS) under the control of the RTDS simulator, in a method previously described in [18]. Most recently, the relative reactive power of a Fronius CL 60 inverter was controlled via its Modbus card, in out-of-band commands not controlled by the RTDS simulation. A Windows PC was used, running the ModbusTools (RTU) software, and equipped with a USConverters RS232-RS485 converter. The appropriate registers were set manually via Modbus, using the SunSpec-standard ports to first define a Volt-VAR curve, and then to enable that control. After

enabling Volt-VAR control in the inverter, the grid voltage in the simulation (and thereby the emulated grid power bus) was changed under controlled conditions.

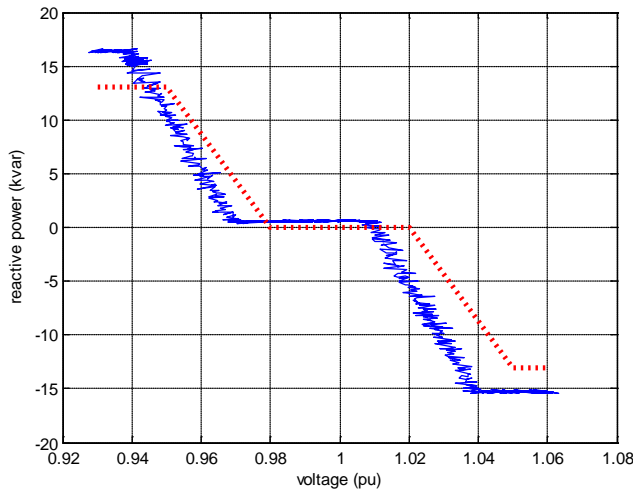


Figure 7-24. Inverter volt_VAR curve response from CHIL test

Figure 7-24 shows a Volt-VAR characteristic curve for commercial 60kW 3-phase inverter in a PHIL simulation at CAPS. The characteristic curve is shown in dotted/red, and measurement results in solid blue. The measurements are taken as 1-second log data, as the system AC voltage was slowly varied; the differences are due to probe inaccuracy.

7.2.5 Strategies and Considerations for Utility-Controlled PV

7.2.5.1 VAR capacity

The amount of VAR exchange (injection or absorption) on a circuit possible from solar PV depends on the installed power capacity, whether or not the PV inverters support volt/VAR control, and, for those that do, the inherent design limitations on the power factor range of

the inverter. As of this writing, the widest range commonly available in smart inverters is a power factor of 0.85 lagging/leading. As a consequence, small systems, such as residential rooftop, can have little impact individually, except on a localized level, in the immediate vicinity of the PV system on the customer side or transformer secondary.

7.2.5.2 Location

For solar PV to be useful in volt/VAR regulation on a circuit, there must be enough installed capacity and in locations where it can have some benefit. PV located where voltage excursions are greatest due to circuit loading and power flow conditions will have the greatest benefit when employed in a regulation scheme.

7.2.5.3 Strategy

There is a question as to which PV systems should be integrated with the utility in a PV-SCADA system. Logical criteria would include some minimum size threshold and location. With respect to location, locations where regulation or some kind of mitigation with traditional devices or system design and construction changes would normally or otherwise be needed might benefit from leveraging solar PV resources for regulation.

With respect to size, there are several reasons why criteria that call for connecting only the larger size plants may be the preferred approach:

Communications cost: If integration of PV is for the purpose of improving operations, the communications and systems integration must be robust, which can be costly. Levelized unit costs (per kW or kVAR) of communications infrastructure will be less for larger systems, compared to having to install and support a sufficiently robust, reliable, high-performance communications network to large numbers of smaller PV systems.

Inverter capabilities: Maximum impact and system benefit will be from larger solar PV installations, and, inverter capabilities will be more extensive for the larger capacity systems as well (at least, that is currently the case).

Complexity: Control strategies and algorithms, as well as maintenance and support, are simpler with fewer connections.

7.2.6 *Communications*

Current utility practices for SCADA at the distribution system level vary considerably depending on the size of the utility. Municipal and cooperative utilities often do not have separate distribution management systems (DMS) and energy management systems (EMS), yet, often, completely separate systems are used for volt/VAR management.

Many utility distribution circuits lack digital communications infrastructure. Communications capabilities are limited, and, where they exist, they often exhibit high latencies due to bandwidth on the types of carriers (e.g. radio or cellular) and signal transmission delays over the long distances associated with electrical circuits.

There is currently no standard approach to communications at the distribution circuit level. Where utilities implement communications at the distribution level, it is often for distribution automation. The most common communications means employed are spread-spectrum radio, cellular, and fiber optic. IEEE 2030.5, which is based on Zigbee wireless standard, is among the likely future standards to be employed for utility-DER, including utility-PV integration at the distribution level.

A promising emerging standard for solar PV integration that has fairly broad industry membership and support is the SunSpec Alliance specifications [17]. This provides standard specifications for communicating with PV inverters, with different options (e.g. MODBUS) possible for the underlying communication layers.

7.2.7 *Control*

Control strategies using PV inverters for regulation may rely on autonomous “smart inverter” controls, where options such power factor or VAR injection curves are activated. Eventually, supervisory control strategies may be employed where regulation options are changed dynamically depending on circuit operation conditions that may vary seasonally, day-to-day, or throughout the day, or actual VAR, power factor, or voltage setpoints are changed continuously by the SCADA system (“immediate” or “direct” control mode).

Some considerations in implementing smart or advanced volt/VAR controls with inverters include:

- Possible dynamic interaction between inverters
- Failsafe operation – shedding from supervisory control to safe local control on loss of communications

7.2.8 *Towards RFP Model Language*

A first step towards a PV-SCADA approach to a greater level of solar PV integration with the EPS and the electric utility is to begin specifying substantial control capabilities in solar PV systems being installed and a communications interface to the utility sufficient for not only monitoring, but supervisory control. Basic tenets are as follows:

- Communications must be reliable so utility-integrated solar PV systems can truly be depended upon in overall system operation and control.
- Control capabilities must be highly configurable and flexible, with provisions for multiple modes of control, and supervisory control changes to modes, configuration settings, and reference values.
- Communications and control systems must employ good cyber-security practices in design and deployment to reduce the possibility of intrusion or compromise.

It would be beneficial to have available model RFP language is on the technical requirements for tighter integration of a solar PV plant or system with the utility. California utilities are likely to accomplish this merely by referencing the updated rule 21, when that process is complete in the coming months. Updated Rule 21 addresses smart inverter functions and communications requirements for integration with the utility. The communications called out are basically IEEE 2030.5, the smart grid communications standard.

7.3 References

- [1] . Liu, J. Bebic, B. Kroposki, J. de Bedout, W. Ren, “Distribution system voltage performance analysis for high –penetration PV,” in Proc. IEEE Energy 2030 Conf., 17-18 November, 2008, pp. 315-320.
- [2] Yang Weidong, Zhou Xia, Xue Feng, “Impacts of Large Scale and High Voltage Level Photovoltaic Penetration on the Security and Stability of Power System”, Power and Energy Engineering Conference (APPEEC), 2010
- [3] IEEE Draft Guide to Conducting Distribution Impact Studies for Distributed Resource Interconnection, IEEE Standard 1547.
- [4] Xiaowei Wang, Jun Gao, Wenping Hu, “ Research of effect on distribution network with penetration of photovoltaic system”, Universities Power Engineering Conference (UPEC), 2010
- [5] F. Katiraei, J. R. Aguero, “Solar PV Integration Challenges”, IEEE Power & Energy Magazine, May/June 2011, pp. 62-71
- [6] ANSI C84.1, “American National Standard for Electric Power Systems and Equipment—Voltage Ratings (60 Hertz)”, 2006
- [7] “Power Distribution Planning Reference Book”, H. Lee Willis
- [8] “Electric Power Distribution Handbook”, T. A. Short, 2004 by CRC Press LLC.
- [9] S. Taniguchi, S. Uemura, “Problems of SVR operation in Large Penetration of Photovoltaic Power Generation and Proposal of Improved Operation”, 21st International Conference on Electricity Distribution
- [10] “Impact of Transient clouds on Utility-Scale PV Fields” EPRI Solar Program Webinar, first published in SOLAR 2010 Conference Proceedings.
- [11] L. Casey, C. Schauder, J. Cleary, M. Ropp, “Advanced Inverters Facilitate High Penetration of Renewable Generation on Medium Voltage Feeders – Impact and Benefits for the Utility”, IEEE Conference on Innovative Technologies for an Efficient and Reliable Electricity Supply, September 2010.
- [12] <http://grouper.ieee.org/groups/scc21/>
- [13] H. W. Dommel, “Digital computer Solution of Electromagnetic Transients in Single and Multi-Phase networks”, *IEEE Trans. On Power Apparatus and Systems*, Vol. 88, No. 4, pp. 388-395, April 1969.
- [14] Feng Li, Wei Li, Feng Xue, Yongjie Fang, Tao Shi, Lingzhi Zhu, “Modeling and Simulation of Large-scale Gridconnected Photovoltaic System”, 2010 International Conference on Power System Technology, Oct 2010
- [15] Tonkoski, R., Lopes, L.A.C., El-Fouly, T.H.M., “Coordinated Active Power Curtailment of Grid Connected PV Inverters for Overvoltage Prevention” IEEE Transactions on Sustainable Energy, Apr. 2011.
- [16] <http://docs.cpuc.ca.gov/PublishedDocs/Efile/G000/M087/K821/87821977.PDF>, “Recommendations for Updating the Technical Requirements for Inverters in Distributed Energy Resources,” January 2014.
- [17] <http://sunspec.org/sunspec-alliance-specifications-4/>, “Open Information Standards for Distributed Energy.”
- [18] J. Langston, K. Schoder, M. Steurer, O. Faruque, J. Hauer, F. Bogdan, R. Bravo, B. Mather, and F. Katiraei. “Power hardware-in-the-loop testing of a 500 kW photovoltaic array inverter”, in IECON 2012 - 38th Annual Conference on IEEE Industrial Electronics Society, pages 4797-4802, Oct 2012.

- [19] A. Hariri, M.O. Faruque, R. Soman, R. Meeker, “Impacts and Interactions of Voltage Regulators on Distribution Networks with High PV Penetration”, North American Power Symposium (NAPS), IEEE 2015.
- [20] H. Ravindra, M.O. Faruque, K. Schoder, M. Steurer, P. McLaren, R. Meeker, “Dynamic Interactions Between Distribution Network Voltage Regulators for Large and Distributed PV Plants”, IEEE Power Engineering Society (PES) Transmission and Distribution Conference and Exposition (T&D), 2012.

8 SUBSTATION PROTECTION

8.1 Overview

Substation protection studies were carried out for two substations supplying utility partner high penetration feeders studied under SUNGRIN. These studies were accomplished by developing detailed models in RTDS from detailed utility-furnished information on the substation electrical layout, equipment ratings, protection schemes, and protection settings. Protection on the feeder, such as fuse coordination and recloser operation, was not considered.

It is also suspected that higher penetration of renewable energy such as PV may require some changes in the traditional protection schemes such as directional (or bi-directional) relaying, communication based transfer trips, pilot signal relaying, and impedance-based fault-protection schemes as [1], [2], [8-13]. Possible issues that have been anticipated include fuse coordination, sympathetic tripping, fault detection, ground source impacts, recloser coordination and conductor burnout when DR penetration is high [3], [15]. Depending on the fault location, the fault current through the protective device (PD) may be changed and a change in the settings of the time-overcurrent relays may be required [1].

8.1.1 Traditional Distribution System Protection

Distribution system protection consists mainly of protection of substation equipment and the feeders serving customers. Generally, it lacks redundancy and various faults can result in the loss of electric power to customers except for critical loads where redundancy is necessary.

Distribution substations generally step down the voltage from transmission level high voltage to medium voltage (4kV- 35kV). The main components of a distribution substation are transmission lines, power transformers, instrument transformers, bus bars, switches, circuit breakers, fuses etc. Appropriate protection schemes need to be employed for all of this equipment and for customer safety. Maintaining a reliable, fault-tolerant and robust system is another objective. Early schemes sought to protect the system from excess current by using relays, reclosers and fuses which respond to phase and residual over-currents and thus protect the distribution systems. Current demand for greater reliability and an increased penetration of Distributed Generation brings the need for distribution systems to be more reliable, with faster protection and control schemes.

8.1.2 Current Practices

Several techniques of protective relay schemes for different equipment include [15], [16]:

I. *Power transformer protection:* Power transformers in the substations can vary from a few MVA's to over a hundred MVA. Internal and external faults and abnormal operating conditions can cause severe damage to transformers. The cost of repair, cost of energy not delivered and possible damage of adjacent equipment can be too expensive and may lead to a system blackout. The transformer protection scheme should disconnect the transformer before extensive damage occurs to the transformer and the power system. Typical faults occurring on a transformer can be classified into winding and thermal faults, core faults, tank and accessory faults, OLTC fault, abnormal operating conditions and uncleared external faults. The transformer protection scheme depends on the application and importance of the transformer. Smaller distribution transformers can be protected satisfactorily by the use of over-current relays. But this method results in time-delayed protection due to downstream co-ordination requirements. Thus the time-delayed approach is not suitable for large or more important power transformers. Differential protection schemes are used for larger power transformers.

II. *Bus bar protection:* Buses are nodes in electric power networks. A bus fault results in opening of all branches connected to that bus. Busbars are left without specific protection, because, 1.) they have a high degree of reliability; and, 2.) accidental operation of busbar protection may cause widespread impact on the power system. Busbar protection is required when system protection does not cover the busbar or

in order to maintain power system stability or when high speed fault clearance is a must. Several types of protection schemes can be applied for busbars: frame-earth protection, differential protection, phase comparison protection, directional blocking protection.

III. *Breaker-Failure protection:* Although transmission systems typically use breaker failure protection, modern distribution systems where fast fault clearance is required employs breaker failure protection. Stability of a power system can be greatly affected if there is a delay in clearing fault due to a breaker failure. Fault clearance time should always be shorter than critical clearing time to preserve transient stability. Depending on the type of fault, the critical fault clearing times can vary according to [1]. Most breaker-failure schemes use phase and ground instantaneous overcurrent elements as fault detectors.

8.1.3 Potential Impacts of PV integration

Typical distribution systems are radial in nature. Distribution feeders typically employ overcurrent protection as the primary method. Protection is based on the principle that power flows from substation to loads and there are no energy sources along the feeder. With the penetration of distributed generation like rotating synchronous generators and new resources like PV and wind systems, new sources of energy are possible and can change fault current paths and magnitudes. Further, these sources can change ground fault current magnitudes which can create problems for operation of overcurrent protection schemes. When DG penetration is low, fault current contributions may not have an effect on the system but with high penetration of DG in the distribution system, changes to the existing power system may be required. Following are the potential issues/concerns raised in different scientific venues [1], [2]:

1. **Increased fault current-** PV and other DG sources would contribute to higher fault current. This may have influence on the existing power system due to increased fault current contribution [1].
2. **Requirement of changes in the rating of protection equipment-** Due to the increased fault current magnitudes with PV fault current contribution, changes in fuse and circuit breaker parameters may be necessary.
3. **Damage of equipment-** The higher fault current may also damage distribution transformers.
4. **Change of fault current flow direction-** PV might create changes in the direction of fault current flows or a new path of fault current
5. **Nuisance trip-** due to the addition of PV, sensitive circuits in another feeder may face sympathetic or nuisance trip of reclosers and circuit breakers.
6. **Desensitization of ground fault scheme-** It may also lead to confusion in automatic switching schemes and can desensitize ground fault protection schemes.

8.2 Substation 1

8.2.1 Substation Overview

Figure 8-1 shows the one line diagram of the local utility distribution substation system used for the study. The substation data was provided by the utility and was modeled in RSCAD environment. The substation is rated at 230kV-24kV level. It has 3 transformers to serve six feeders with different types of loads. The secondary of the transformers (24 kV bus bars) are connected through tie-lines and necessary protective devices. Currently, two Distributed Generation (DG) units (one PV

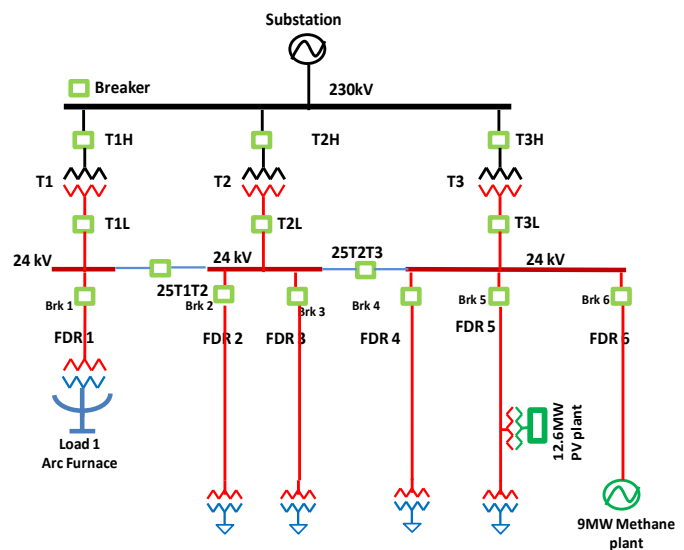


Figure 8-1. Single line diagram of substation 1

and one Bio-gas plant) are connected to feeder 5 and feeder 6. However, in this study, for hypothetical analysis, one scenario would be studied where each feeder will have one PV plant. Transformer T1 has one feeder, FDR 1, which has a steel mill that houses an arc furnace. The steel mill is located next to the substation. Transformer, T2 has 2 feeders FDR 2 and FDR3 which have rural loads on them. Transformer T3 has 3 feeders of which FDR 4 serves rural and commercial loads. FDR 5 has rural loads on it and it also has a 12.6MW PV plant at 4.8miles from the substation. FDR 6 is an express feeder with a 9MW bio-gas plant feeding back to the substation. Table shows the feeder lengths and their characteristics. The substation protective relays consist of overcurrent relays only. The protective relay data and settings were provided by the utility.

8.2.2 Modeling

The 24kV high penetration PV feeder out of the substation hosts a 12.6 MW AC (15 MW DC) PV plant which is connected to a 24 kV feeder was simulated using a real-time transient simulation tool. Since it is a computation intensive tool and it is not practical to model each load separately, total loads of each feeder were carefully represented by 5-8 aggregated loads (instead of the actual load distribution) so that computational burden is minimized. This has been done in such a way that there is very little or no effect on the protective device settings due to the load aggregation. The rationale for using such a tool for this study is that it is very fast and it produces time-domain waveforms at a resolution of several μ s (time-step of the simulation).

The 230 KV substation source was modeled as an infinite source with small series impedance shown in the documents provided by the utility. Transformer ratings, configuration, voltage level, leakage reactance, winding resistance and saturation characteristics were also obtained from the utility and used to model the power transformer in the transient environment.

Typical circuit breaker resistance for medium voltage systems was used to model breakers. The operation time of the circuit breaker was set to 150 ms. Current transformer (CT) and potential transformer (PT) models were added from the library of the simulation programs and were updated with the ratings obtained from the utility.

The built-in RTDS library also includes relays and they were used in the model as required.

The line sections for feeders were modeled as RL branches since the sections were too small to model as lines with distributed parameters.

The loads in the system were modeled as a mixture of constant power and constant impedance type.

Typical distribution transformer data were used to model the service transformers. All loads were connected at 120 V level.

PV system PCC voltage was set to 315 V since that is the output voltage of the inverter. Controllers for each PV inverter were modeled using the DQ control theory so that real and reactive power can be controlled independently. A built-in library model for the 3-phase arc furnace was used which behaves like a non-linear load. The arc length is dynamically varied for each phase at every half cycle using statistical variations. An SVC was also connected with the arc furnace so that harmonics generated by the non-linear furnace can be suppressed. The 9 MW bio-gas plant was modeled as a synchronous generator with typical parameters.

Table 8-1. Feeder data

Feeder No.	Length (miles)	X/R ratio	Max. Loading (MVA)	Max. PV Penetration (MW)
1	Arc Furnace Load (next to substation) – 12 MW			
2	5	4	6	10
3	6	3	7	6
4	5	4	6	8
5	9	3	12	12.6
6	Express feeder with no loading.			

8.2.3 Simulation Setup

As mentioned earlier, the substation model was built in a real-time EMTP type simulation environment using RTDS/RSCAD. The simulation time step was set to 1 μ s. Two case studies were performed to see the impact of PV penetration on protective relay operation.

The first case is the base case where faults were applied at a feeder in three different scenarios. Scenario 1 is without adding any PV power injection to observe the relay operating times. Second scenario considers injection of 12.6 MW from the PV plant at FDR 5, as shown in Figure 8-1, and, in the third scenario, all the feeders have PV plants, as shown in Figure 8-2(b). Their corresponding PV ratings are also given in Table 8-2.

The second case investigates the effect of fault impedance on fault clearing time. The investigation is done by inducing the fault at three different locations as shown in Figure 8-2(a). Based on the maximum PV penetration and loads on each feeder, FDR 2, FDR 4 and FDR 5 is feeding power to the substation and hence can be considered in reverse power flow situation. The amount of reverse power flows are 4.127 MW for FDR2, 2.398 MW for FDR4 and 2.706 MW for FDR5. The 12.6 MW PV plant on FDR 5 has a recloser, which has a Transfer trip operation mode. The PV plant recloser opens if the FDR 5 breaker opens or if T3L breaker and 25T2T3 tie breaker opens.

8.2.4 Results

8.2.4.1 Case 1: Effect of PV penetration on relay operation

A single line to ground fault was applied on Phase A of FDR 4 at location. The fault impedance was set to 0.1 ohm. Three scenarios that were studied for this case are:

- (1) *Scenario 1*- in this scenario, there was no PV injection on any feeder. This has been studied to find out the operating time of the protection devices in the absence of PV plants.
- (2) *Scenario 2*- 12.6MW PV plant is connected on FDR 5 and it supplies 12.6 MW power.
- (3) *Scenario 3*- in this scenario, each feeder has at least one PV (Figure 8-2(b)) except FDR1 and FDR6. Table shows the loadings and PV penetration for each scenario. The PV Systems are current limited to 1.3 p.u. during fault condition.

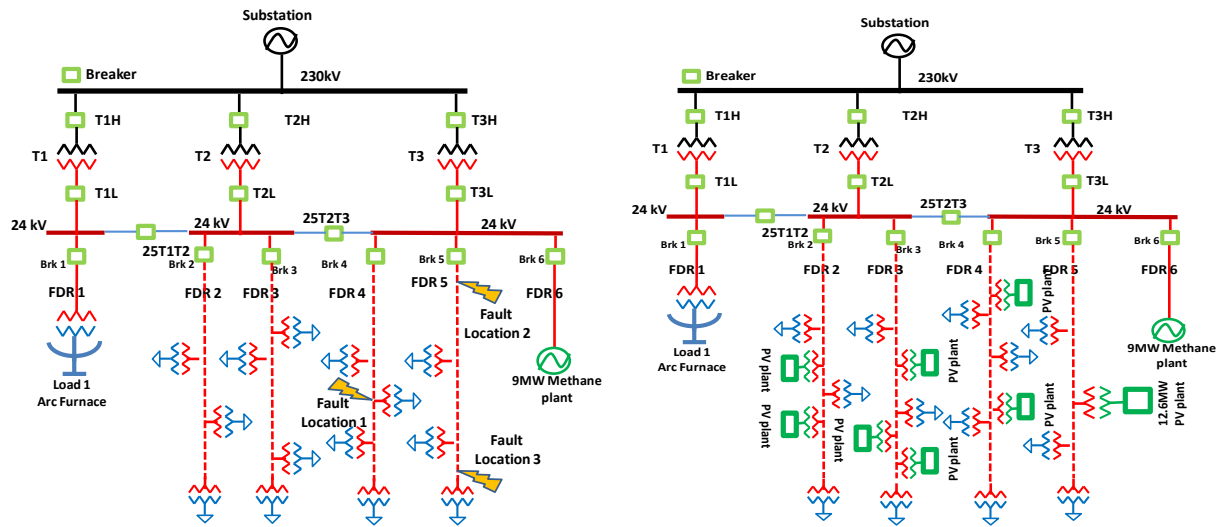


Figure 8-2. (a) left, Case 1, Scenario 2, (b) right, Case 1, Scenario 3

Peak fault current magnitudes and exact breaker trip times were recorded for the three mentioned scenarios. The fault isolation time includes the relay operation time and the breaker operation time (150 ms). Trip times for all three scenarios did not vary by more than a few msec. In all cases, the change in PV current or contribution of fault current by the PV was insignificant in comparison to the fault current from the grid. BKR5, on FDR5 does not trip due to the fault on FDR4. This establishes the fact that if relays are coordinated with proper settings, the chance of having nuisance trip or sympathetic trip is a remote possibility.

Fault current injected by PV is close to 390 A and fault current from the DG on FDR 6 is around 650 A. The fault current contributed from the system is around 3.95 kA, which is a few times higher than both DGs.

Table 8-2. Feeder loadings and PV Capacity for Case 1

Feeder No.	Feeder Loading (MVA)	PV power (MW)		
		Scenario 1	Scenario 2	Scenario 3
2	6	0	0	10
3	8	0	0	6
4	6	0	0	8
5	10	0	12.6	12.6

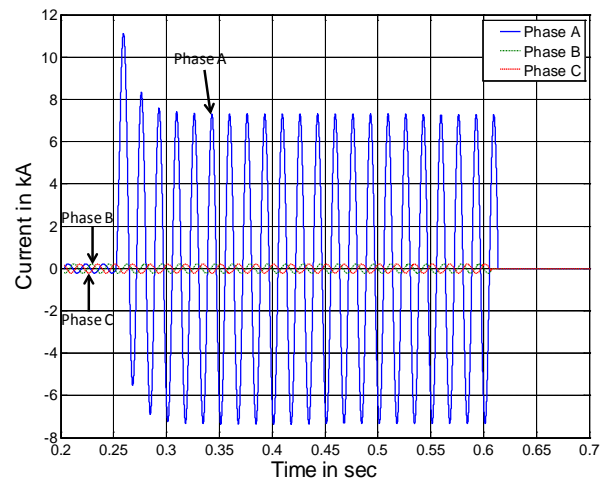


Figure 8-3. Current through BKR, FDR4, Scenario 1

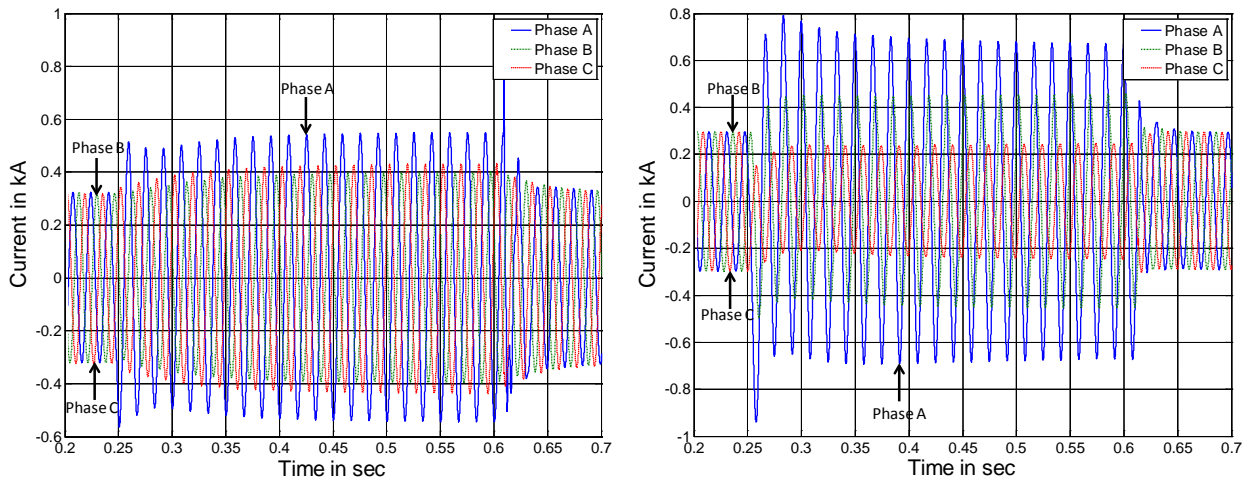


Figure 8-4. Fault currents, Scenario 1, (a) left, 12.6 MW PV plant on FDR5, (b) right, at synchronous machine DG on FDR6

8.2.4.2 Case 2: Effects of fault impedance and PV location on relay operating time

This case study was done to observe how PV location and the fault impedance influences the protective relay operation. This case also has three scenarios and in all these scenarios, the 12.6 MW PV plant that is located at 4.8 miles from the substation on FDR 5 was supplying full power. The three scenarios were:

(1) *Scenario 1*- in this scenario, the impact of fault impedance was observed when the fault was at feeder 4 (FDR 4), a feeder that does not have PV.

(2) *Scenario 2*- in this case, the fault was on FDR 5 that has 12.5 MW PV plant. The location of the fault was at a distance of 0.2 mile which is between the BRK 5 and the PV plant.

(3) *Scenario 3*- in this scenario, the fault location was at the end of FDR 5. So the location of the PV plant is upstream to the fault location.

A single line to ground fault was applied on phase A and the fault impedance was varied in the range of 0.1 – 50 ohm. Fault impedance, fault current magnitude and trip times were recorded for all three scenarios. Results revealed that a fault at FDR 4 did not create any nuisance trip or sympathetic trip for FDR 5 where the PV is connected. This was true over the range of expected fault impedances.

For scenario 2, the fault current is higher than Scenario 3 due to the fact that the fault location is close to the substation. For scenario 3, the fault current at BRK5 is less than the fault current when there is no PV injection. This can be attributed to: (1) the fault path has comparatively high impedance and (2) the fault current injection from the PV will cause a higher voltage across the fault resistance and thereby reduce the fault current from the grid. Therefore, it can be concluded that the location of the PV with respect to the fault location has slight impact on the breaker fault current and trip times of protective relays. As expected, with increasing fault impedance, fault current decreased and relay operation time increased.

Results obtained suggest that issues arising from the potential concerns identified for this particular set of studies may not be that prevalent. Table 8-3 summarizes the observations with respect to each issue.

Table 8-3. PV system integration and protection issues

Issues related to PV penetration and protective relay operation	Comments based on the study performed
Fault current contributions from DG on a feeder can reduce fault current through breaker which may desensitize relay operation [3].	PV inverters are current limited and therefore has slight impact on reducing the fault current and hence the relay operation time. However, this is much smaller than the grid contribution to the fault.
PV penetration may have an impact on protective relay operation by reducing the reach distance of relay [4].	For the current study, only time – inverse overcurrent relay was used which does not encounter such problem
PV fault current contribution can cause conductor damage or damage to transformers [1].	PV fault current is limited and the magnitude is not high enough to damage the mentioned equipment.
PV's can cause sympathetic trip of reclosers or circuit breakers [13].	No such incident was observed
PV's can desensitize ground fault relaying protection [17].	The system used in the study had a high ground fault setting and PV penetration did not desensitize the relay operation

8.3 Substation 2

8.3.1 Substation Overview

For this study, the substation data and relay settings were provided by the utility. SCADA data for the substation was also provided by utility. Some of the basic features of the substation are given below:

- The substation serves six 12.47 kV feeders (F1-F6).
- Feeder 5 has 2.6 MW of PV systems installed on the feeder.
- Feeder 3 has 2 MW of PV installed on the feeder.
- The substation connects 12.47 kV feeders to the transmission system (138 kV level).
- 3 transmission lines are fed into the substation with one of the lines normally open.
- A 24.6 MVAR capacitor bank is installed at the substation on the 138 kV side which is switched during summer season.
- The substation has two 22.4 MVA, 138/12.47 kV transformers.
- The transmission lines are protected with SEL 311 transmission system protection relays with distance relay schemes
- The 24.6 MVAR capacitor bank is protected with SEL 451, protection automatic and bay control system with overcurrent protection.
- The substation transformers are protected with SEL 351 relays which have differential protection as primary and overcurrent element as backup.
- The 12.47 kV distribution feeders are protected using SEL 351 relays which have differential element as primary and overcurrent element as backup.
- Most relays are setup with either one or two reclose attempts.

8.3.2 Modeling of Substation in RTDS

Modeling of the substation has been done in RTDS with a 70 μ s time step. Figure 8-5 shows the substation model that was built in RTDS. Since 66 (72 on newer cards) nodes can be modeled on each rack in RTDS, the model of the substation was split over three racks. With the case built over three racks, signals sent from one rack to another rack have a one time-step delay.

The 138 kV section of the substation is modeled in rack 1. The system is split at the 22.4 MVA transformers. The 22.4 MVA transformers are modeled using the cross rack transformer model of RTDS. The cross rack transformer allows one to model the high side of the transformer and its connection on one rack and

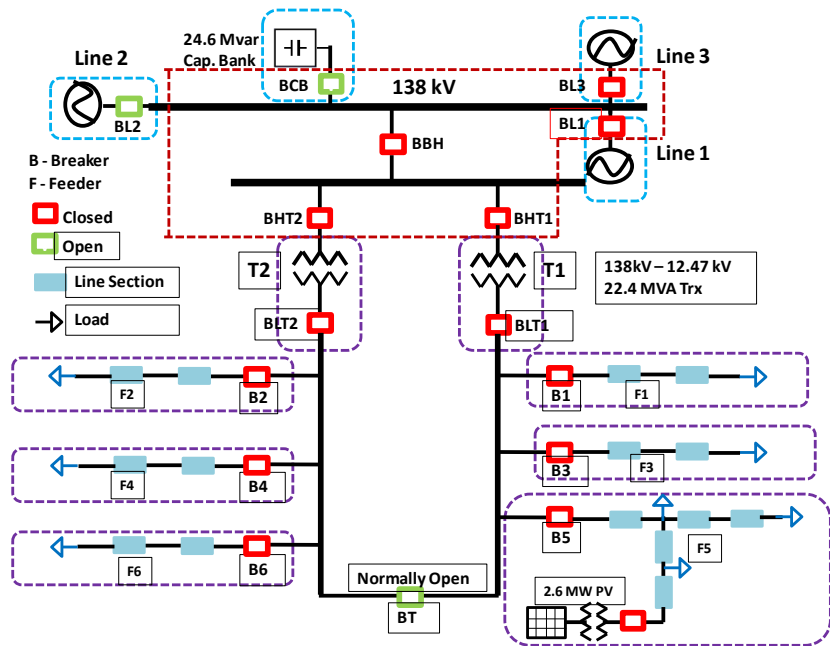


Figure 8-5. Substation 2 modeled in RTDS

the low side of the transformer and its connection in the other rack. Use of the cross rack transformer eliminates the need for using a transmission line model or an additional transformer thus preserving the accuracy of the model and facilitating the modeling of the system across multi-racks.

Distribution feeders fed from transformer T42 are modeled in rack 2 and feeders fed from T41 are modeled in rack 3. Feeders 1 - 5 are modeled with two line sections with load at each section. The fault can be applied on each feeder at three locations, at the beginning of the feeder, midpoint of the feeder and at the end of feeder. Feeder 6 is modeled with a little more detail with five line sections and three loads. Since the PV plants are very closely located, they were aggregated to one single large 2.6 MW PV plant. Single line to ground faults (SLG), double line to ground faults (DLG), line to line fault (LLF) and three phase faults (3PHF) can be applied at any location in the system. The fault angle, fault duration and fault impedance can also be controlled in the model.

The RTDS relay database is used for modeling the relays. Since the RTDS relay library does not have integrated relay functions of a digital relay, several relay components are used to model a single digital relay installed on the substation. The feeder loadings are chosen based on the SCADA data provided by the utility.

8.3.3 Modeling of PV system

An average model of the PV converters is used for simplicity. The PV system controls are modeled using a DQ control scheme with the 'd-axis' controlling real power and the 'q-axis' controlling reactive power. The PV system is current limited to 1.2 pu, i.e. under no circumstance the inverter would allow more than 1.2 pu current. The PV system connects to the rest of the system through a breaker on the 12.47 kV system.

The breaker at the PV plant is set to operate in transfer trip mode. If Breaker B5 trips, then the PV breaker is set to trip automatically. For Feeder 5, all the distributed PV systems are modeled as single large 2.6 MW PV system. The PV connects to the feeder using a 480V/12.47kV, ungrounded wye/ grounded wye transformer. The PV system is designed not to inject any zero sequence current into the grid.

8.3.4 High Penetration PV and protection studies

As with the Substation 1 studies, a variety of cases and scenarios were created to explore impact of fault current contribution of PV inverter systems, potential for sympathetic tripping of relays, and possible desensitization of ground fault detection. Faults applied for the Substation 2 cases included single-line-to-ground faults, bolted 3-phase faults, and double-line-to-ground faults.

With PV inverters normally being current limited (most in the range of 1.1-1.5 p.u.), PV systems should not significantly impact tripping times of relays, as borne out by the Substation 1 studies. For the Substation 2 simulation studies, the inverters were current limited to 1.2 p.u. Case studies below show fault current contribution by PV for different fault types and fault impedances. The results show that although PV inverters account for a part of the fault current, the trip times of relays are not significantly changed since the PV inverter fault currents are limited to 1.2 p.u. of rated current of the PV plant which is much smaller in comparison to the fault current contribution from the grid.

The following Scenarios were studied:

- Fault Current Contributions and Impact
 - Scenario 1 – Single Line to Ground fault on Feeder 5
 - Scenario 2 – Line to Line fault on Feeder 5
 - Scenario 3 – Bolted 3 phase fault on Feeder 5
- Sympathetic Tripping
 - Scenario 1 - Single line to ground fault on feeder 3

- Scenario 2 - Three phase fault on feeder 1
- Scenario 3 - Double line to ground fault on feeder 3
- Sensitivity to Ground Fault Detection

Detailed results and data for the Fault Current Contribution studies and the Sympathetic Tripping studies for Substation 2 are omitted here for brevity. The results and conclusions are similar to those for the feeders on Substation 1, in that fault current contribution from PV was limited and caused no protection issues, and, sympathetic tripping was not observed for any of the scenarios.

8.3.5 Sensitivity to Ground Fault Detection

To examine potential impact on sensitivity of ground fault detection for Substation 2 feeders, parametric sweep studies were conducted by varying PV penetration, fault impedance, and load unbalance.

8.3.5.1 Trip Time as a function of PV penetration and fault impedance

Tables 8-4 and 8-5 show trip times for a single line to ground fault on phase A of feeder 5. plots trip time as a function of PV penetration and fault impedance. The fault angle was set to 0 deg on phase A voltage. PV penetration was varied from 0 MW – 6 MW. The fault impedance was varied from 2 Ω to 10 Ω. It can be observed that as the PV penetration increases, the trip time for the relay decreases. This is due to the fact that the relay monitoring the breaker has a neutral setting element that is more sensitive than the phase setting.

The zero sequence current on the breaker actually increases as the PV penetration increases. Figure 8-6 shows the phenomenon of increase in zero sequence current with increase in PV penetration. This increase in zero sequence current can be attributed to the fact that the load impedance in the system which is in parallel with the fault impedance has an effect on zero sequence currents.

Since the PV system does not inject any zero sequence current, increases in PV penetration make the load behave as a lightly loaded system with higher load impedance. Thus as PV penetration increases, the load impedance looks higher than before. This higher impedance of load diverts more current into zero sequence networks and hence more current will be seen at the breaker. The net effect causes a higher zero sequence current at the fault and hence more zero sequence current at the breaker.

Table 8-4. Trip Times for fault impedance 2 - 5.5 ohm

PV Penetration [MW]	Trip Time in seconds for breaker B5							
	Fault Impedance in Ohms							
	2 Ω	2.5 Ω	3 Ω	3.5 Ω	4 Ω	4.5 Ω	5 Ω	5.5 Ω
0	1.212	1.346	1.501	1.681	1.882	2.106	2.359	2.634
1.3	1.205	1.337	1.491	1.668	1.866	2.088	2.338	2.609
2.6	1.197	1.327	1.478	1.653	1.848	2.066	2.312	2.578
4	1.189	1.317	1.468	1.638	1.831	2.045	2.286	2.548
5	1.186	1.313	1.46	1.629	1.82	2.036	2.271	2.53
6	1.184	1.31	1.456	1.625	1.814	2.024	2.257	2.514

Table 8-5. Trip Times for fault impedance 6-10 ohm

PV Penetration [MW]	Trip Time in seconds for breaker B5								
	Fault Impedance in Ohms								
	6 Ω	6.5 Ω	7 Ω	7.5 Ω	8 Ω	8.5 Ω	9 Ω	9.5 Ω	10 Ω
0	2.937	3.272	3.663	4.102	4.589	5.13	5.732	6.403	7.155
1.3	2.907	3.244	3.634	4.068	4.55	5.084	5.678	6.341	7.09
2.6	2.871	3.211	3.596	4.023	4.496	5.021	5.605	6.257	7.008
4	2.839	3.179	3.559	3.979	4.445	4.961	5.535	6.188	6.93
5	2.82	3.159	3.535	3.952	4.414	4.926	5.497	6.15	6.88
6	2.806	3.141	3.514	3.928	4.385	4.891	5.464	6.111	6.837

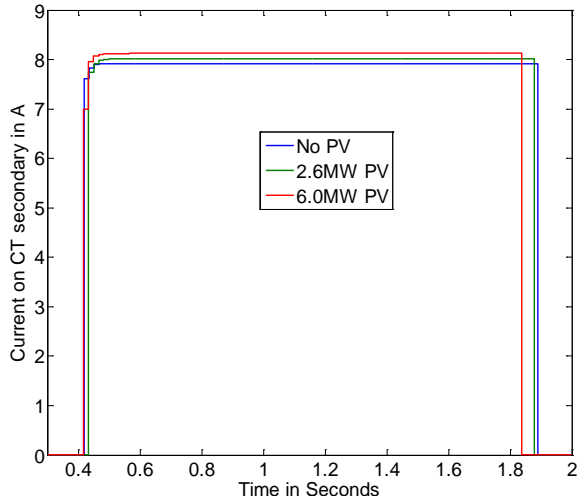


Figure 8-6. Increase in neutral current with change in PV penetration

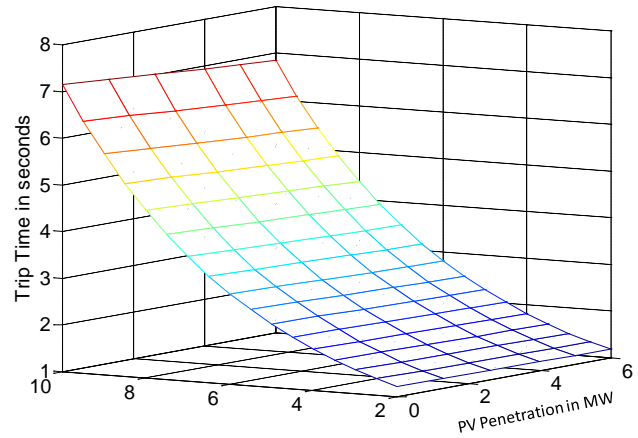


Figure 8-7. Trip times of relay as function of PV penetration and fault impedance

Figure 8-8 plots percentage change in trip times from no PV case for various fault impedances. Tables 8-6 and 8-7 show the percentage change in trip times from no PV case for different fault impedances.

Although trip time increases as the fault impedance increases from 6 Ω to 6.5 Ω , percentage change decreases from about 4.5% to around 4.1% for 6 Ω to 6.5 Ω . This issue can be attributed to the fact that although the current decreases as fault impedance increases, the current proportion change did not increase accordingly.

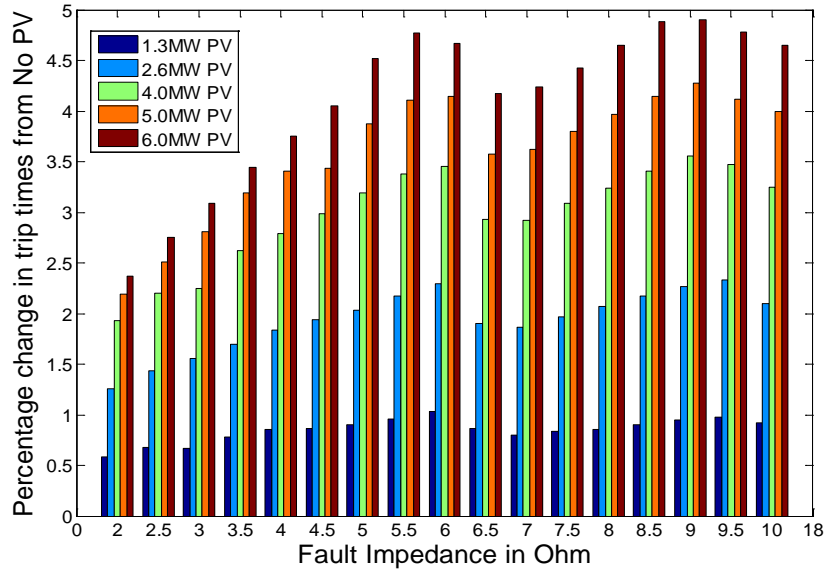


Figure 8-8. Percentage change in trip times for different PV penetration

Table 8-6. Percentage change in Trip Times for fault impedance 2 - 5.5 ohm

PV Penetration [MW]	Percentage change in Trip Time compared to no PV Penetration (in %)							
	2 Ω	2.5 Ω	3 Ω	3.5 Ω	4 Ω	4.5 Ω	5 Ω	5.5 Ω
1.3	0.58	0.67	0.67	0.77	0.85	0.86	0.89	0.95
2.6	1.25	1.43	1.55	1.69	1.83	1.93	2.03	2.17
4	1.93	2.2	2.24	2.62	2.78	2.98	3.19	3.37
5	2.19	2.51	2.8	3.19	3.4	3.43	3.87	4.11
6	2.36	2.74	3.09	3.44	3.74	4.05	4.51	4.77

Table 8-7. Percentage change in Trip Times for fault impedance 6 - 10 ohm

PV Penetration [MW]	Percentage change in Trip Time compared to no PV Penetration (in %)								
	6 Ω	6.5 Ω	7 Ω	7.5 Ω	8 Ω	8.5 Ω	9 Ω	9.5 Ω	10 Ω
1.3	1.03	0.86	0.79	0.83	0.85	0.9	0.95	0.97	0.91
2.6	2.29	1.89	1.86	1.96	2.06	2.17	2.26	2.33	2.09
4	3.45	2.92	2.92	3.09	3.23	3.4	3.55	3.47	3.24
5	4.14	3.57	3.62	3.79	3.96	4.14	4.27	4.11	3.99
6	4.66	4.17	4.24	4.42	4.65	4.88	4.9	4.77	4.65

8.3.5.2 Trip time as a function of PV penetration and load unbalance

For this scenario, the impact of load unbalance and PV penetration on trip times of the breaker was investigated. A single line to ground fault was applied on phase A of feeder 5 with a fault impedance of 2 Ω for 2 sec. Two load unbalance scenarios were simulated.

Unbalance of current or voltage in percentage is calculated as

$$UB \text{ in } \% = \frac{(\text{Mean Deviation of maximum from Average}) * 100}{\text{Average}}$$

8.3.5.3 Scenario 1: Phase A load unbalance

For this scenario, the load unbalance was varied from 0% to 50% on Phase A. The PV penetration was varied from 0 – 6 MW. Trip times were observed for the above mentioned faulted scenarios. Table 8-8 shows the trip times for scenario 1. It can be observed that as the unbalance percentage on phase A increases, the trip time of the breaker decreases. Figure 8-9(a) shows percentage change in trip times compared to 0 % unbalanced loading case for Phase A. The change in trip time is roughly the same for various amounts of PV penetration for a specific load unbalance percentage.

Table 8-8. Trip times for phase A unbalance scenario

PV Penetration in MW	Trip Time for breaker B5 in seconds					
	Phase A Unbalance in %					
	0	10	20	30	40	50
0	1.212	1.195	1.185	1.169	1.155	1.14
1.3	1.205	1.188	1.178	1.163	1.148	1.134
2.6	1.197	1.181	1.17	1.155	1.141	1.128
4	1.189	1.173	1.163	1.149	1.134	1.121
5	1.186	1.169	1.158	1.144	1.13	1.117
6	1.184	1.165	1.154	1.14	1.127	1.113

8.3.5.4 Scenario 2: Phase C load unbalance

For this scenario, the load unbalance was varied from 0% to 50% on Phase C. The PV penetration was varied from 0 – 6 MW. Trip times were observed for the above mentioned faulted scenarios. Table I shows the trip times for scenario 2. It can be observed that as the unbalance percentage on phase C increases, the trip time of the breaker increases. Figure 8-9(b) shows percentage change in trip times compared to

Table I Trip times for phase C unbalance scenario

PV Penetration [MW]	Trip Time for breaker B5 in seconds					
	Phase C Unbalance in %					
	0	10	20	30	40	50
0	1.212	1.234	1.25	1.274	1.3	1.326
1.3	1.205	1.226	1.242	1.265	1.291	1.316
2.6	1.197	1.218	1.233	1.258	1.281	1.306
4	1.189	1.209	1.227	1.248	1.27	1.298
5	1.186	1.205	1.222	1.247	1.268	1.292
6	1.184	1.205	1.219	1.24	1.262	1.287

0 % unbalanced loading case for Phase C. The change in trip time is roughly the same for various amounts of PV penetration for a specific load unbalance percentage.

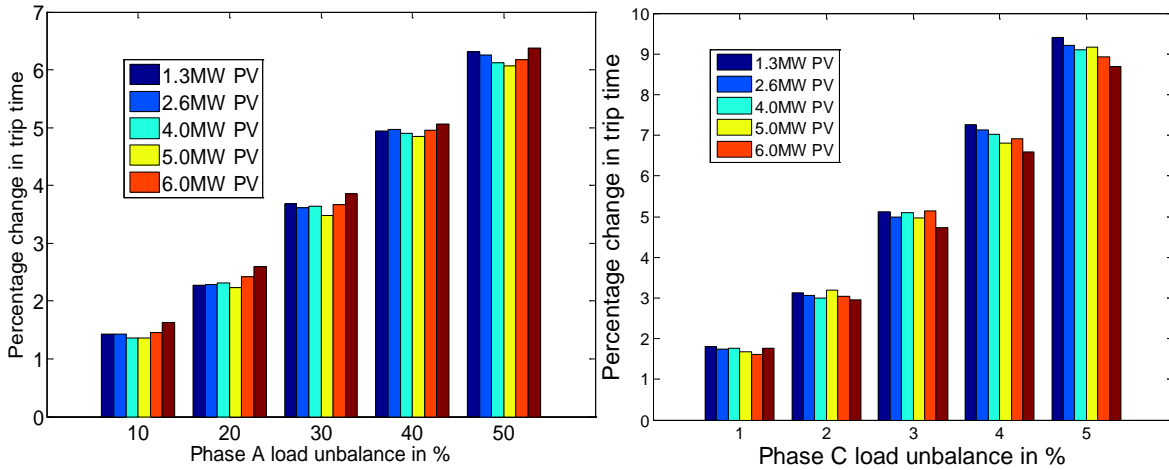


Figure 8-9. Percentage change in trip times for phase A (left) and phase C (right) unbalance

Figure 8-10 shows rms of neutral current on the CT secondary for breaker B5 for a single line to ground fault on Phase A. The figure shows the current for no unbalance scenario, 50% unbalance on phase A and 50% unbalance on phase C. For 50% unbalance on phase A, the relay trips faster than zero unbalance scenario. This is due to the fact that the unbalance loading is on phase A and the zero sequence current is already constituted by phase A. With the fault on phase A, the zero sequence current increases and the relay time inverse over current element is triggered faster than the zero unbalance loading case. But for 50% unbalance on phase C, the zero sequence current is constituted by phase C. With fault on phase A, the zero sequence current decreases as compared to no unbalance scenario and thus the relay time inverse overcurrent element takes longer to trip.

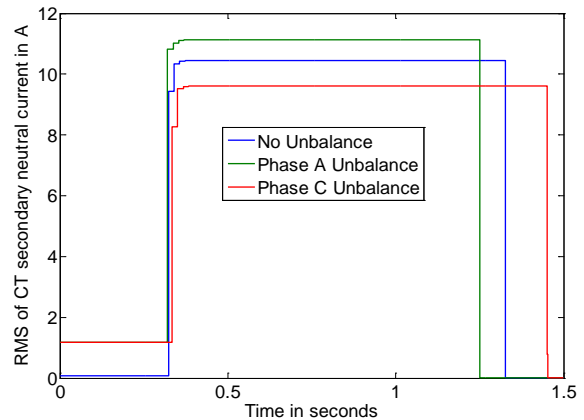


Figure 8-10. Comparison of zero sequence currents for 3 unbalanced scenarios

8.4 Conclusions

From the results of the cases studied in detail, which are actual substations with high-penetration PV feeders represented with full protective relaying details and settings in EMTP simulation, it has been found that the fault current contribution from the PV, in these particular cases, is too small compared to the fault current supplied by the grid to have impact on the protection. The short circuit capacities of these feeders, particular for Substation 1, were very high in comparison with the PV fault current. The results might be slightly different for a weak system but it would require a very large fault current contribution from the PV to result trip failures on the local feeder or sympathetic trips on adjacent feeders.

Based on the Substation 2 ground fault sensitivity studies, as PV penetration increases on a feeder, the trip times for sensing ground faults decrease for a balanced load scenario. For the unbalanced loading scenario, the trip times for sensing ground faults decrease if a ground fault happens to be on the least-loaded phase. Although the trip times change, the changes do not seem to be large enough to significantly affect operation of system ground fault detection devices.

Results and conclusions presented here are based on detailed studies involving many different test scenarios for two actual utility substations, but, nonetheless, they are specific to these systems and care should be exercised in attempting to generalize these results to other circuits. If conditions and substation and circuit design and configuration are sufficiently different, additional studies should be performed.

8.5 References

- [4] M. McGranaghan, T. Ortmeyer et al., “Advanced Grid Planning and Operations”, Sandia National Laboratories. Feb. 2008.
- [5] IEEE standard 1547.7- Guide to Conducting Distribution Impact Studies for Distributed Resource Interconnection , 2012.
- [6] R.A. Walling, R. Saint, R.C. Dugan, J. Burke, L.A. Kojovic, “Summary of distributed resources impact on power delivery systems”, IEEE Transactions on Power Delivery, Volume 23, Issue 3, July 2008, Pages: 1636 – 1644.
- [7] J. Driesen, and R. Belmans, “Distributed generation: challenges and possible solutions,” IEEE PES General Meeting, 2006.
- [8] Zhi-hai Tan, Liang Ge, Qiu-peng Sun, Fend-qing Zhao, Ahi-hong Li, "Simplified model of distribution network based on minimum area and its application," Electricity Distribution (CICED), 2012 China International Conference on 10-14 Sept. 2012.
- [9] H. L. Willis, “Power Distribution Planning Reference Book”, Marcel Dekker Inc., 2004.
- [10] H. Ravindra, M. O. Faruque, K. Schoder, M. Steurer, P. McLaren, R. Meeker, “Dynamic Interactions Between Distribution Network Voltage Regulators for Large and Distributed PV Plants” in IEEE Transmission and Distribution Expo., Orlando, FL, 2012
- [11] Ravindra, H.; Faruque, M.O.; McLaren, P.; Schoder, K.; Steurer, M.; Meeker, R., "Impact of PV on distribution protection system," *North American Power Symposium (NAPS)*, 2012 , vol., no., pp.1,6, 9-11 Sept. 2012
- [12] H. J. Altuve, M. J. Thompson and J. Mooney, “Advances in breaker-failure protection”, in 33rd Annual western Protective Relay Conference, Spokane, WA, Oct. 2006.
- [13] IEEE standard 1547.7- Guide to Conducting Distribution Impact Studies for Distributed Resource Interconnection, 2012.
- [14] R.A. Walling, R. Saint, R.C. Dugan, J. Burke, L.A. Kojovic, “Summary of distributed resources impact on power delivery systems”, IEEE Transactions on Power Delivery, Volume 23, Issue 3, July 2008, Pages: 1636 – 1644.
- [15] J. Driesen, and R. Belmans, “Distributed generation: challenges and possible solutions,” IEEE PES General Meeting, 2006.
- [16] H. Cheung, A. Hamlyn, L. Wang, C. Yang, R. Cheung, “Investigations of impacts of distributed generations on feeder protections”, IEEE PES General Meeting, 26-30 July 2009, Pages: 1 – 7.
- [17] M. E. Baran, H. Hooshyar, Z. Shen, A. Huang, “Accommodating High PV Penetration on Distribution Feeders”, Proc. of IEEE Trans. on smart grid, Vol. 3, No. 2, June 2012, pp. 1039-1046.
- [18] Network Protection and Automation Guide”, ALSTOM T&D, 1st ed. 2002.
- [19] H. J. A. Ferrer, E. O. Schweitzer, “Modern Solutions for Protection, Control, and Monitoring of Electric Power Systems”, Schweitzer Engineering Laboratories (SEL), Inc. 2010.
- [20] K. Maki, S. Repo, P. Jarventausta, “Protection planning development for DG installations”, 20th International Conference and Exhibition on Electricity Distribution, 8-11 June 2009, Pages: 1 – 4.
- [21] Y. Lu, J. Du, X. Lin, and J. Ma, “An asymmetrical fault line selection based on I2 scalar product research in distribution system with DGs,” IEEE PES General Meeting, 2008, Pages: 1 - 6.

9 DISTRIBUTION FEEDER OPEN-USE DATASETS, MODELS, AND TOOLS

9.1 Open-Use Solar PV Plant Production Data Sets

9.1.1 Approach – Data Synthesis Using Wavelets

Open use data sets have been synthesized from raw PV plant output data sets for various size plants. The procedure used to synthesize PV power data is outlined in the following steps:

- Segregation** – This involves partitioning the available data per day into its respective types depending on the weather condition. Day types are based on adaptations of a base set of day types based on weather (Clear, Fog, Rain, Thunderstorm), further modified to provide combinations of weather behavior types in a particular day (Fog_Rain, Rain_Thunderstorm, Fog_Rain_Thunderstorm), resulting in 7 day types based on weather type. Data is segregated by day type and season (Summer=SU, Autumn=AU, Winter=WI, and Spring=SP), amounting to a possible 28 unique types of days (e.g. ClearSU, ClearAU, ClearWI, ClearSP, FogSU, FogAU, etc.), which reduce to 23 in practice, with 5 day types that never occur when the data is run through the classification process. An example distribution of day types for one of the synthetic data sets for 365 days is shown in Figure 9-1.

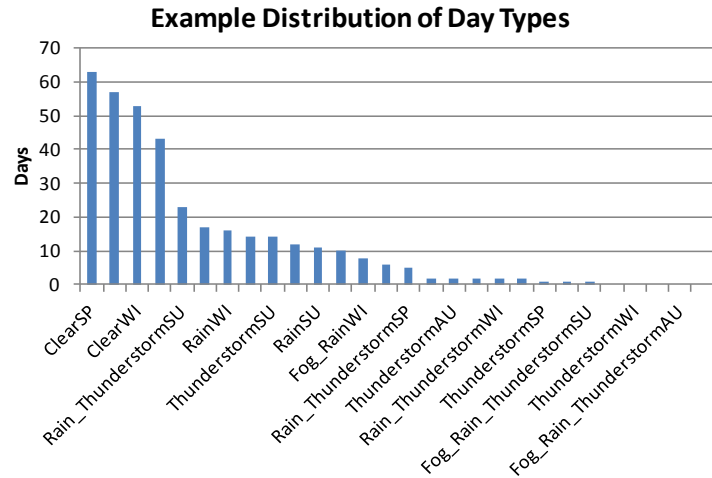


Figure 9-1. Example distribution of day types

- Dividing into quadrants** – Here, the overall data, for each day, is divided into 4 equal parts of 6 hours each (6am – noon, noon – 6pm, 6pm – midnight, midnight to 6am).
- Moving RMS waveform generation** – This step results in the generation of a base signal, one each for the type of day. This step has two parts,
 - Retaining the sign of the power reading per column of the array is crucial to increase accuracy of the overall RMS signal. The number of negative values per column are counted and if this exceeds the total number of rows, then a negative sign is attached to the column. Otherwise the column is positive. The moving

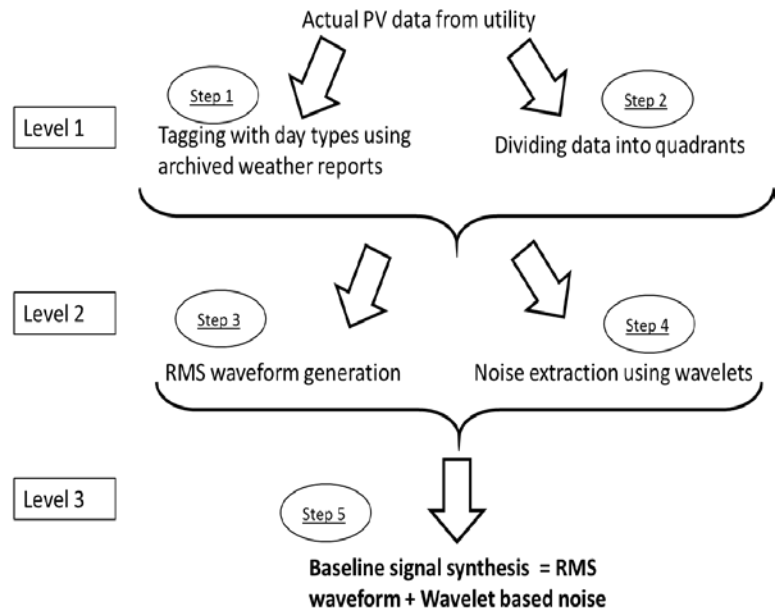


Figure 9-2. Approach for production of synthetic data sets

RMS is calculated taking 2 rows of the matrix at a time and looped until only 1 row remains. This essentially generates only positive values. These are multiplied by the sign retention array in part 3.a to get the actual signs as per the original data stream.

- *Wavelet noise calculation* – To include a more short-term stochastic variation in the averaged signal from step 2, a noise component is added. The noise components are calculated using wavelet transforms [1]. An important aspect of carrying this out is the selection of the mother wavelets as per the type of day. For this work, the following were adopted,
 - db3 – Clear
 - db4 – Mostly cloudy, Partly cloudy, Scattered clouds
 - db8 – Fog, Overcast, Rain, Thunderstorm
- *Signal synthesis* – The final synthesized signal is the sum of the RMS signal (step 3) and the wavelet noise (step 4). One may further average individual synthesized signals depending on the number of data sets available. In this study, four data sets measured at 1min. intervals are used to from which separate synthesized signals per day type were obtained, for each data set. These were averaged to produce “baseline” signals for each day type. Another important factor to note is the division of annual data available per season i.e. summer and winter.

The power capacities of the four data sets used in development of the synthetic data sets are listed in table n.

Table 9-1. Individual PV data sources

Source data set no.	Rated capacity [MW]	Measurement interval [min.]
1	0.315	1
2	0.250	1
3	2.5	1
4	2.5	1

Example synthetic waveforms based on day type distribution and time-series patterns derived from a 315 kW plant are shown in Figure 9-3.

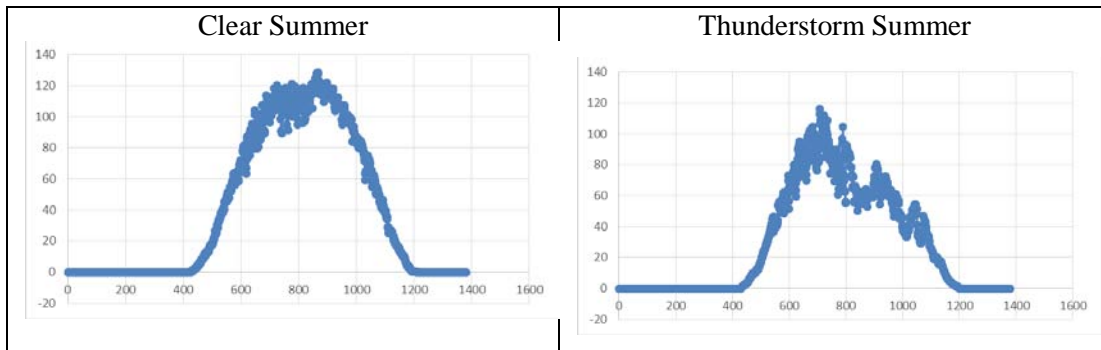


Figure 9-3. Typical baseline synthetic data profiles, two day types

9.1.2 Using baseline data

The approach elaborated previously extracts from actual PV data generic base profiles for a given day type. The example shown here pertains to four utility PV power data sets measured at 1min intervals. In a scenario where a researcher has the day type information for a given series of dates, a continuous waveform could be patched by utilizing the given baselines.

Associated MATLAB functions, codes and plots of sample results are given in the appendix.

9.1.3 Comparison of Results from Simulations with Actual and Synthetic Profile Sets

The distributions of the normalized power from the actual and synthetic data sets over a year-long duration are compared in Figure 9-4(a) (here, only non-zero values are considered). A t-test applied to

the two data sets do not indicate consistent mean values of the data sets, with a t-statistic of 32.3. However, a simple regression of the CDF for the synthetic data onto the CDF of the actual data gives an R^2 value of 0.932. A similar comparison of CDFs for the normalized power ramp rates (pu/s) are given in Figure 9-4(b). The results for the t-test show good agreement for the mean values of the ramp rates with a t-statistic of 0.0096. A regression of the CDF for the synthetic data onto the CDF of the actual data gives an R^2 value of 0.999.

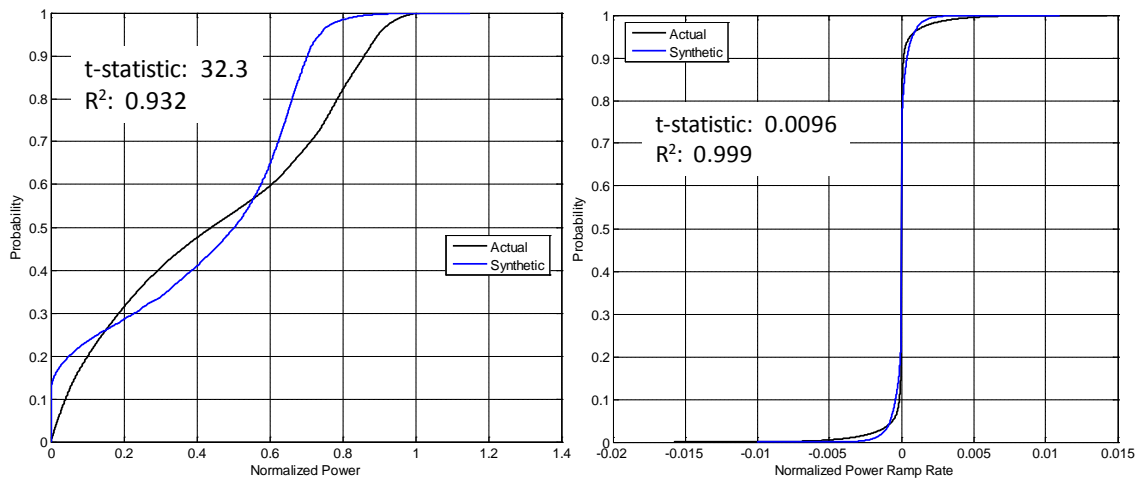


Figure 9-4. (a) left, comparison of CDF's for normalized power, actual and synthetic, over 1 year
(b), right, comparison of CDF's for normalized ramp rates, actual and synthetic, over 1 year

9.1.4 Future work

Some possible enhancements and improvements that could be pursued include:

- Produce data sets of different sampling intervals, shorter and longer than the 1-min. sets provided
- Develop reliable, validated method for scaling synthetic sets to different PV plant capacities, properly including aggregation smoothing effects for different locations and types of plants.
- It is anticipated that with a larger number of data sets available, it is possible to improve upon the accuracy and precision of the synthetic baseline waveforms generated.
- Tagging data with unique hybrid day types could be further assessed. As an example and based on observed data, the weather events taking place in every quadrant of a day might further be incorporated into determining “day type”. The approach used depends on properly classifying type of weather, which often changes during the course of a day. Improving on how the day is divided and what “hybrid” day types to use, and experimenting further with formal clustering techniques to group with an appropriately selected day types could substantially improve results.
- Experiment further with selection of mother wavelets to more closely match the general daily PV profile of a given day.
- Apply curve-fitting and residuals, where, the residuals generated correspond to the noise equivalents of wavelet transforms.

9.2 References

- [1] Moaveni, H.; Click, D.K.; Meeker, R.H.; Reedy, R.M.; Pappalardo, A., “Quantifying solar power variability for a large central PV plant and small distributed PV plant,” Photovoltaic Specialists Conference (PVSC), 2013 IEEE 39th , vol., no., pp.0969,0972, 16-21 June 2013

9.3 Software Tools and Open-use Models

9.3.1 Functions and Framework

In order to facilitate studies with the feeder models, including impact mitigation, parametric studies, and model reduction studies, a set of functions and classes were written in MATLAB. These functions and classes provide a modular tool set for crafting and conducting studies of feeder models using OpenDSS.

The numerous functions can be grouped and classified as follows:

- Execution of a simulation with an openDSS model and retrieval of results (e.g. `sg_runOpenDSSSim()`, `sg_runModel()`, `sg_resultExtBase()`)
- Computation and visualization of metrics describing system behavior based on time-domain results (e.g. `sg_loadImpact()`, `sg_NumVregActions()`, `sg_vHistograms()`, `sg_VarContributions()`)
- Implementation of reactive power controls for inverters and control of capacitor banks (`sg_CapCtl_pf_Q`, `sg_DGVarCtl`)
- Execution of parametric studies (e.g. `sg_evalSet()`, `sg_evalSim()`, `sg_buildRM()`)
- Model reduction (e.g. `sg_openDSSModelReduction()`, `sg_openDssSplitBus()`, `sg_openDssRemoveBus()`, `sg_openDssCombineLoads()`, `sg_voltageDropMetric()`)
- Helper functions for setting/getting information to/from OpenDSS models (e.g. `sg_getLineFlow()`, `sg_FeederInfo()`, `sg_getParam()`, `sg_scaleParam()`)
- Miscellaneous helper functions (e.g. `sg_updateOpts()`, `sg_loadTable()`, `sg_rgrep()`)

As an example of how the functions can be used together, Figure provides an illustration of the use of some of the functions in executing a time-domain simulation of an openDSS model.

Here, “runModel” serves as a script to execute the simulation by calling the other necessary functions. The `sg_startOpenDSS()` function is first called to initialize the COM interface to OpenDSS.

The `sg_runOpenDSSSim()` function is then called, passing the name of an OpenDSS case file, and the file name for the profile set to execute. The `sg_runOpenDSSSim()` function, in turn, loads the OpenDSS case file using the COM interface to OpenDSS and loads the profile set using the `sg_loadTable()` function. The `sg_runOpenDSSSim()` function runs through the set of load and PV profiles, on each iteration obtaining a solution from OpenDSS and retrieving the results using the `sg_resultsExtBase()` function. The `sg_runOpenDSSSim()` function returns the time-domain results from the simulation, and these are written to a file in the runModel script.

Additionally, the runModel script calls several functions (`sg_plotMaxMinVoltageProfile()`, `sg_plotFeeder()`, and `sg_plotVoltageProfile()`) which are used to compute metrics from the time-domain results and generate figures for visualization of the results.

This is one example of the use of these functions for a simple task, but the developed functions were generally intended to provide a modular framework to support a range of analyses. Uses of the functions for particular purposes are discussed in many portions of this document.

standalone SUNGRIN Tool executable is available that provides both a command line and a Graphics User Interface (GUI). The following provides information on obtaining and installing the necessary software components.

9.3.2.1.2 Disclaimers:

- OpenDSS is a copyrighted product of Electric Power Research Institute, Inc., <http://www.epri.com/>
- MATLAB® is a registered trademark of The MathWorks, Inc., <http://www.mathworks.com/>

9.3.2.1.3 OpenDSS

The OpenDSS is an electric power Distribution System Simulator actively developed by the Electric Power Research Institute (EPRI). Its main www-site is located at <http://electricdss.sourceforge.net/>. Follow the links to download the installation files (which includes both the MS Windows 32-bit and 64-bit versions). OpenDSS provides the information necessary to successfully install the software and register the corresponding COM-library (note: need to have administrator privileges to register the COM-library).

After installation, the OpenDSS is available as a power flow tool on its own. The SUNGRIN tool is based on its COM-interface to setup, execute, and post-process power flow time series studies.

9.3.2.1.4 MATLAB Runtime

To run the SUNGRIN tool without having the software MATLAB itself available, the MATLAB Runtime environment needs to be installed. It is freely available. Information on the MATLAB Runtime is available from MathWorks at <http://www.mathworks.com/help/compiler/working-with-the-mcr.html>. Note that a specific Runtime must be installed: the version must match the MATLAB used to compile and create the executable.

Note: Installation will require administrator privileges.

9.3.2.2 Using the SUNGRIN Tool

The executable can be used in two different ways: command line and GUI-based feeder studies. The following provides information on getting started in using the SUNGRIN tool. Note that the command line and the GUI versions may take a long time after starting before showing any results/response as both the initialization of the MATLAB Runtime and loading of large time series data files require

9.3.2.2.1 Command line environment

When using the tool from the Windows command line, all input and output is through the use of data files. To execute a function that was developed for the SUNGRIN feeder DER impact analysis, its name (or short name) needs to be provided as argument. Functions available provide the means to interactively load required data files to simplify the command line use. But, if desired, additional arguments to the function call can be provided to, e.g., specify the data files to be used. This capability allows to setup batch execution of feeder studies. The following provides usage examples (shown for the 64 bit version). See the individual functions documentation for additional information on functions available corresponding and function parameters.

Note: In the following **sg_DERtool_64bit.exe** is used as an example file name. The actual (latest) version will have a different name as it also includes the MATLAB version number.

- **sg_DERtool_64bit.exe** or **sg_DERtool_64bit**
Opens the GUI-based interface as no function to execute has been specified.

- **sg_DERtool_64bit fn FunctionName fp FunctionParameterPairs**
Calls the function FunctionName with function arguments as provided in “FunctionParameterPairs.” A Parameter pair consists of a parameter name and its value.

Note that in general, a function called without arguments will prompt for the required data files before continuing to execute the function.

- **sg_DERtool_64bit fn sg_gui** or **sg_DERtool_64bit fn gui**
Opens the GUI-based interface.
- **sg_DERtool_64bit fn sg_plotmaxminvoltageprofile** or **sg_DERtool_64bit fn mmv**
Prompts for a feeder study results data file and plot the minimum and maximum feeder voltage profiles.
- **sg_DERtool_64bit sg_plotvoltageprofile** or **sg_DERtool_64bit vp**
Prompts for a feeder study results data file and plots the first power flow result’s feeder voltage profile.
- **sg_DERtool_64bit sg_plotFeeder** or **sg_DERtool_64bit feeder**
Prompts for a feeder study results data file and plots the feeder structure (as based on x-y-coordinates that were included in the OpenDSS feeder setup).

Two examples of calling a function with parameters (the following assumes that the executable in the search path and/or the executable and data files are in the same folder):

- **sg_DERtool_64bit fn feeder fp \"fname\", \"Result.mat\"**
This calls the function to plot the feeder structure using results computed earlier and saved in the file “Results.mat”. Note that both of these are strings and require the backslash as escape character. Also, the parameter pair(s) needs to be provided without any spaces; it is one string on the command line.
- **sg_DERtool_64bit fn vp fp \"fname\", \"Result.mat\", \"step\", 5**
Shows (animates) voltage profile plots by stepping through the data using every 5th result.

9.3.2.2.2 Graphical User Interface (GUI) Environment

Running the executable from the command line or by simply double-clicking, starts the graphical user interface. The GUI facilitates loading data files and execution of a time series study. A limited number of functions is currently available, but additional analysis and reporting functionality will be added. Currently available are: plotting of min-max feeder voltage profiles, feeder structure (based on the first power flow result in the data), feeder voltage profiles (either manually or automatically stepping through the results), and feeder voltage analysis in form of histograms. Once loaded and/or computed, feeder and profile information is displayed. Brief messages are displayed to inform about ongoing operations and status. The GUI is depicted in Figure 9-6.

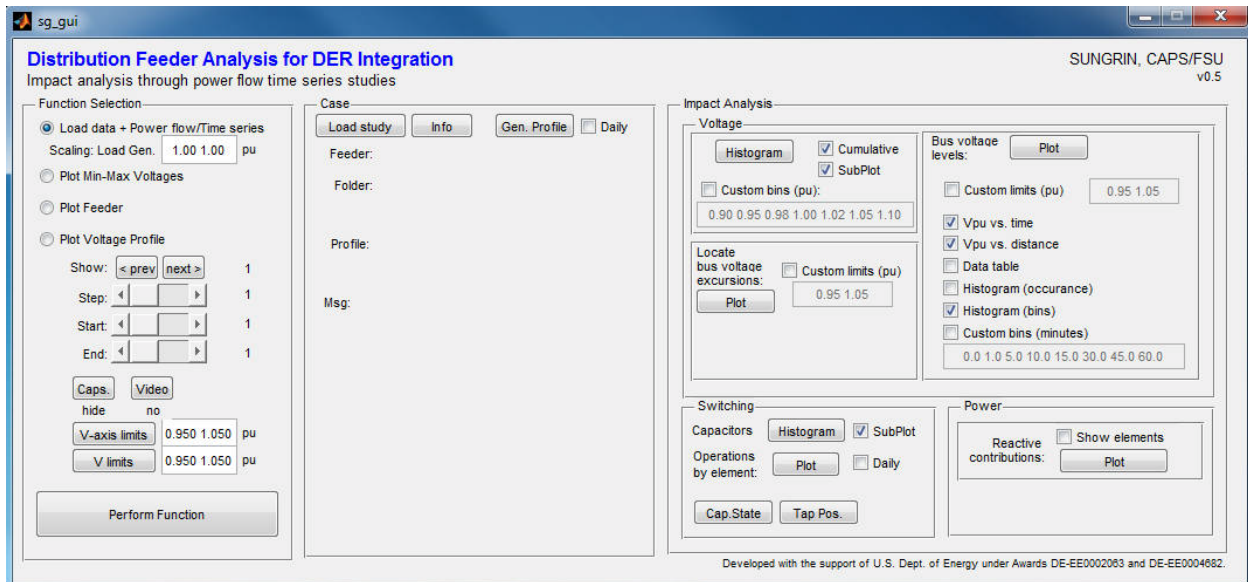


Figure 9-6. SUNGRIN DER Analysis Tool GUI

The GUI currently consists of three main areas:

- Basic functions to load and perform studies,
- Case information, and
- Impact analysis centric functions.

The basic functions allow the following:

- Functions to **load data** feeder (i.e., feeder/OpenDSS and profile/Excel files) and perform **time series studies**;
- Plot minimum and maximum voltage profiles;
- Plot **feeder structure** (based on xy-coordinates as included in the OpenDSS data file(s));
- Plot **voltage profiles** (either manually stepping through results or automatically).

The impact analysis sections includes

- Analysis of voltage levels and changes;
- Analysis of switching analysis information;
- Reactive power contribution analysis;
- Analysis voltage excursions.

All the plotting functions will ask for results data files (MATLAB *.mat files) in case data are not already available in memory to allow loading and analyzing previously computed results.

Several of these functions allow customize settings. For example, in the impact analysis section, feeder voltage information can be shown in form of histograms. The histogram bins can be defined manually or automatically in 1% steps from minimum-to-maximum.

9.3.2.3 Data Files and Formats

The feeder analysis tool is based on or uses the following files and formats:

- **Electric distribution systems:** OpenDSS files that define all the electric characteristics of a feeder; including solar PV sites. Specific settings (parameter values) can and will be updated from the SUNGRIN tool while executing a study. For detailed information see the OpenDSS documentation.
- **Profile data:** Information on specific settings as used in the power flow time series analysis. For example, load demand (active (kW) and reactive power (kVAr) demand; solar PV/generation power injected into system (kW), power factor, substation voltage. An example (part) of a profile file is shown below. The first column is the time in seconds. All other columns follow OpenDSS convention: Element type (dot) Element name (space) Parameter. Note that the load and generation data can be scaled by factors entered in the GUI to facilitate comparative studies.

Table 9-2. Input profile data file form at example

time	Load.B20021A_1 kva	Load.B20031A_1 kva	Generator.B20082P_1 kW	Vsource.source pu
0	127.4935034	283.3188966	0	1.029720906
60	127.0887828	282.4195172	0	1.029780722
120	126.7020497	281.5601103	0	1.029835132
180	126.0305131	280.0678069	0	1.029943226
21180	122.1973149	271.5495887	0.001	1.024851111
21240	122.0914111	271.3142469	0.0395	1.024656667
21300	122.0375387	271.1945305	0.104	1.024528889
21360	122.1453867	271.4341928	0.18	1.024465556
21420	122.324674	271.832609	0.303	1.024444444

- **Feeder study result files:** Feeder studies are saved as MATLAB (*.mat) files to facilitate later processing and analysis. The data are in the format of a data structure and can be (re)used within the SUNGRIN tool or used within MATLAB on their own.

9.3.2.4 Documentation

More documentation can be found with the downloadable open use feeder models and standalone executable files. A document is also available describing all functions. And, all functions, scripts, and source code contain comments.

9.4 A Model Reduction Tool for OpenDSS Models

9.4.1 Introduction

The SUNGRIN project has relied on a reduced model approach to simulation assisted analysis. RTDS models were reduced versions, which was necessary to fit distribution models within the per-rack node-limits of an RTDS. However, there are many other advantages of a reduced model approach, including faster development, less detailed information required to build, easier sharing of models, reduced maintenance and upkeep requirements, simplified validation with limited field data, less prone to errors in development, use, and upkeep, reduced computational burden / faster execution times, and ability to run on real-time simulation platforms. Reduced models fill a need for models that enable large-scale studies involving many iterations, long simulation time periods, or scaling the scope to larger portions of the electric power system.

A methodology was developed and improved upon over the course of the project for developing reduced models, initially primarily for the RTDS. More recently, with a focus on OpenDSS models, an automated tool has been developed for producing a reduced OpenDSS model from a larger, more detailed OpenDSS distribution circuit model.

The OpenDSS reduction tool incorporates lessons learned and ideas developed and refined from prior phases of the project. The processes developed and utilized previously for reducing models have been effective, but, mostly manual and relying largely on experience and engineering judgment. The OpenDSS model reduction tool is automated, embedding knowledge and experience along with application of relevant electrical engineering principals to arrive at a reduced model that is validated, meaning the electrical state at key busses retained in the reduced model compares closely with those same busses in the full source model.

9.4.2 Approach

9.4.2.1 Equivalent reduced models

The automated model reduction approach was based on the key objectives used in earlier phases. The objectives were to both retain salient feeder structure and operating characteristics. To achieve these objectives, the following steps were followed.

- Identify key elements and buses in the system. These buses were to be kept in the final model. To retain the feeder structure, a list of key locations was established including substation, breakers and reclosers, voltage regulators, capacitor banks, large-scale solar PV sites, and medium-voltage feeder branches with significant load demand.
- After the key feeder locations were identified, corresponding feeder sections could be assigned and the equivalent impedances between the key buses computed. Short-circuit currents were determined for selected test points and compared to the results obtained using the original model.
- Design load demand data, i.e., utility installed customer transformer ratings, were aggregated into demands at the nearest retained key bus locations and scaled based on available feeder current and power flow measurements.

Several circuit reduction techniques have been developed by others, along with an approach geared towards application in distribution systems. This method computes lumped load representations for feeder sections with a large number equal loads, assuming a constant current load model and uniform load distribution. The resultant representation is a lumped load at the feeder section's midpoint. In a second step and based on achieving the same voltage drop, it is recognized that half of the lumped load may be connected at the end of the feeder section. Examining the feeders section representations' corresponding power losses, a difference is recognized and an alternate representation derived, which yields a feeder

section with the lumped load connected one third down the line, but yields the same power loss term as the initial midpoint representation.

In conclusion, the same model cannot correctly represent voltage drops and power losses at the same time. The feasibility of a model that does achieve both goals is shown with the derivation of an additional lumped load representation that splits the one equivalent lumped load into two parts of and of the initial load, connected at the distance and the end of the section. Though this final model is useful for converting the distributed load of a section into an equivalent representation, it is not directly applicable to the feeder circuit reduction process.

A variation of the lumped load model approach that does support model reduction was demonstrated and discussed in [6]. It is again based on using a constant current model to represent loads but allows to split a load into two parts and connects these parts to the two neighboring buses. The load fractions are derived with the constraints of reproducing the same voltage drops and the same power consumption, i.e., sum of load and line losses. Once the load is split and moved to the neighboring buses, the initial bus can be removed from the feeder model and the two line sections combined into a single section. This bus and section reduction process is feasible as long as the two line sections are compatible, i.e., the number of phases is equal and the resulting load parts can be correctly connected at the neighboring buses, i.e., preserving phase relationships.

A proof of equivalency with respect to voltage drop and power was developed that considers all quantities involved to be complex numbers, but is omitted here for brevity. The proof shows that the total power flows of the original and equivalent models are the same. A graphical representation of the process of splitting and moving a load to neighboring buses is shown in Figure 9-7.

As used in the derivation, line section impedances are used to compute the load ratios. In the algorithm implemented, these line section impedances are based on the positive sequence components. Also, the scaling as implemented for 3-phase loads assumes balanced conditions.

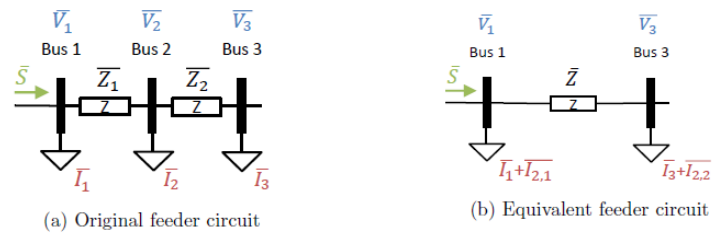


Figure 9-7. Splitting and moving a node to neighboring buses

9.4.2.2 Model Reduction Steps

With the above demonstrated feasibility of splitting and moving a load to neighboring buses without impacting voltage profiles and power flows, two key steps of reducing a model have been identified. These steps can be applied to any load bus that is deemed a candidate bus for reduction, i.e., not a key bus to be retained. While reducing a feeder circuit model, the following process and model reduction steps are applied.

- **Build a list of key buses:** Key buses are to be retained in the reduced model. Typical choices for key buses includes the substation, transformer and voltage regulator buses, capacitor bank locations, feeder branching nodes, distributed resource locations, and components that are deemed significant. The following provides a list of specific choices available in configuring the key bus selection process.
 - Buses explicitly identified by the user (an array of names to be passed to the function);
 - Buses with names matching a regular expression, can be used in conjunction with naming conventions to easily select portions of a feeder that are of interest to be retained;
 - A capacitor bank kVAR rating threshold, such that buses containing a capacitor bank with a rating exceeding the specified threshold are automatically retained;
 - An option to automatically retain buses including a tap changing transformer;

- A generator kVA rating threshold, such that buses including a generation unit with a rating exceeding the specified threshold are automatically retained;
 - A load kVA rating threshold, such that all buses including loading with a rating exceeding the specified threshold are automatically retained;
 - An option to retain all three-phase buses;
 - A threshold voltage rating, such that all buses with a voltage rating above the threshold would be retained, can be used, for example, to select all of the buses of a main trunk to be retained; and
 - A per unit voltage deviation threshold, such that all buses within the solved model having voltages that differ from nominal by more than this threshold value would be retained in the reduced model.
- **Split loads:** As described above, in case a candidate bus with loads is identified, the loads can be split using the ratios derived above. The resulting load components are connected to the two neighboring buses and the initial loads removed. The load ratios are used in a separate step to update profile data accordingly. Note, this step can also be applied to loads connected through a transformer. In this case the transformer and all connected elements on the secondary side are scaled accordingly. The steps' implementation handles single-phase, phase-phase, and 3-phase connected loads accordingly, and the possibility of different phase-ordering at the neighboring buses is considered as well.
 - **Move elements:** in case a candidate bus at a leaf-end of a feeder model has been identified, the connected elements (loads) can be moved to the bus “before,” i.e., one bus closer to the substation in case of a radial feeder, and the leaf-end bus be removed from the circuit. The resulting current flows will be same and only the bus voltage information for the removed bus will be lost. As mentioned in the step above, the different load types and possibility of different phasing is considered when connecting the loads to the new bus.
 - **Remove bus:** Any candidate bus without any load can be removed from the feeder circuit by combining the two adjacent line sections into one. Certain restrictions apply: the two adjacent line sections need to be compatible with respect to number of phases.
 - **Move line:** One end of a line can be moved (i.e., reconnected) at another bus by considering the line impedance of the section the line is moved across. The reconnected line section's impedance is combined with the impedance of the section it is moved across. Three additional considerations and steps may be necessary:
 - **Compensate for moved line:** The demand along the moved line section caused a voltage drop across the line section it was moved across. Therefore, an equivalent load-generation pair needs to be added to ensure the same voltage at the original connection point. Step: add moved line's power flow as equivalent load to the initial connection point. Add the same amount as generation to the new connection point (or through a negative load).
 - **Compensate for other connected lines:** The flows of the remaining line sections caused a voltage drop. Again, an equivalent load-generation pair needs to be added to ensure the same voltage at the other end of the moved line. Step: add the sum of the other sections' power flows as equivalent load to the end of the moved line section. Add the same amount as generation to the new connection point. Note, the added load-generation pair needs to be scaled as the moved line section impedance increased. The original power flow would cause a larger voltage drop and a scaling ratio of $\frac{\bar{Z}_1}{\bar{Z}_1 + \bar{Z}_2}$, where \bar{Z}_1 is the impedance of the section the line is moved across and \bar{Z}_2 is the impedance of the moved section, has to be used.

- **Compensate for local load:** In case loads were connected at the original point of connection, an equivalent load-generation pair needs to be added to ensure the same voltage at the end of the moved line section. Step: add the sum of the local load as equivalent load to the end of the moved line section. Add the same amount as generation to the new connection point. As in the step above, this load-generation pair needs to be scaled to account for the larger line impedance.

Again, the step's implementation considers different load type and possibility of different bus phasing when reconnecting.

- **Combine loads:** The step of splitting and moving a load to neighboring buses may result in a large number of loads in the reduced feeder model. In case of compatible loads, i.e., phasing, connection types, and voltage rating, a single equivalent load can be computed. The profile data entries are updated accordingly, i.e., the original entries are mapped to the new equivalent load.

As stated above, the reduction process finds equivalent circuit under the assumption of constant current loads. The constant current as used during the power computations is given by a load's active and reactive power demand and its nominal voltage. As the nominal voltage is a constant scaling factor, the implemented algorithm handles and updates the power components directly rather than the currents. The same applies to the updates made to associated profile data.

Though the algorithm can handle all the situations of interest with respect to the SUNGRIN feeder reduction requirements, restrictions of the implemented model reduction algorithm apply:

- Combining line sections only succeeds in case of compatible line sections, i.e., number of phases. Also, only sequence based line information is handled.
- Only loads are currently handled but not generators, i.e., already connected distributed resources are not mapped to neighboring buses. It is assumed that the distributed generation will be connected at identified key buses after deploying model reduction.
- Load ratios are determined by using the positive sequence information only. Shunt line impedances are not considered.
- Three phase loads are assumed to be balanced.
- As outlined above, the "move line" step is involved due to the need to trace all downstream connected components to properly match power flows. This process step is computationally expensive and only been implemented by an approximate approach.

The implementations of the fundamental reduction steps keep track of both the actions taken and the actions it would take to reverse (undo) steps. Therefore, alternate algorithm implementations may be feasible that probes individual reduction steps and follows the best path forward, possibly back-tracking earlier steps in case a better choice of steps has been found.

9.4.2.3 Model Reduction Process

The basic model reduction steps need to be applied in a logical and automated process that scales from small demonstration models to actual large-scale feeder models. The following describes the two approaches implemented, which themselves may be combined to arrive at the final reduced model.

9.4.2.3.1 Topology Walking

The topology walking algorithm is based on the following iterative concept.

- **Build key and candidate bus lists:** Initially, all buses are candidates for removal. Based on the user selected choices, iterate over all buses and determine if the bus should be moved to the key bus list and making it part of the reduced model. The available list of choices includes substation, transformers, voltage regulators, capacitor bank locations, loads larger than a certain rating, branching points, bus voltage level.
- **Build topology tree:** Iterate over the feeder model from substation (root) to the feeder end points (leaves) and build the associated feeder structure tree.
- **Topology walk:** For every leaf found, walk bus-by-bus back to the root. For each bus visited, determine if the bus belongs to the set of key buses or the set of candidate buses. If the bus is a key bus then move to the next bus upstream. If the bus is newly identified as a key bus, add it to the key bus list and move to the next bus upstream. If the bus is a candidate bus then evaluate which steps should be followed to remove the bus from the feeder model. Possible intermittent steps may be to move connected loads, split connected loads, move a line section, and remove the bus. Once the bus is removed, eliminate it from the candidate list and move to the next bus upstream. The algorithm exits if no candidate bus is left or all the leaf-root paths have been followed.
- **Apply model reduction steps:** Once the list of actions (steps) has been generated, all actions are executed in order. Some actions may fail due to additional consistency checks such as phasing of sections to be combined. If an action does not succeed then the associated bus is kept as part of the model, the current action is terminated, and the next action applied. As a last step, individual, compatible loads at buses are combined into one.
- **Update profile data:** If a profile data file was specified, an update profile file is automatically generated that maps the initial load data to the newly connected loads. As the ratios of loads that are split and moved to neighboring buses are complex factors, both active and reactive power (or magnitude and angle) need to be updated.
- **Save reduced feeder model:** The reduced circuit model is exported as a set of OpenDSS files. These files, together with the updated profile data, can be used to setup high-penetration studies and evaluate salient feeder conditions using a time series approach and/or perform parametric studies.

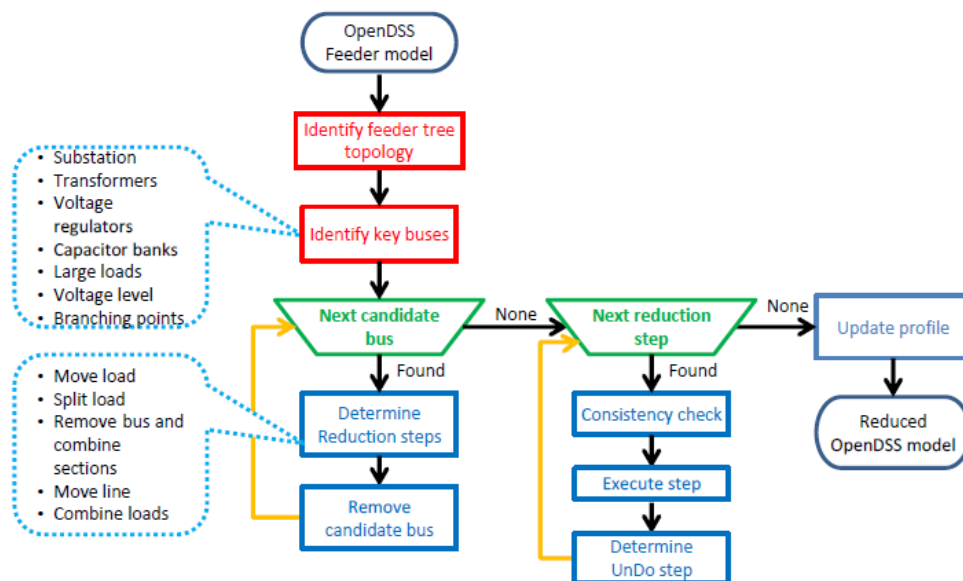


Figure 9-8. Topology walking model reduction process

A graphical representation of the model reduction process based on topology walking is shown in Figure 9-8. It is noted that the automated procedure of the topology walking currently requires a radial feeder structure though loops may be recognized and broken with additional logic.

9.4.2.3.2 Least Voltage Sensitivity

The Least Voltage Sensitivity algorithm is based on the following iterative concept. Based on an equivalent voltage drop index, selection of significant loads and line sections are made. The index that serves this role considers the local load and adjacent line impedances. Both, the loading and impedances are expressed in per unit values for a chosen base power and voltage rating. If a bus contains a total load of S_{load} and the adjacent line impedances are Z_1 and Z_2 , corresponding to two connected lines, the voltage drop indices associated with this bus are given by

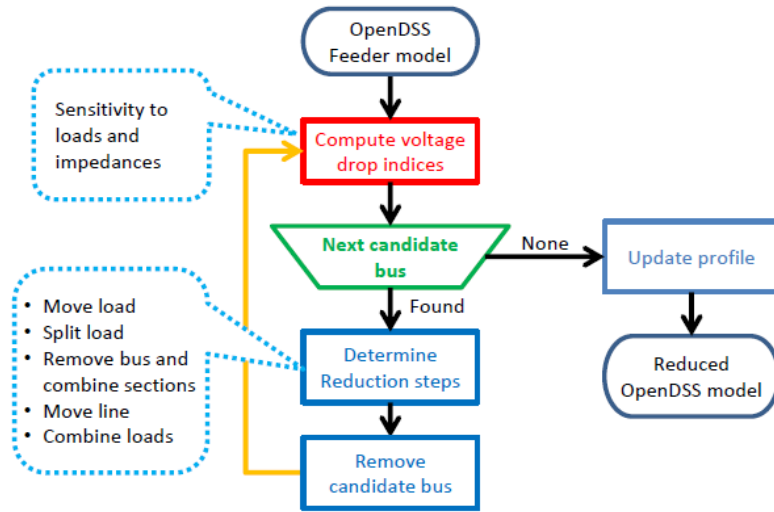


Figure 9-9. Model reduction algorithm based on voltage drop index.

Both, the loading and impedances are expressed in per unit values for a chosen base power and voltage rating. If a bus contains a total load of S_{load} and the adjacent line impedances are Z_1 and Z_2 , corresponding to two connected lines, the voltage drop indices associated with this bus are given by

$$VI = \max(|S_{load}Z_1|, |S_{load}Z_2|)$$

This index is computed for every bus with two adjacent lines, and the bus with the smallest index is removed. In this way, all buses with zero loading will be selected for removal before any buses containing loads. Similarly, buses with low impedance branches (lines, transformers, etc.) relative to the loading on the bus will be selected early in the process.

In a given iteration, once the candidate bus has been selected, the base reduction functions introduced above are used to make the necessary changes to the OpenDSS model to effect the bus removal. If a bus is connected to only one branch, the load on the bus is simply moved to the connected bus, and the branch is removed. If a bus is connected to two branches, the split-and-move approach as described above is used. The resulting algorithm is depicted in Figure 9-9.

9.4.1 Model Reduction Functions

MATLAB functions developed provide the required functionality to setup and execute the model reduction process, interacting with OpenDSS through the COM-interface. Five base reduction steps are necessary to achieve model reduction. Besides this core reduction functions several additional are required to setup the feeder model and execute the reduction process. The functions specifically developed to implement the model reduction process are listed in Appendix C. The core functions are indicated by their short description in the “Reduction step” column, and others are facilitating functions.

The functions have been written in the MATLAB environment and interact with the OpenDSS feeder model through the COM-interface. The set of functions allow the use of OpenDSS models as a starting point for model reduction, and depending on the algorithm chosen additional parameters can be set to configure the reduction process. Additional information is available in the functions documentation, MATLAB help for each of the functions, and browsable function documentation.

9.4.2 Examples

Several examples were developed to test the process and show how the model reduction tool that can be applied to OpenDSS feeder models. In the implementation of the tool, MATLAB functions interact with OpenDSS model via COM-interface. The design is a modular implementation, with the possibility to extend and replace as improvements or refinements are available. As part of the process, input profile data files are updated to match reduced feeder model.

For the current version of the tool, not all OpenDSS elements are handled, but this is not expected to be a limiting factor in power flow time series study feeders (reactors; and generators to be placed after reduction) and/or can be included by building on current functions. Positive sequence impedance is used in splitting loads.

9.4.2.1 Feeder 6

The example chosen to demonstrate the model reduction procedure and algorithms is taken from [6]. The example feeder is referred to herein as “Feeder 6,” and a simplified circuit diagram is shown in Figure 9-10. The diagram also gives the substation voltage, the positive sequence impedance data, and active and reactive load demands. All elements are assumed to be 3-phase and symmetric/balanced, and loads are represented by constant current loads using OpenDSS model type 5. The power flow computation results for the bus voltages and feeder section currents are shown as well. In the following different reduced feeder models are determined and compared.

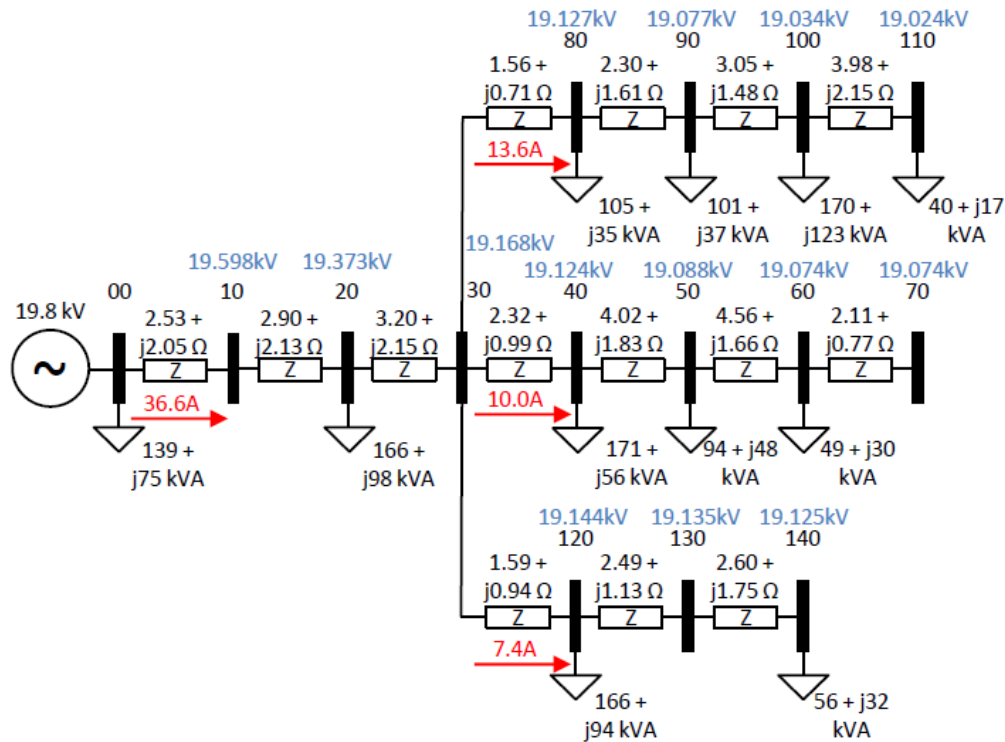


Figure 9-10. Feeder 6 single-line diagram, before reduction.

As a first reduction application example, the feeder is reduced following the steps given in [6] to arrive at a model with only four buses remaining. The reduction steps taken include the custom steps of moving the connection points of two of the branches one section closer to the substation. Note that as no automated procedure can be implemented do detect the need for these two steps, all steps were manually generated and ordered. The possibility to manually implement the reduction process allowed testing the

code implemented. But just as important, the developed program scripts can also be reused by other users. The program scripts available can be used as a starting point to configure reduction steps and to apply reduction steps to other feeder models. Approximately 20 steps are applied in doing so (Table 9-3). The steps are not unique, and several steps can be exchanged while nevertheless still arriving at the same reduced model. Also, the steps and parameters as used here serve an example for the reduction steps automatically generated by the reduction algorithms once a decision of how to handle a bus has been made. The 4-bus reduced model that results from applying these steps is shown in Figure 9-11.

Table 9-3. Steps in first pass reduction of model

No.	Step	Parameters	Comment
1	Move elements	Bus 110	Dangling end, move connected load up
2	Remove bus	Bus 110	Nothing connected, can be removed
3	Remove bus	[Bus 10, Bus 130]	Nothing connected, can be removed, combines adjacent lines
4	Move line	Bus 30, [Bus 20, Bus 80]	Reconnect line 30-80 at Bus 20, updates line impedance and adds load-generation pairs as necessary
5	Move line	Bus 30, [Bus 20, Bus 120]	Reconnect line 30-120 at Bus 20
6	Move elements	[Bus 140, Bus 120],[Bus 120, Bus20]	Moves loads from Bus 140 to 120 and 120 to 20
7	Remove bus	[Bus 140, Bus 120]	Nothing connected, can be removed
8	Split bus	Bus 80, [Bus 20, Bus 90]	Split load at bus 80 and move parts to Buses 20 and 90
9	Remove bus	Bus 80	Nothing connected, can be removed, combines adjacent lines
10	Split bus	Bus 90, [Bus 20, Bus 100]	As above: Split load and move parts to neighboring buses
11	Remove bus	Bus 90, [Bus 20, Bus 100]	Nothing connected, can be removed, combines adjacent lines
12	Split bus	Bus 60, [Bus 50, Bus 70]	As above: Split load and move parts to neighboring buses
13	Remove bus	Bus 60	Nothing connected, can be removed, combines adjacent lines
14	Split bus	Bus 50, [Bus 40, Bus 70]	As above: Split load and move parts to neighboring buses
15	Remove bus	Bus 50	Nothing connected, can be removed, combines adjacent lines
16	Split bus	Bus 40, [Bus 30, Bus 70]	As above: Split load and move parts to neighboring buses
17	Remove bus	Bus 40	Nothing connected, can be removed, combines adjacent lines
18	Split bus	Bus 30, [Bus 20, Bus 70]	As above: Split load and move parts to neighboring buses
19	Remove bus	Bus 30	Nothing connected, can be removed, combines adjacent lines
20	Combine loads		Replaces individual loads by one equivalent, performed for all buses

An example for applying the topology walking algorithm is as follows. The algorithm accepts a list of key buses and parameters as input, and the following has been specified: keep buses 00, 20, 70, and 100, and keep branching points. The algorithm automatically identifies a list of actions to take, followed by applying the actions one at a time. The resulting feeder model is shown in Figure 9-12.

As can be observed by comparing the previous power flow results with respect to the line section currents, the reduction process yields models that do not allow to direct comparison of current flows (though these can be recovered by considering portions of the reconnected loads.)

To demonstrate that current could be preserved if desired, the topology walking algorithm is repeated, but adding the first buses after the branching point (Buses 40, 80, and 120) to the list of key buses. This yields the result depicted in Figure 9-13.

As described above, one of the core reduction steps is to split a load into two parts and connect the load parts at the neighboring buses. This step requires the associated load profile data to be updated accordingly. While the reduction algorithm perform the reduction steps, it keeps track of the ratios computed for the new load parts. Therefore, once the reduction process ended, these ratios can be used to map the original load profile data to the loads in the reduced circuit. This load update process may mean that several of the originally individual loads get mapped into a single equivalent load.

The power flow results for the key bus voltages and feeder current are shown in Figure 9-14. The results for the two feeder circuits are basically indistinguishable.

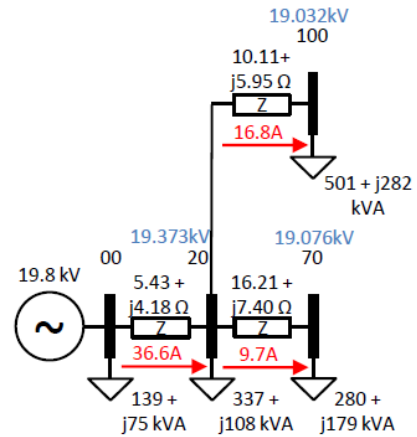


Figure 9-11. 4-bus reduced model

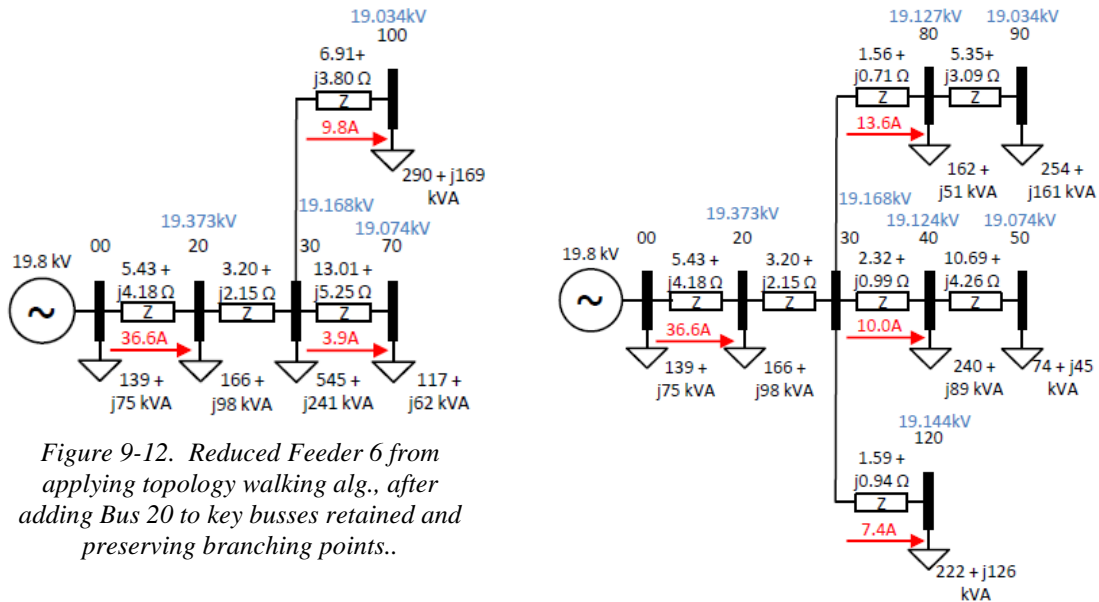


Figure 9-12. Reduced Feeder 6 from applying topology walking alg., after adding Bus 20 to key busses retained and preserving branching points..

Figure 9-13. Reduced Feeder 6. Result for topology walking alg. And preserving section current flows.

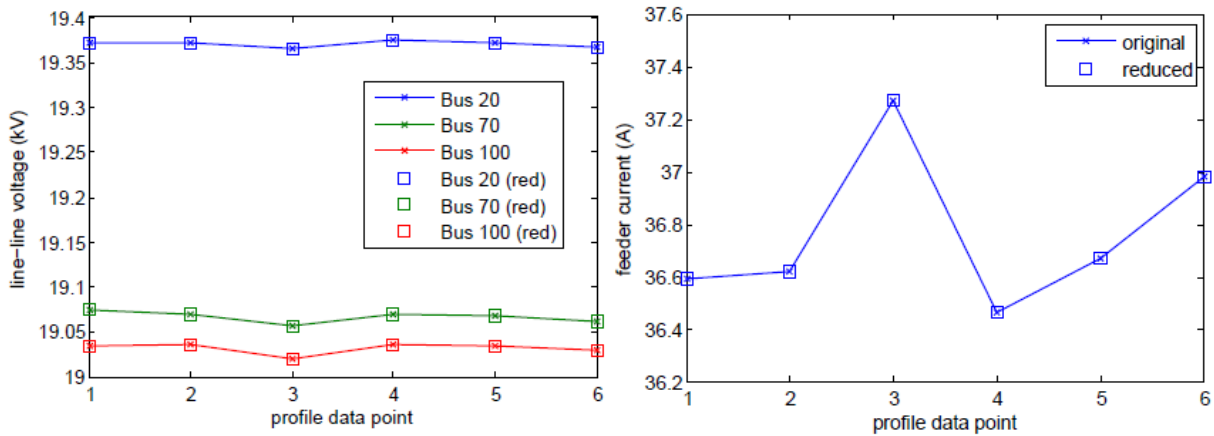


Figure 9-14. Feeder 6 – comparing selected bus voltages and feeder current, original vs. reduced model (topology walking)

9.4.2.2 Feeder 7

The Feeder 6 example documents the fundamental steps in model reduction with simple examples. The Feeder 7 case is used to test the concept on a larger system. The reduction steps and tree walking algorithm are applied to one of the OpenDSS example feeders, “Ckt. 7,” referred herein as Circuit 7. Circuit 7 original feeder structure is shown in Figure 9-15(a), and the locations of the three key buses (181991, 158676, and 182162) used are indicated. The feeder’s corresponding OpenDSS model summary lists 1255 buses, 2232 devices, and 2452 nodes. Note that only 290 buses are used to draw the circuit structure in the original model, i.e., these are the buses with existing x-y-coordinate information available.

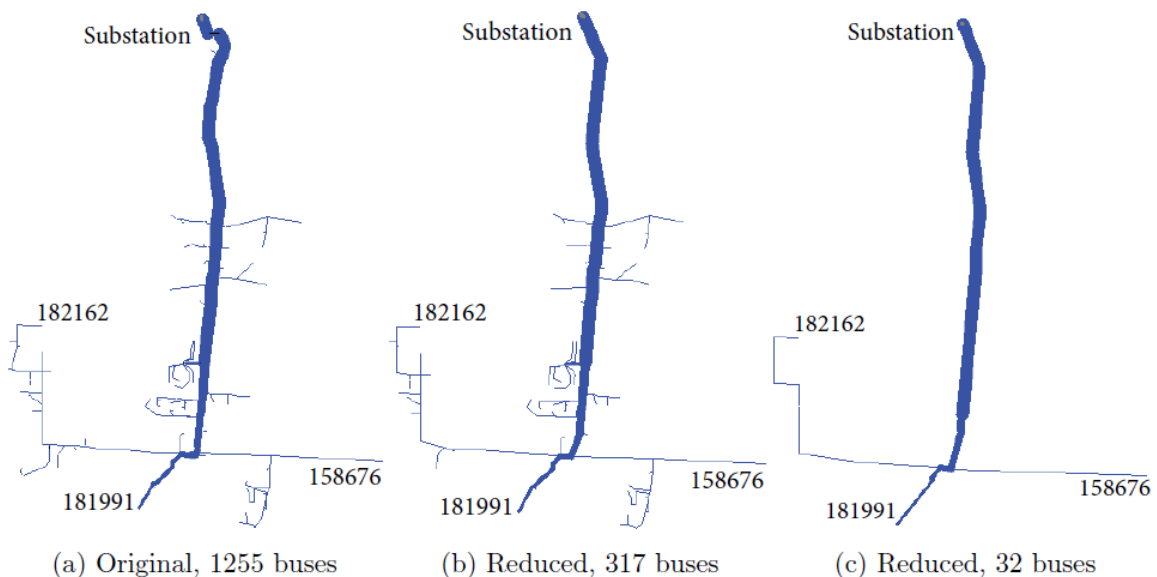


Figure 9-15. Feeder 7 – original circuit and reduced versions

The feeder is basically treated as a grey box and only a few key buses are manually identified in the original model and used as key buses in the reduction algorithm. In the first reduction algorithm application, choices are to not move branching points and keep capacitor banks and transformers. In

addition to the key buses indicated in the figure, the buses at the substation feeding Circuit 7 are specified (SourceBus, Ckt7, and 318412). After model reduction 317 buses, 487 devices, and 636 nodes remain, and 187 buses represent the reduced model in Figure 9-15(b). With respect to buses, a 75% reduction was achieved. By comparing the two feeders, it can be seen that the number of buses can be significantly reduced without losing valuable features in the structure. Note, the coloring and line thickness reflects the power flow as drawn by OpenDSS.

Several power flow computation results were compared to ensure the validity of the reduced model. The following provides a summary of results when modeling all loads as constant current loads, i.e., model=8 and zipv=(0 1 0 0 1 0 0) with minimum voltage of $V_{min} = 0.85$ pu. The selected items of interest are the key bus voltages and feeder current, and the results of the comparison are shown in Table 9-4. To further check on results of the reduced models, the bus distances of the original and reduced model were compared and all found to be correct in the reduced model. Also, there were no significant differences in node voltages.

Further circuit reduction is feasible and shown as a second example here. By specifying the key buses as listed above, including capacitor banks but excluding transformer buses, the circuit is reduced to 32 buses, 122 devices, and 96 nodes. With respect to buses, the outcome reflects a 97.5% reduction. The resulting feeder structure is shown in Figure 9-15(c), and the numerical results for the corresponding voltages and current are listed in Table 9-4. The maximum

Figure 9-4. Comparing original and reduced models (magnitude & angle)

Quantity	Phase	Original	317 bus	32 bus
Voltage at Ckt7 (kV)	1-2	12.660 \angle -4.7	12.659 \angle -4.7	12.667 \angle -4.7
	2-3	12.621 \angle -124.8	12.620 \angle -124.8	12.628 \angle -124.8
	3-1	12.613 \angle 115.4	12.612 \angle 115.4	12.620 \angle 115.4
Current at feeder head (A)	1	207.320 \angle 159.9	207.300 \angle -159.8	206.970 \angle 160.2
	2	215.200 \angle 38.6	215.190 \angle -38.6	214.860 \angle 38.9
	3	207.360 \angle -82.7	207.360 \angle -82.7	206.980 \angle -82.3
Voltage Bus 182162 (kV)	1-2	12.434 \angle -6.0	12.433 \angle -6.0	12.457 \angle -6.1
	2-3	12.402 \angle -126.3	12.402 \angle -126.3	12.426 \angle -126.4
	3-1	12.369 \angle 114.0	12.368 \angle 114.0	12.391 \angle 113.9
Voltage Bus 181991 (kV)	1-2	12.428 \angle -6.0	12.427 \angle -6.0	12.450 \angle -6.1
	2-3	12.399 \angle -126.3	12.399 \angle -126.3	12.423 \angle -126.3
	3-1	12.364 \angle 114.0	12.363 \angle 114.0	12.386 \angle 113.0
Voltage Bus 158676 (kV)	1-2	12.455 \angle -6.0	12.455 \angle -6.0	12.477 \angle -6.1
	2-3	12.427 \angle -126.3	12.426 \angle -126.3	12.449 \angle -126.3
	3-1	12.392 \angle 114.0	12.391 \angle 114.0	12.414 \angle 113.9

difference in bus voltages is 24 V and, based on a nominal voltage of 12.47 kV, this difference is less than 0.2%. The magnitude difference in currents is less than 0.38 A (Phase C), or 0.2% with respect to the original feeder current of 207.36 A.

The corresponding voltage profiles are shown in Figure 9-16. All three profile plots are scaled with the same settings, i.e., the y-axis setting of the 317 bus circuit have been applied to the other two. As chosen in the model reduction setup, the 317 bus feeder differs from the original by eliminating the final line sections that feed customers, and the associated voltage drops are missing in this model. The 32 bus version eliminates all the load transformers but keeps the PV plant interconnection transformer.

The two model reductions required the following number of actions and steps. First, the algorithm generated a list of actions to be taken, e.g., “move elements.” Second, each action was implementing by executing individual steps, e.g., all loads at a bus are moved to a neighboring bus. Reduction to a 317 bus model took 1,877 actions and 3,032 steps, and, reduction to a 32 bus model took 2,447 actions and 29,861 steps.

9.4.3 Conclusion

The availability of reduced distribution feeder circuit models has been important for several reasons. As full-scale models may include several thousand buses, line sections, and loads, parametric time series studies become quickly infeasible. This restriction applied even though today’s power flow solvers are able to handle such systems and may solve for a single solution within seconds. Reduced models allow

researchers and engineers to focus on salient feeder and operation aspects without compromising the results from a quantitative and qualitative view.

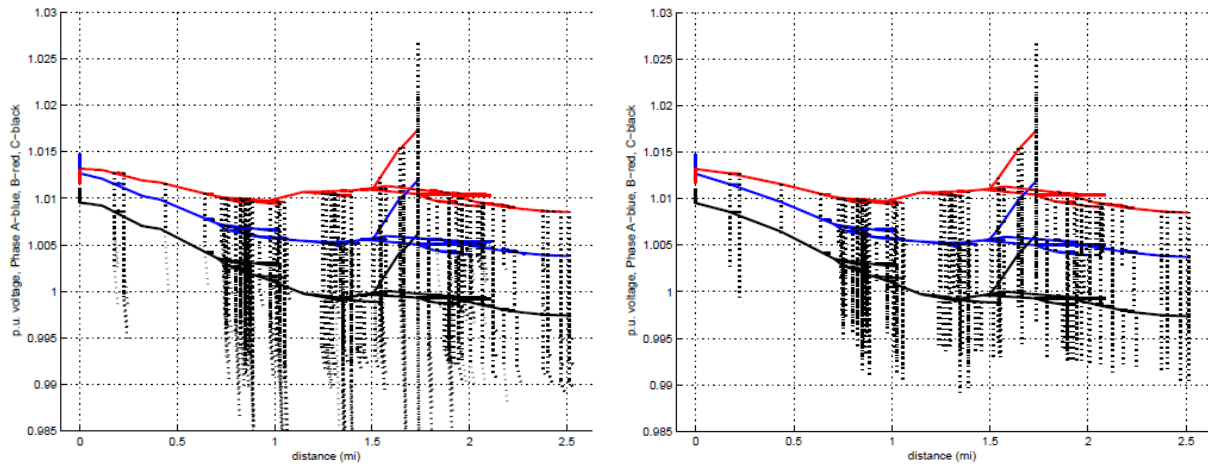


Figure 9-16 . Voltage profiles for (a) left, original 1255 bus system ,and, (b) right, 317 bus model

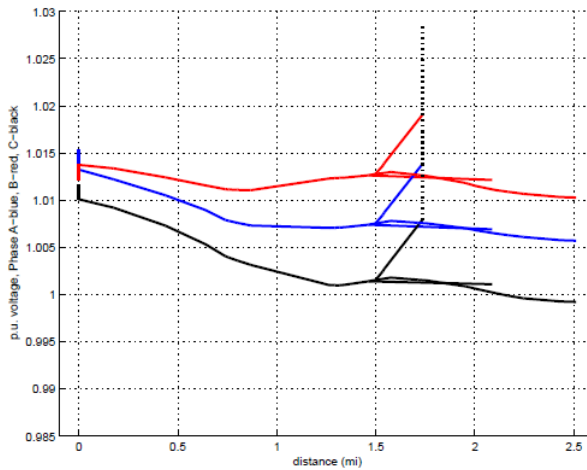


Figure 9-16(c) Voltage profiles for 32 bus model_

This report describes the model reduction approach and salient implementation aspects of both individual reduction steps and algorithms. The algorithms allow automation of the reduction process and are based on the core concept of identifying key buses to keep and candidate buses to remove. Once a candidate bus is identified, steps to remove it from the model are taken. Several customizable parameter choices are provided to allow tailor the reduction process to a specific feeder. The MATLAB functions developed provide the required functionality to setup and execute the model reduction process, interacting with OpenDSS through the COM-interface. As demonstrated in the examples, the reduction process has been successfully tested and the validity of results confirmed. Based on the constant current load model, power flow results for the reduced feeder circuits compare well to the original circuits.

9.5 References

- [1] Electric Power Research Institute, Inc. (EPRI). OpenDSS. <https://sourceforge.net/projects/electricdss/>, 2013.
- [2] The MathWorks Inc. Matlab. <http://www.mathworks.com/>, 2015.
- [3] Harsha Ravindra, M.O. Faruque, Karl Schoder, Rick Meeker, Michael Steurer, and Peter McLaren, “Modeling and validation of a utility feeder for study of voltage regulation in the presence of high PV penetration”, Proceedings of the IEEE PES T&D Conference and Exposition, 2014.
- [4] Harsha Ravindra, “Investigation of dynamic interactions of PV inverters and traditional devices in regulation of voltage on distribution feeders with high penetration levels of solar PV”, Master's thesis, Florida State University, 2013.
- [5] W.H. Kersting, “Distribution System Modeling and Analysis”, Third Edition. Taylor & Francis, 2012.
- [6] Matthew J. Reno, Robert J. Broderick, and Santiago Grijalva. “Formulating a simplified equivalent representation of distribution circuits for PV impact studies”, Sandia National Laboratories, SAND2013-2831, 2013.

10 SYSTEM IMPACT ASSESSMENT – A PARAMETRIC STUDY APPROACH

10.1 Introduction

A systematic method is needed for assessing high penetration solar PV impact and adoption measures on distribution feeders that covers the wide variety of feeder types, operating characteristics, and PV deployment scenarios that are possible. With that as a goal, a system and set of tools for conducting parametric studies of high penetration PV impact using the OpenDSS feeder models has been developed and applied. The variation in feeders, operating characteristics, and deployment scenarios, along with the numerous, often interdependent, influencing factors involved, makes development of an effective and practical systematic approach somewhat challenging.

The approach developed makes use of quasi-steady state power flow simulation using OpenDSS, nominally using a one-minute simulation time-step size. This allows exploration of potential impacts on the system such as voltage regulation, the numbers of operations of voltage regulation devices, reverse power flow, losses, and line loading. However, the approach described here is not used in the analysis of some of the other important impact considerations, such as the short-circuit impact of DG, grounding issues, unintentional island detection, and some power quality issues such as harmonic distortion or flicker. Thus, while the method and studies presented are certainly not comprehensive, the goal is to gain general insight into the relationships between some of the important influencing factors and some of the important impact categories in order to more easily identify situations in which high penetration PV may present challenges and some of the mitigation methods that may be most appropriate.

The approach employed generally consists of identifying parameters of the system to be studied, defining an experimental design for exploring the parameter space, executing the simulations at the specified points, computing response quantities, and studying the relationships between input parameters and output response quantities. While no set of parameters is universally applicable or comprehensive, an attempt has been made to identify parameters that are as widely applicable as possible.

The experimental design (sets of parameter values at which to evaluate the simulation model) may be tailored to specific purposes of the parametric studies, such as factor screening or sensitivity analysis, or for developing a regression model, for example. While generating an experimental design is a large topic beyond the scope of this document, several methods are described herein, and references to additional material on this subject have been included. Examples for generating designs using the freely available and open-source software package, R, have also been included.

To facilitate variation of parameters and manipulation of the OpenDSS feeder models, a set of MATLAB functions has been developed, which make use of a COM interface with OpenDSS. While the output of each OpenDSS simulation is inherently a set of time-domain waveforms, an attempt is made to summarize the results of each simulation run through a set of scalar response quantities. These scalar response quantities are intended to quantitatively reflect impacts on the system, such as the number of operations by voltage regulation devices, or the amount of time voltage excursions beyond acceptable limits are observed. Again, to the extent possible, an attempt has been made to identify response quantities that are as widely applicable as possible, in order to allow comparison from one feeder to another.

The approach is described in further detail in the full System Impact Assessment - Parametric Study report, along with examples applying the methods. Examples are given making use of several feeder models, which are reduced models of feeders that are based on actual circuits in Florida. These models were described in Sections 6 and 9.3. The developed MATLAB functions that are employed are listed in Appendix~D.

10.2 Approach

MATLAB is generally used to set up and initiate simulations, while OpenDSS is used as the simulation engine. The approach generally begins with identifying the parameters of the system to be varied, and an attempt has been made to identify parameters which are as generally applicable (meaning applicable to a wide range of feeder models) as possible. It is then necessary to implement a MATLAB function to allow these parameters to be modified.

10.2.1 Process Description

The general approach employed for studying the relationships between impact factors and behavior of the feeders includes:

- Identifying the system parameters to be varied, and implementing a function to manipulate the OpenDSS models, execute simulations, and save time-domain results.
- Constructing one or more experimental designs (sets of parameter values for which the simulation model is to be executed) for exploration of the parameter space.
- Executing the simulation at each point in the experimental design set through calling the implemented function.
- For each point in the experimental design, convert the set of time-domain results into a representative set of scalar response quantities.
- Study and characterize the relationships between the parameters and response quantities.
- Augment the experimental design and repeat the process, or craft additional studies to better characterize relationships.

It is expected that this process is iterative, and depending on results obtained, may require additional parameters to be included, refinement of the ranges of parameters, augmentations to experimental designs to be added, additional response quantities included, and new studies to be executed. The selection of parameters is described in more detail in the full System Impact Assessment - Parametric Study report.

The overall process is illustrated by Figure 10-1, in relation to the implemented MATLAB functions. An input matrix is first generated based on an experimental design to explore the parameter space. The input matrix is then provided to the function, which sequentially calls the function which has been configured for this set of parameters. For each entry (set of parameter values) in the input matrix, a set of time-domain results is generated. The function is used to generate a set of scalar response quantities used to summarize the time domain response from a simulation run. This function is called for each entry in the input matrix, and is then used to generate a response matrix containing the response quantities for each simulation run. The response matrix can then be used in conjunction with the input matrix to analyze the influence of the input parameters on each of the response quantities for characterization of the relationship between the influencing factors and the impact indices.

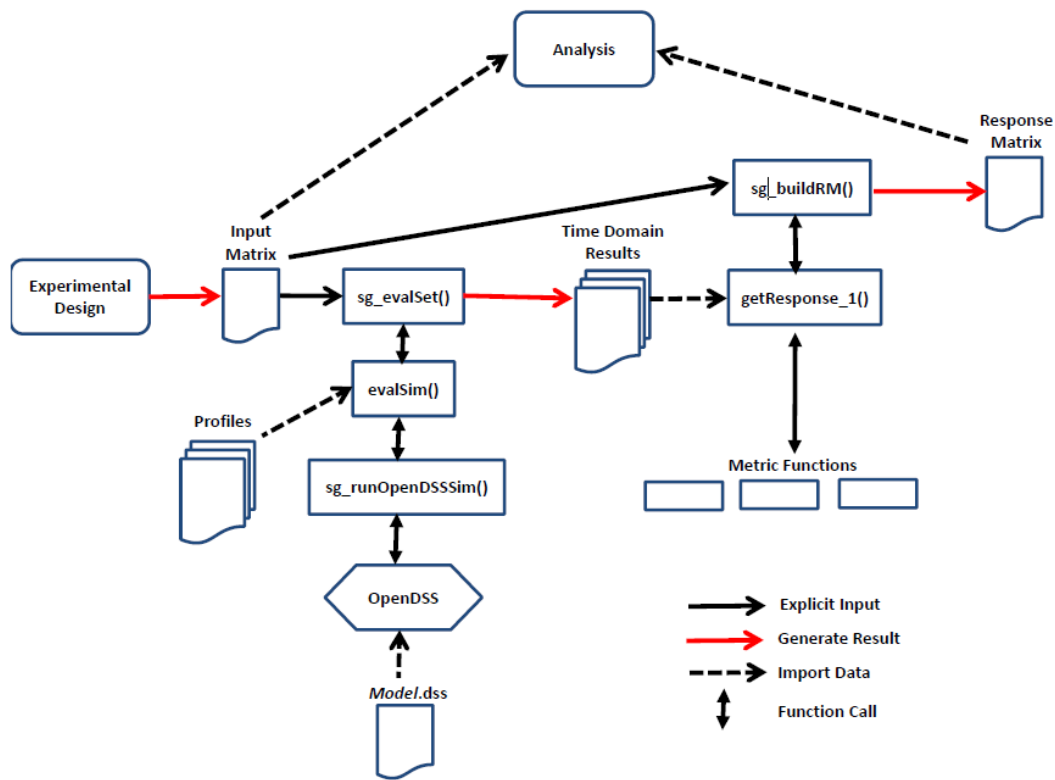


Figure 10-1. Approach

An attempt was made to allow the function to be used with different feeder models. To support this, the function accepts a structure of constants as an optional argument, with these constants providing key information about the feeder (e.g. the OpenDSS file, the base MVA of the substation transformer, maximum loading of the feeder, etc.) that is needed for interpretation of the parameters passed in.

10.2.2 PV and Load Profiles

One of the key decisions in structuring the approach for this work was in handling the PV and load profiles for the parametric studies. One option was to parameterize these profiles such that random, synthetic PV and load profiles would be generated based on characterizing parameters. However, due to the challenges (and uncertainty of suitability) in determining this set of descriptive parameters and implementing functions for random generation of realistic profiles, this approach was not taken.

Rather, the approach employed in this work makes use of representative sets of actual profiles, broken into single-day durations. Normalized (measured power divided by the rated power of the PV plant), one-year sets of profiles were constructed for several plants with different power ratings. All sets make use of one-minute resolution data, as this was chosen as the time-step size to be used for the OpenDSS simulations. This choice was motivated by a desire to consider the impacts of PV on voltage regulation controls (which typically have operation times on the order of several minutes), a desire to maintain a reasonable execution time for the simulations, and by the availability of data with this time-resolution from PV sites. Thus, the parameters specifying the PV and load profile were treated as discrete parameters which specified a particular day's profile (from the available sets) to be used for each.

In general, the approach was intended to study the effects based on a one-year set of profiles. However, as the computational effort required for simulating an entire year would severely burden the exploration of a

parameter space including numerous parameters, an approach was used whereby a representative subset of the profiles from the annual set were used to approximate the behavior of the feeder over a year.

10.2.3 Model Parameters

There are numerous ways to parameterize the system.⁷ As a starting point, parameters are selected that are applicable to a wide set of feeder models and that, as much as possible, are uncorrelated with each other.

In this work, the matrices of parameter values (input matrices) were generated using R, and these were saved as comma separated value (csv) files for use by the MATLAB functions used to execute the simulations.

To begin with, a set of feeder model constants are defined, as shown in Table 10-1.

Important basic feeder parameters are defined in Table 10-2, including source impedance, load utilization factor (LUF), load power factor, several parameters that define the nature of the PV on the system, including capacity and how it is distributed. Some parameters are normalized to feeder capacity and load transformer rating.

Figure 10-2 illustrates how load scale, total residential PV power, total bulk PV power, and total PV power are determined from the feeder parameters. Generally, residential PV power refers to smaller distributed PV systems and bulk PV power refers to larger systems (large commercial or utility scale systems).

To support studies involving PV participation in voltage regulation, a set of parameters is defined that allows selection of several voltage regulation options and the ability to set, to a limited degree, the behavior of those options (i.e. the shape of the control ‘curves’). These parameters are shown in Table 10-3, along with, as an example, the volt-VAR curve option.

Table 10-1. Feeder Model Constants

Symbol	Description
SSXfmrSb	The base apparent power (MVA) for the substation transformer supplying the feeder.
SSBasekv	The base voltage rating (kV) for the bus representing the substation.
SSXfmrXtoR	The X/R ratio for the substation transformer.
ScapacityFeeder	The maximum capacity (MVA) of the feeder. This corresponds to ratings of lines and/or over-current relay settings.
SmaxFeeder	The maximum loading (kVA) on the feeder. This is based on known loading data for the feeder.

Table 10-2. Feeder Parameters

Symbol	Description
Zsrc	Source impedance (pu).
LUF	Load utilization factor, defined as ratio of maximum load on feeder to rated feeder capacity.
LoadPF	The power factor to be applied to all loads in the system.
PVpen	PV penetration level (total).
PVres	Residential PV power capacity as a fraction of load transformer kVA rating.
BulkPVPos	A value on the interval [0 1] specifying the distance from the substation (as a fraction of the maximum bus distance from the substation) at which the bulk PV is located.
PVProfile	A discrete parameter specifying the normalized PV power profile to be used.
LoadProfile	A discrete parameter specifying the normalized load power profile to be used.

⁷ The construction of experimental designs to explore the parameter space is a broad and involved topic, the full discussion of which is beyond the scope of this document. Detailed information can be found in the references.

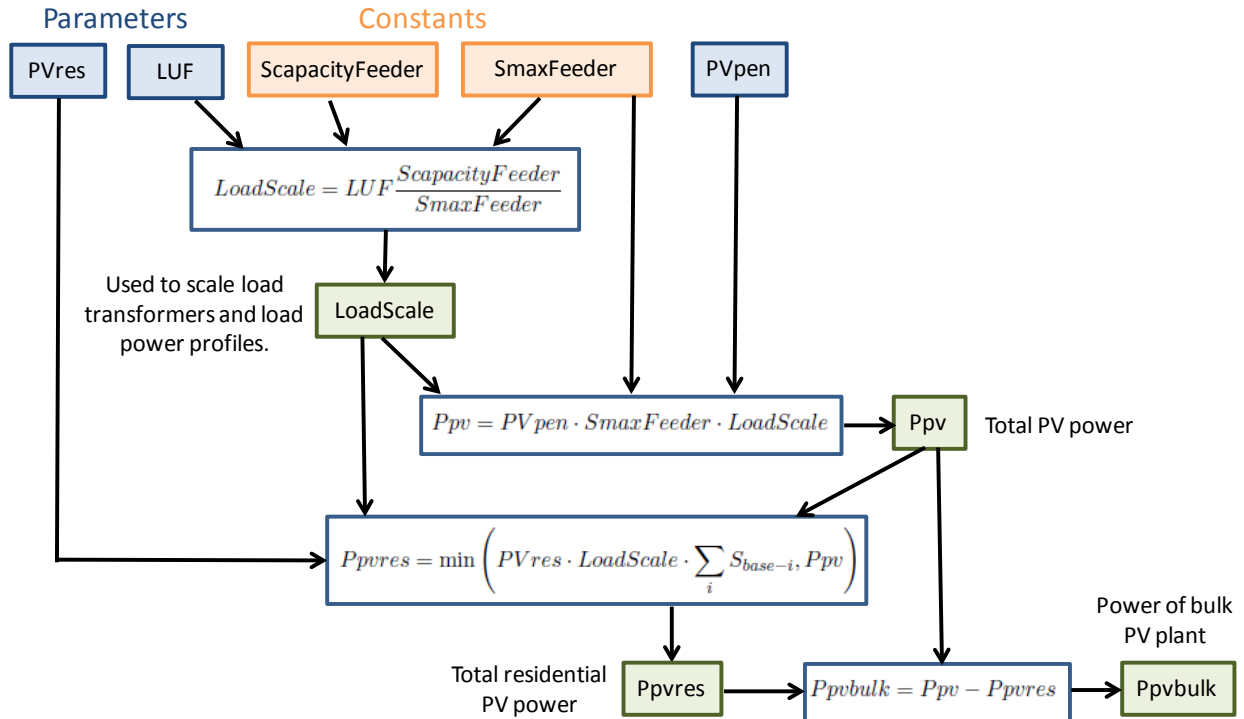


Figure 10-2. Calculation of load and PV power scaling factors

Table 10-3. PV Reactive Power Control Parameters

Symbol	Description
PVctl	Control mode (none, Volt-Power Factor, Volt-VAR, Power-Power Factor)
PVctlXDBwidth	Used to control the width of the deadband in the characteristic.
PVctlXwidth	Range used for X-axis of characteristic.
PVctlXCenter	Specifies center of X-axis of characteristic.
PVctlYwidth	Range used for Y-axis of characteristic.
CapDisable	Disables capacitor bank controls.
PVctlRes	Restricts reactive power controls to only the bulk PV or applies to residential, as well.

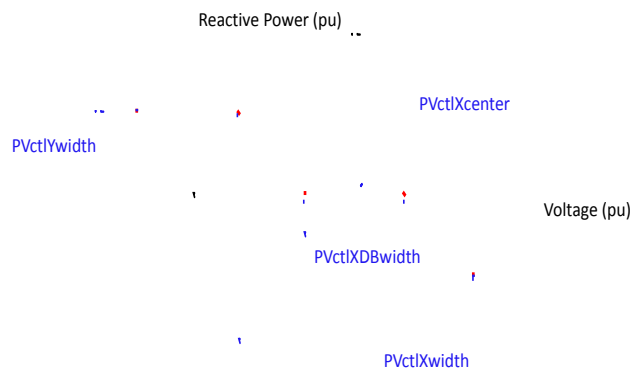


Figure 10-3. Configurable Volt-VAR curve

10.2.4 Response Quantities

A number of scalar response quantities are defined and used to summarize the time-domain results from each run. For each execution of the simulation, results included the voltage at each bus, the real and reactive power contribution from PV sources, the real and reactive power of loads, and the status of capacitor banks and voltage regulators. .

The response quantities are implemented in a MATLAB function. The function is called for each rung in the input matrix, returning the associated matrix of response quantities computed from the time-domain results. The response matrix is written to a csv file, so that the analysis of the results (characterization of relationships between parameters and response quantities) can be done with R, MATLAB, or any other software package capable of importing ASCII files. The methods for analysis of the results are closely related to the experimental design approaches.

Response quantities are selected that are comparable for disparate feeders. As pre-defined load and PV power profiles are used, “response quantities” are also defined as a convenient and flexible way to characterize the profiles.

The entire list of response quantities and their descriptions are shown in Table 10-4. Several are unique and were developed as part of this effort to be particularly useful for the purpose of studying high-penetration solar PV impact.

Inspired by the widely used distribution system reliability indices defined in IEEE standard 1366, two new indices, for use as response quantities in these systematic impact studies, were defined, SALII and CALII. These indices provide a weighted measure of voltage excursions over time, one based on all loads, one based on loads having experienced an excursion. SALII and CALII are calculated as follows:

$$SALII = \frac{\sum_{i \in L_{ex}} \int P_i(t) I_{ex}[V_i(t)] dt}{\sum_{i \in L} \int P_i(t) dt} \quad (10.1)$$

$$CALII = \frac{\sum_{i \in L_{ex}} \int P_i(t) I_{ex}[V_i(t)] dt}{\sum_{i \in L_{ex}} \int P_i(t) dt} \quad (10.2)$$

$$I_{ex}(V) = \begin{cases} 0, & \text{for } V_{limit-min} \leq V \leq V_{limit-max} \\ 1, & \text{otherwise} \end{cases} \quad (10.3)$$

Here, L represents the set of all loads in the system, and L_{ex} represents the set of loads that experience an excursion in terminal voltage beyond the specified limits. Functions $P_i(t)$ and $V_i(t)$ represent the instantaneous power into load i and the instantaneous per unit voltage at the terminals of load i, respectively. The function $I_{ex}()$, defined in (10.3), is used as an indicator function, which assumes a value of 0 when its argument voltage falls within the specified voltage limits, and assumes a value of 1, otherwise. Thus, in the numerator of (10.1) and (10.2), the load power at each load is integrated over the time durations for which voltage excursions at the terminals of the load occur. In (10.1), this integrated power is normalized by the total power of all loads integrated over the entire time duration. In (10.2), the numerator is normalized by the total power of all loads experiencing excursions, integrated over the entire time duration. If the excursion of the voltage at a load were treated as an interruption, these indices reflect the proportion of the total energy to all customers and to affected customers that would be expected to be lost on a daily basis.

Table 10-4. Response Quantities

Symbol	Description
CapSwAvg	The average number of capacitor switching actions per capacitor per day (switching actions during a one hour initialization period are ignored).
VregSwAvg	The average number of voltage regulator switching actions per voltage regulator per day (switching actions during a one hour initialization period are ignored).
Vmax	The maximum voltage (pu) observed over any bus over the duration of the run.
Vmin	The minimum voltage (pu) observed over any bus over the duration of the run.
dVmax	The maximum absolute deviation from nominal (pu) of any bus over the duration of the run.
Vrange	The maximum difference (pu) between the highest and lowest bus voltages at any time over the duration of the run.
SALII_A	System average load impact index evaluated for ANSI A voltage limits.
CALII_A	Customer average load impact index evaluated for ANSI A voltage limits.
SALII_B	System average load impact index evaluated for ANSI B voltage limits.
CALII_B	Customer average load impact index evaluated for ANSI B voltage limits.
FLLR_u	Mean of feeder loss-to-load ratio [5].
FLLR_std	std Standard deviation of feeder loss-to-load ratio [5].
RPFp	Proportion of time for which there is a reverse power flow.
Pgen_u	The mean of the total power supplied by all PV sources (kW).
Pgen_std	The standard deviation of the total power supplied by all PV sources (kW).
PgenVI	The high frequency power variability index associated with the total power supplied by all PV sources.
Pgenrate2_u	The mean of the ramp rates associated with the total power supplied by all PV sources (kW/s).
Pgenrate2_std	The standard deviation of the ramp rates associated with the total power supplied by all PV sources (kW/s).
PgenRampMag2_u	The mean of the ramp magnitudes associated with the total power supplied by all PV sources (kW).
PgenRampMag2_std	The standard deviation of the ramp magnitudes associated with the total power supplied by all PV sources (kW).
PgenRampDur2_u	The mean of the ramp durations associated with the total power supplied by all PV sources (s).
PgenRampDur2_std	The standard deviation of the ramp durations associated with the total power supplied by all PV sources (s).
Pload_u	The mean of the total power for all loads (kW).
Pload_std	The standard deviation of the total power for all loads (kW).
Qload_u	The mean of the total reactive power for all loads (kVAR).
Qload_std	The standard deviation of the total reactive power for all loads (kVAR).

Other response quantities related to the behavior of the feeder include FLLR_u, FLLR_std, and RPFp. The feeder loss-to-load ratio (FLLR) is defined as in (10.4), providing a measure of system losses, normalized by the system load. As the introduction of PV may increase or decrease system losses, response quantities FLLR_u and FLLR_std provide indications of the mean and standard deviation, respectively, of the FLLR over the duration of a simulation run. The response quantity RPFp indicates the proportion of time during which a reverse power flow is experienced at the substation.

$$FLLR(t) = \frac{P_{loss}(t)}{\sum_{i \in L} P_i(t)} \quad (10.4)$$

Response quantities Pgen_u, Pgen_std, PgenVI, Pgenrate2_u, Pgenrate2_std, PgenRampMag2_u, PgenRampMag2_std, PgenRampDur2_u, and PgenRampDur2_std are used to describe the characteristics of the power produced by the PV sources.

In the case where the PV power injections are all scaled versions of the specified profile, these primarily just provide characterization of the applied PV profile. As such, these may also be treated as input parameters in some of the analyses.

Response quantity suffixes ‘u’ and ‘std’ indicate the mean and standard deviation of the total power produced by the PV sources over the duration of the simulation.

A new metric defined for use as a response quantity, again particularly useful for high penetration PV studies, is the high frequency power variability index (HFVI) given by (10.5),

$$HFVI = \frac{\sum_{k=2}^n \sqrt{[1000\hat{P}(k) - 1000\hat{P}(k-1)]^2 + \Delta t^2}}{\sum_{k=2}^n \sqrt{[1000\hat{P}_{lf}(k) - 1000\hat{P}_{lf}(k-1)]^2 + \Delta t^2}} \quad (10.5)$$

This index is motivated by the variability index described in [6], which computes the ratio of the “length” of an irradiance profile to the “length” of the corresponding global horizontal irradiance (GHI) curve. However, as power profiles from PV plants with tracking systems do not necessarily closely follow the associated irradiance curve, and because irradiance data is not always available with power profiles, the modified metric defined here was used. For this metric, a low frequency version of the normalized (by the rating of the PV plant) PV power profile, \hat{P}_{lf} , is first obtained by filtering the normalized profile, \hat{P} .

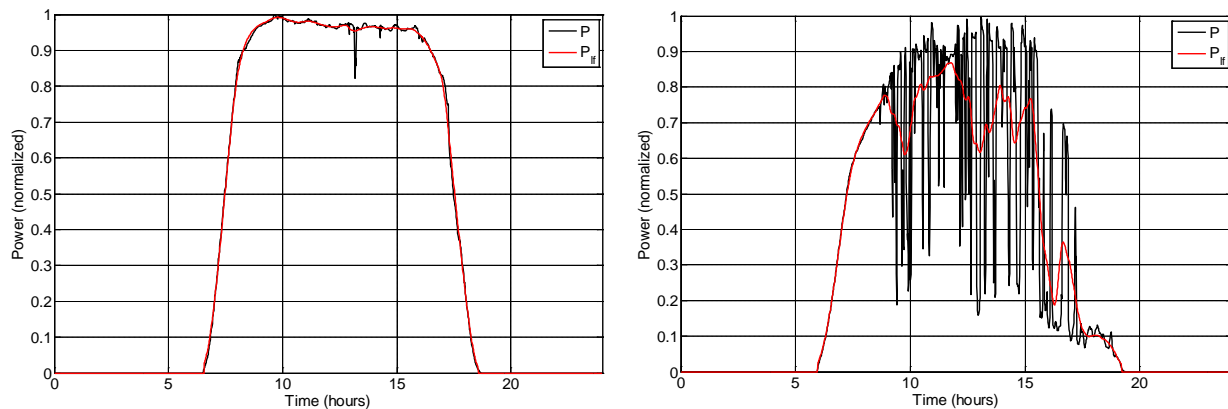


Figure 10-4. Normalized power and filtered power for calculation of HFVI, (a) left, HFVI=1, (b), right, HFVI=10

For filtering, a second-order Butterworth filter with a cutoff frequency of $1.74e-4$ Hz (corresponding to the 15th harmonic with a 1 day fundamental period) is applied. Using a time increment, Δt , of 1 minute, the HFVI is then calculated using (10.5), where the profiles are discretized and k is used as the index. Because the “distance” measure of the variability index is taken over incompatible dimensions, results are very sensitive to the units. Thus, the multiplication of the normalized power quantities by 1000 is necessary to obtain index values comparable to those obtained with the irradiance variability index. This metric essentially provides an indication of the variability of the high frequency portion of the profile. Example profiles, showing the original profile and the filtered, low frequency version, are illustrated in Figure 10-4].

Response quantities $P_{genrate2_u}$, $P_{genrate2_std}$, $P_{genRampMag2_u}$, $P_{genRampMag2_std}$, $P_{genRampDur2_u}$, and $P_{genRampDur2_std}$ indicate the mean and standard deviation of the rates, magnitudes, and durations of the ramps and are based on decomposing the power profile into a series of ramps. This is done using the GE Archive Compression algorithm from the GE Proficiency Historian software [7], [8].

Response quantities P_{load_u} , P_{load_std} , Q_{load_u} , and Q_{load_std} indicate the mean and standard deviation of the real and reactive components of the total load. Like the response quantities associated with the total PV power, these response quantities may also be useful to treat as inputs in analyses.

10.3 Design and Analysis of Experiments

The design and analysis of experiments focus on efficiently exploring a parameter space in order to characterize the influence of input parameters on outputs of a system or model. These topics are addressed in a number of fields, including design of experiments [9],[10], design and analysis of computer experiments [11],[12], data mining and machine learning [13],[14], as well as in specific application areas, such as sensitivity analysis [15]. Some of these fields and approaches focus on application to physical experiments, which inherently include uncontrolled factors and random variation, while others focus specifically on deterministic simulations, such as those considered herein.

However, while some considerations may be needed in applying some of the methods to exploration of simulation models, a large volume of the methods in these fields can be brought to bear in analyzing the feeder models considered. Some of the methods are aimed at specific purposes, such as identifying the most influential factors or studying effects of particular factors, while other techniques more generally focus on developing empirical models of the input-output relationships. These empirical models can then be used as surrogates for the actual simulation models in performing computationally intensive analyses such as uncertainty propagation or robust design. While a complete treatment of the subject is well beyond the scope of this document, a summary of some of the potentially useful techniques is given below, along with references to sources providing additional detail.

10.4 Selection of Representative Subsets of PV and Load Profiles

In studying the impact of PV penetration on feeders, it is often necessary to consider the effects over an extended period, such as a year. However, the computational burden of simulating a full year of operation can present difficulties when attempting to explore a parameter space of even moderate dimensions.

Thus, it is desirable to select a subset of representative profiles from a set, and use this subset to estimate the response quantities that would be associated with execution of the larger set. While a simple approach might be to randomly select a set of profiles from the larger set (e.g. select one profile from each month of an annual set), this may not produce a set that is very representative of the overall characteristics of the larger set.

An alternative approach that may yield a more representative set is to develop a set of scalar quantities that generally characterize the time-domain profiles, and employ a clustering algorithm to categorize the profiles into sets of similar profiles. Points near the centers of each of the groups can then be selected as

representatives for the groups. As the combination of load and PV profile plays a significant role in the behavior of the feeder circuit, it may be useful to apply the clustering algorithm to a set of response quantities representing both the PV and load profiles.

Figure 10-5 illustrates example clusters selected from a one-year set of load and PV profile data. In this case, the clustering was done based on the PgenVI, Pgen_u, and Pload_u response quantities, and results are illustrated in terms of the PgenVI and Pgen_u response quantities.

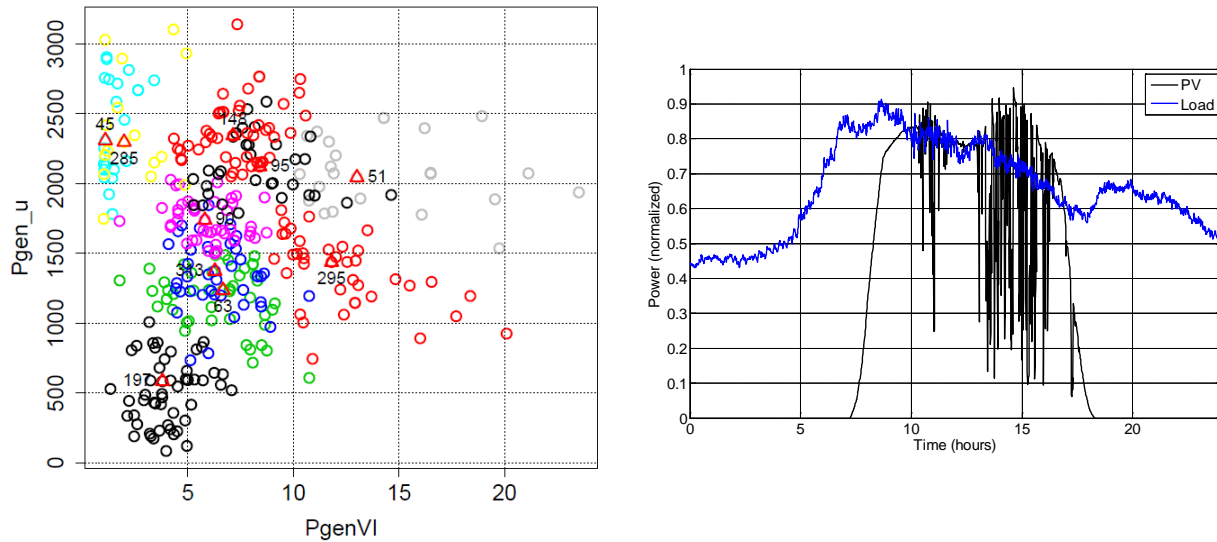


Figure 10-5. (a), left, Clusters Selected using Pgen_u, PgenVI, and Pload_u Based on One Year Profile Set; (b), right, PV-load profile pair 51

By taking a weighted average of each of the response quantities (weighted by the number of points in each cluster), the annual average of each response quantity can be approximated by the results based on the representative set. The accuracy of this approximation is dependent on a number of factors, including the number of groups (and, hence, points) selected, the variation in the original set of points, and the characteristics of the system being studied. While there is no guarantee that results from a selected subset will provide a good approximation over the entire space of system parameters to be varied, it is expected that results based on subsets selected through only the characteristics of the input profiles (as opposed to system response quantities based on simulations with these profiles) would be less sensitive to changes in the system and system parameters. The approach described above may be a reasonable method to approximate the year-long performance of a system using a subset of the profiles in order to facilitate exploration of the parameter space.

10.5 Examples and Selected Results

One of the studies performed using these methods examines effects of source impedance (Z_{src}), PV penetration level (PVpen), and load utilization factor (LUF) on Feeder 3, using a Latin Hypercube Sample experimental design method. Executing the simulation (using the Feeder 3 OpenDSS model and appropriately configured parameters and input matrices), results from representative profile pairs are used to estimate response quantities for an annual set. The results are shown in Table 10-5, with 20 sets of values for the three input parameters on the left and the resulting response quantities (in this case, capacitor bank and voltage regulator switching) on the right.

Relationships between input parameters and output response quantities are then examined for single days and annual averages, and, an attempt is made to fit regression models, initially to quadratic models, then pared down with stepwise regression. The resulting regression equations for 12 response quantities are shown in Table 10-6.

Table 10-5. Response Quantities for Feeder Losses and Reverse Power Flow

No.	Zsrc	LUF	PVpen	No.	CapSwAvg	VregSwAvg
1	0.115	0.309	0.907	1	0.188	1.638
2	0.102	0.511	1.734	2	0.608	3.153
3	0.094	0.488	0.662	3	0.298	1.000
4	0.114	0.433	0.548	4	0.475	2.186
5	0.108	0.551	0.404	5	0.780	2.597
6	0.109	0.690	1.317	6	0.620	7.181
7	0.112	0.287	1.250	7	0.188	1.671
8	0.104	0.411	1.091	8	0.586	2.151
9	0.087	0.618	1.066	9	0.773	3.359
10	0.104	0.657	0.946	10	0.620	5.674
11	0.120	0.637	0.801	11	0.663	6.323
12	0.081	0.598	1.628	12	0.813	3.934
13	0.091	0.326	1.589	13	0.188	0.638
14	0.083	0.536	0.336	14	0.662	1.000
15	0.100	0.262	0.754	15	0.142	1.389
16	0.097	0.744	0.619	16	0.586	3.874
17	0.117	0.456	1.433	17	0.245	2.507
18	0.090	0.723	1.520	18	0.625	4.121
19	0.095	0.367	0.272	19	0.264	1.704
20	0.085	0.397	1.224	20	0.527	2.016

Table 10-6. Response Quantities for Feeder Losses and Reverse Power Flow

Response Quantity	Formula	R^2	R^2_{adj}	κ
CapSwAvg	$k_0 + k_1 PVpen + k_2 Zsrc + k_3 LUF + k_4 LUF^2 + k_5 PVpen \cdot Zsrc$	0.791	0.716	3.09
VregSwAvg	$k_0 + k_1 PVpen + k_2 Zsrc + k_3 LUF + k_4 PVpen^2 + k_5 Zsrc^2 + k_6 LUF^2 + k_7 PVpen \cdot LUF + k_8 Zsrc \cdot LUF$	0.913	0.850	5.11
Vmax	$k_0 + k_1 PVpen + k_2 LUF + k_3 LUF^2 + k_4 PVpen \cdot LUF$	0.979	0.973	3.19
Vmin	$k_0 + k_1 PVpen + k_2 Zsrc + k_3 LUF + k_4 LUF^2 + k_5 PVpen \cdot Zsrc$	0.986	0.981	3.09
dVmax	$k_0 + k_1 PVpen + k_2 LUF + k_3 LUF^2 + k_4 PVpen \cdot LUF$	0.979	0.973	3.19
Vrange	$k_0 + k_1 PVpen + k_2 Zsrc + k_3 LUF + k_4 PVpen \cdot Zsrc + k_5 PVpen \cdot LUF$	0.969	0.958	2.86
SALILA	$k_0 + k_1 PVpen + k_2 LUF + k_3 PVpen^2 + k_4 PVpen \cdot LUF$	0.922	0.901	3.36
CALILA	$k_0 + k_1 PVpen + k_2 LUF + k_3 PVpen^2 + k_4 LUF^2 + k_5 PVpen \cdot LUF$	0.922	0.895	4.43
SALILB	$k_0 + k_1 PVpen + k_2 Zsrc + k_3 LUF + k_4 PVpen^2 + k_5 PVpen \cdot Zsrc + k_6 PVpen \cdot LUF + k_7 Zsrc \cdot LUF$	0.948	0.917	4.26
CALILB	$k_0 + k_1 PVpen + k_2 Zsrc + k_3 LUF + k_4 PVpen^2 + k_5 PVpen \cdot Zsrc + k_6 PVpen \cdot LUF + k_7 Zsrc \cdot LUF$	0.952	0.923	4.26
FLLR_u	$k_0 + k_1 PVpen + k_2 Zsrc + k_3 LUF + k_4 PVpen^2 + k_5 PVpen \cdot LUF + k_6 Zsrc \cdot LUF$	0.997	0.996	4.06
RPFp	$k_0 + k_1 PVpen + k_2 PVpen^2$	0.969	0.966	3.17

A study was performed on Feeder 3 to examine the use of power factor control for PV inverters to regulate voltage on the feeder. There is a single bulk PV plant at the end of the feeder. For the design matrix, a sweep of PVpen was performed and the design replicated for 10 representative profile pairs. Multiple cases of voltage mitigation were considered, including no PV participation in control, reactive power control with PV inverters, and reactive power control with PV inverters with different deadband settings on the existing step voltage regulators.

For the *base case*, load impact indices (SALII, CALII) increase significantly with PV penetration and voltage regulator switching increases slightly. For the *PV inverter control case*, inverter participation in voltage regulation is found to help mitigate effects on load impact indices, but, causes a significant increase in voltage regulator switching operations. However, increasing the deadband on the voltage regulators is found to mitigate the effects on the voltage regulator switching.

And, as a final example, a study was done using a two-level factorial design to explore influence of Source impedance (Z_{src}), Load utilization factor (LUF), PV penetration (PVpen), Position of bulk PV (BulkPVPos), and Residential PV (PVres). The design was replicated for 10 representative profile pairs and applied to Feeders 1, 2, 3, and 4 and compare relative influence of factors. The results were analyzed based on annual estimates using half-normal plots of the effects.

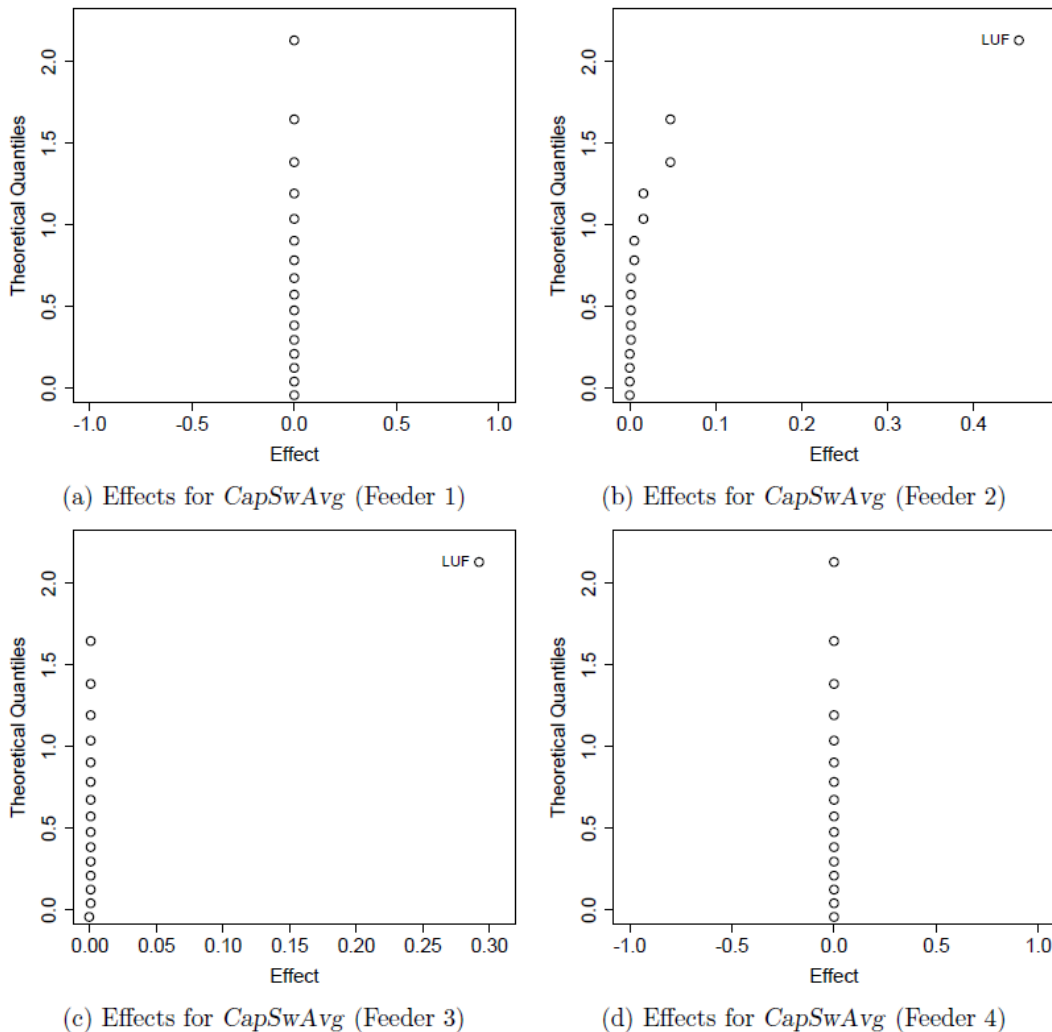


Figure 10-6. Half normal plots showing influencing factors on SCB switching.

Figure 10-6 shows half-normal plots of average number of capacitor switching events per day for each feeder. Feeders 1 and 4 do not have switched capacitor banks (SCB's). The plots indicate that LUF is the dominant factor affecting SCB switching count for Feeders 2 and 3.

Figure 10-7 examines average number of voltage regulator switching events per day. Feeders 1 and 4 do not have step voltage regulators (SVR's) either. Voltage regulators for Feeder 2 do not show switching response. LUF and source impedance appear as the dominant factors affecting switching for Feeder 3.

Figure 10-8 examines impact on the ANSI A voltage impact load index, SALII_A. LUF is found to be influential for all four Feeder models, with less impact on Feeder 2. Source impedance, Zsrc, is found to be influential on Feeder 1, but not PVpen. PVpen and BulkPVpen appear to play an important role on Feeders 3 and 4. And, interaction of BulkPVpen is particularly influential on Feeder 4 (parts of feeder have higher impedance).

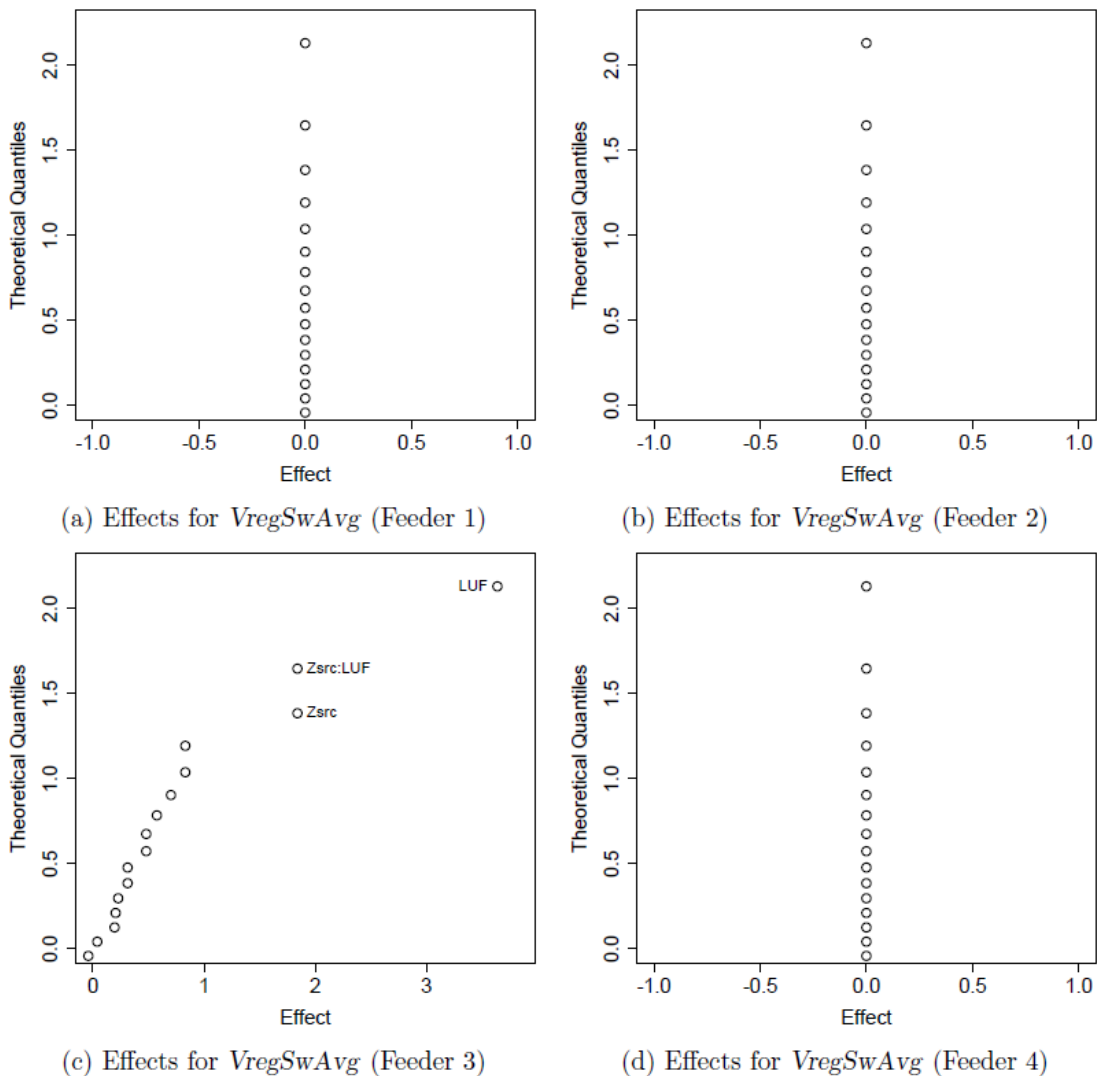


Figure 10-7. Half normal plots showing influencing factors on SVR switching.

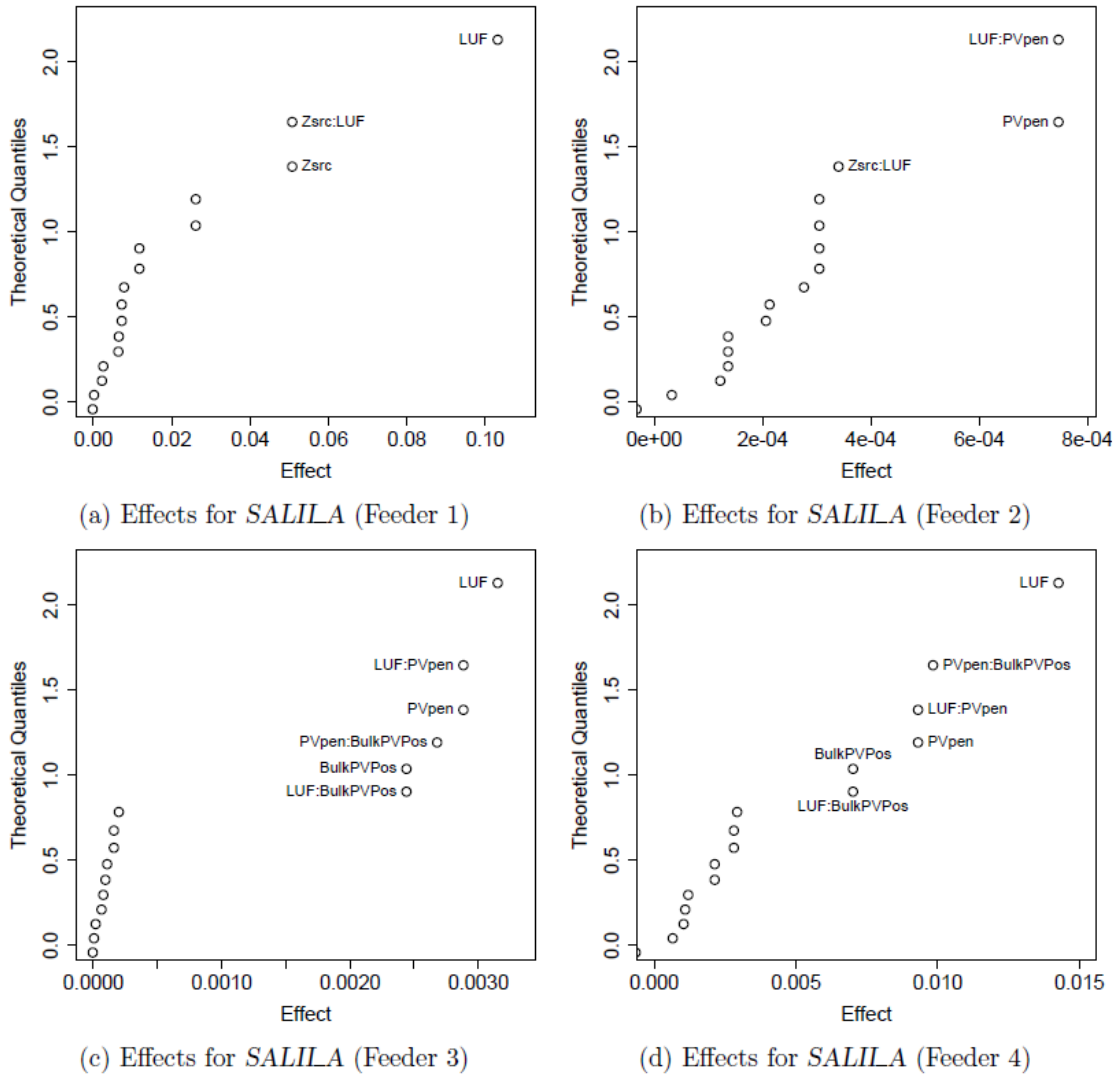


Figure 10-8. Half normal plots showing influencing factors on SALIIA.

10.6 Conclusion

Herein, an approach for conducting parametric studies for high penetration of PV with feeder models is presented. The approach focused on time-domain, quasi-steady-state analysis of distribution feeders in order to investigate the impact of high penetration PV on such aspects of system behavior as voltage excursions and operation of voltage regulation devices. In particular, the approach was intended to allow consideration of a variety of mitigation techniques such as possible reactive power control strategies for PV inverters. However, the approach was not tailored to consider some of the other points of concern for high penetration of PV, such as system harmonics, grounding issues, fault current contributions, or unintentional island detection. Additionally, a number of simplifications have been made in order to accommodate the parameterization with a small set of largely independent and generally applicable parameters. Some of the simplifications and points of consideration include the following:

- PV and load power profiles were not parameterized. As an alternative, single-day profiles were drawn from available data sets. PV power data was available from a number of sites within Florida with one-minute resolution. One-year sets of profiles were assembled for representative PV sites of

sizes ranging from a few kilowatts up to several megawatts. Inevitably, days with missing or erroneous data prevented full, one-year sets from being directly composed. However, same-day data from other years was substituted in most cases to produce a reasonably representative one-year set. A small set of load profiles was constructed from substation real and reactive power measurements with synchronized PV power measurements. However, only a small set of load profiles was used in the parametric studies, and a one-week set was recycled over the one-year profile sets. A more comprehensive approach might generate randomized, representative synthetic data sets based on descriptive parameters.

- For a simulation, a single PV profile was applied to all PV sources in the model. Thus, all of the profiles were correlated, which would be somewhat unrealistic. Phase-shifting the profiles was considered as a means to make the simulation more realistic, but this reduces the variation in the total profile, deviating from the intended overall profile. Thus, the variation in the individual profiles would need to be increased in order to include these random variations. This was also an issue with the load profiles, as applying the same profile to all loads made the load powers completely correlated. Additionally, these profiles were not changed as the PV plants and loads were scaled. It is expected that variability would decrease as PV power increases, for example. However, for these cases, the profiles were not filtered or modified to account for these types of trends.
- The load profile was distributed in proportion to the apparent power ratings of the load transformers. Thus, unless single phase transformers were employed, with different ratings for transformers on different phases, all loads were balanced, which generally would represent an unrealistic, best-case scenario. One approach to make the simulations more realistic might be to explicitly include a parameter to control unbalance of the load between phases. However, this was not done as part of the work described.
- In most cases, the model was not executed for a full one-year set of profiles at each point explored in the parameter space. Rather, in order to reduce the required computational effort, a representative set of PV and load profile pairs was chosen based on a clustering algorithm that was applied. Descriptive characteristics of the profiles (e.g. mean PV power, high frequency variability index, mean load power) were used as inputs to the clustering algorithm. Results from execution of the small representative sets were used, along with the numbers of points in the associated clusters, to estimate annual feeder behavior using a weighted average. This was shown to provide reasonable estimates when applied to one of the feeder models for a few sets of parameter values, but estimates using this approach may not be accurate in all cases.
- Clustering of residential PV was not directly considered, as residential PV was simply distributed in proportion to the apparent power ratings of the associate load transformers. In a related point, only one bulk PV power plant was considered. Thus, while the chosen parameterization afforded some flexibility in the concentration and location of the PV sources along the feeder, a more general parameterization might be considered in future work.
- Impedance values for line sections were not included in the parameterization. The source impedance (generally representing the substation transformer impedance) was included in the parameterization, but the line section impedance values were held constant. Consideration of variations in the line impedances through one or more parameters may help to better provide insight into the role of such feeder characteristics on the overall behavior of the feeders with increased PV penetration.
- While a parameter was included to vary the power factor of the loads, this single parameter was applied to all loads in the system. Some method for variation in the power factor values for loads might also be useful.

- The simulations and formulation of parameters considered herein focused on analysis of a single feeder model in order to simplify and focus the analysis. As a substation may likely supply multiple feeders through multiple transformers, the parameterization in terms of a single feeder connected through a single substation transformer is a simplification. Thus, a widening of the analysis to include multiple feeders could provide additional insight.

Although a number of simplifications were made, a fairly flexible parameterization of the system was presented, and a set of software tools were developed to allow parametric studies to be conducted on feeder models. Some of the key points from these include the following:

- A set of generally applicable parameters was identified for controlling many of the characteristics of a distribution feeder, the incorporation of PV sources into the feeder, and potential reactive power controls for PV sources. While not comprehensive, these provide for considerable variation in the considered system, and can be applied to a wide range of feeder models.
- A set of generally applicable response quantities was identified for characterizing the behavior of a feeder. These response quantities allow comparison of behavior for relatively disparate feeder models in order to attempt to better understand the implication of feeder characteristics, PV penetration, and mitigation methods on feeder behavior. As part of this work, two new load impact indices, SALII and CALII, were also formulated, motivated by reliability indices commonly used by utilities. An analog of the variability index applied for analysis of solar irradiance was also described, which can be applied to measured PV power profiles. This allows characterization of the variability in power profiles in a manner similar to the variability index, but is applicable to cases in which irradiance data is not available or not as directly applicable (as with tracking PV systems).
- A set of software tools was developed to facilitate execution of parametric studies on OpenDSS models. This included development of a number of MATLAB functions to serve as a general tool set for crafting parametric studies, as well as a standalone tool for conducting studies using the pre-configured parameters described in this work.
- An approach for approximating the behavior of a feeder when exposed to a year-long set of PV and load profiles was described. This approach was based on selecting a small, representative set of load and PV profiles using a clustering algorithm targeted at characteristics of the profiles. A weighted average is applied to the results from the selected set based on the numbers of points within the cluster associated with each selected profile.
- In one of the example studies, a case was considered in which increasing PV penetration led to voltage excursions at some of the loads, as indicated by the increased values for the load impact index response quantities. A power-factor control scheme based on power was considered for reactive power control of the PV inverters as a potential mitigation method. While this method reduced the impact on the system in terms of the load impact indices, an unintended consequence was an increase in the number of switching operations of the voltage regulators in the feeder. In order to address this issue, relaxation of the voltage control band for the voltage regulators was considered. It was shown that by including the power-power factor compensation for the PV inverters and relaxing the voltage control band for the voltage regulators, the feeder was able to support increased penetration without substantial negative impacts on the feeder operation. This served as an example case for use of the parametric study tools presented.

In general, while a number of issues were not addressed with the approach described herein, the approach may be useful for investigating, understanding, and addressing some of the issues that may surface through increased penetration of PV in distribution feeders.

10.7 References

- [1] R Core Team. R: A Language and Environment for Statistical Computing. R Foundation for Statistical Computing, Vienna, Austria, 2013.
- [2] MATLAB. version 7.12.0 (R2011a). The MathWorks Inc., Natick, Massachusetts, 2011.
- [3] VDE. Generators connected to the low-voltage distribution network - technical requirements for the connection to and parallel operation with low-voltage distribution networks (German). VDE-AR-N 4105, pages 1{80, August 2011.
- [4] IEEE guide for electric power distribution reliability indices. IEEE Std 1366-2012 (Revision of IEEE Std 1366-2003), pages 1{43, May 2012.
- [5] M JE Alam, Kashem M Muttaqi, Darmawan Sutanto, L Elder, and A Baitch. Performance analysis of distribution networks under high penetration of solar PV. In Proceedings of the 44th International Conference on Large High Voltage Electric Systems, pages 1-9, 2012.8-61
- [6] Joshua Stein, Cli_ord Hansen, and Matthew J Reno. The variability index: A new and novel metric for quantifying irradiance and PV output variability. Technical report, Sandia National Laboratories (SNL-NM), Albuquerque, NM (United States), 2012.
- [7] DC Barr. The use of a data historian to extend plant life. 1994.
- [8] Yuri V Makarov, Clyde Loutan, Jian Ma, and Phillip de Mello. Operational impacts of wind generation on california power systems. Power Systems, IEEE Transactions on, 24(2):1039-1050, 2009.
- [9] D.C. Montgomery. Design and analysis of experiments. Wiley, 2008.
- [10] R.H. Myers, D.C. Montgomery, and C.M. Anderson-Cook. Response surface methodology: process and product optimization using designed experiments, volume 705. Wiley, 2009.
- [11] K.T. Fang, R. Li, and A. Sudjianto. Design and modeling for computer experiments, volume 6. Chapman & Hall/CRC, 2005.
- [12] T.J. Santner, B.J. Williams, and W.I. Notz. The design and analysis of computer experiments, Springer, 2003.
- [13] Trevor Hastie, Robert Tibshirani, and Jerome Friedman. The elements of statistical learning, 2nd Ed. Springer, 2009.
- [14] Christopher M Bishop et al. Pattern recognition and machine learning, volume 4. Springer, New York, 2006.
- [15] Andrea Saltelli, Karen Chan, E Marian Scott, et al. Sensitivity analysis, volume 1. Wiley New York, 2000.
- [16] Max D Morris. Factorial sampling plans for preliminary computational experiments. Techno-metrics, 33(2):161{174, 1991.
- [17] Gilles Pujol, Bertrand Iooss, and Alexandre Janon. sensitivity: Sensitivity Analysis, 2013. R package version 1.7.
- [18] Ulrike Grmping. R package FrF2 for creating and analyzing fractional factorial 2-level designs. Journal of Statistical Software, 56(1):1-56, 2014.
- [19] Joseph Adler. R in a nutshell: A desktop quick reference. " O'Reilly Media, Inc.", 2010.
- [20] Julian J Faraway. Linear models with R. CRC Press, 2014.
- [21] Julian J Faraway. Extending the linear model with R: generalized linear, mixed e_ects and nonparametric regression models. CRC press, 2005.
- [22] John M Chambers and Trevor J Hastie. Statistical models in S. CRC Press, Inc., 1991.
- [23] Jerome H Friedman. Multivariate adaptive regression splines. The annals of statistics, pages 1-67, 1991.

- [24] Carl Edward Rasmussen and Christopher K. I. Williams. Gaussian processes for machine learning. MIT Press, 2006.
- [25] A Samad Hedayat, Neil James Alexander Sloane, and John Stufken. Orthogonal arrays: theory and applications. Springer Science & Business Media, 1999.
- [26] S original by Trevor Hastie, Robert Tibshirani. Original R port by Friedrich Leisch, Kurt Hornik, and Brian D. Ripley. mda: Mixture and exible discriminant analysis, 2013. R package version 0.4-4.
- [27] Robert B. Gramacy. tgp: An R Package for Bayesian Nonstationary, Semiparametric Non-linear Regression and Design by Treed Gaussian Process Models., 2007. Journal of Statistical Software, 19(9), 1-46.
- [28] Garrett M. Dancik. mlegp: Maximum Likelihood Estimates of Gaussian Processes, 2012. R package version 3.1.3.
- [29] Rob Carnell. lhs: Latin Hypercube Samples, 2012. R package version 0.10.
- [30] James R Hockenberry and Bernard C Lesieutre. Evaluation of uncertainty in dynamic simulations of power system models: The probabilistic collocation method. Power Systems, IEEE Transactions on, 19(3):1483{1491, 2004.
- [31] MS Eldred and John Burkardt. Comparison of non-intrusive polynomial chaos and stochastic collocation methods for uncertainty quanti_cation. AIAA paper, 976(2009):1-20, 2009.
- [32] Martin Maechler, Peter Rousseeuw, Anja Struyf, Mia Hubert, and Kurt Hornik. cluster:Cluster Analysis Basics and Extensions, 2013. R package version 1.14.4 | For new features, see the 'Changelog'_le (in the package source).

11 TRANSMISSION SYSTEM MODELING AND SIMULATION

11.1 Motivation

As solar PV penetration becomes widespread, the capacity of solar PV generation as a percentage of the peak load served for entire substations and even entire control areas, rather than just individual circuits, can reach the point where high-penetration solar PV will affect the bulk power system (BPS). To facilitate studies and research and development involving the bulk power system, FSU CAPS has been engaged in a collaborative effort with the FRCC to develop a reduced bus model of the Florida electric grid. The intent is to produce a model significantly reduced in size and complexity from the detailed planning models used by the FRCC and the electric utilities, but, sufficiently capturing salient features of the system to reflect important steady state and dynamic behavior. Once reduced, sanitized or notionalized versions of such a model could also be produced that would not constitute Critical Energy Infrastructure Information (CEII), making it easier to leverage the capabilities of a larger community of experts to study power systems questions, especially the long-range questions involving the future of the power grid.

As with reduced distribution system models, advantages in working with a reduced BPS model include reduced places for error in model development, improved manageability and maintainability, and faster execution times (useful for EMTP studies, real-time simulation runs, and detailed studies requiring multiple simulation runs). A reduced model approach can also simplify and speed the process of producing notionalized models, where, for example, geographically identifying information must be removed.

11.2 Approach and Results

The goal was to produce a model of less than 300 busses from a statewide or regional model having many thousands of busses. 300 busses was initially chosen, in part, because this would run on an RTDS system the size of that at the FSU CAPS facility (14 racks).

Initially, in prior work, a 154 bus model of the Florida system was produced with a great deal of engineering judgment. During the course of the SUNGRIN effort, the built-in model reduction tools within PSSE were applied with carefully selected criteria to produce reduced versions directly from the detailed PSSE model of the system. The 154 bus system and a system produced with PSSE reduction tools are shown in Figure 11-1.

Several reduced versions were produced with PSSE tools, including a 600 bus version and a version of less than 150 busses that could run on 5 racks of the RTDS. The validation of the 600 bus version is shown in Figure 11-2, with voltage magnitudes at

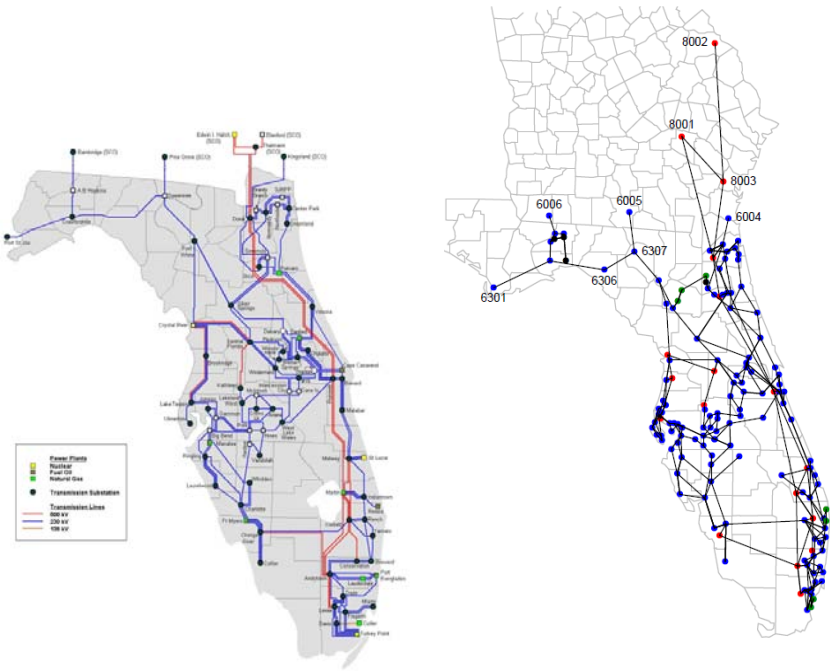


Figure 11-1. 154 (left) and <600 (right) bus models of the FL grid

every retained bus in very good agreement, and, net reactive power flows at the busses in fairly good agreement, though with some outliers to be examined.

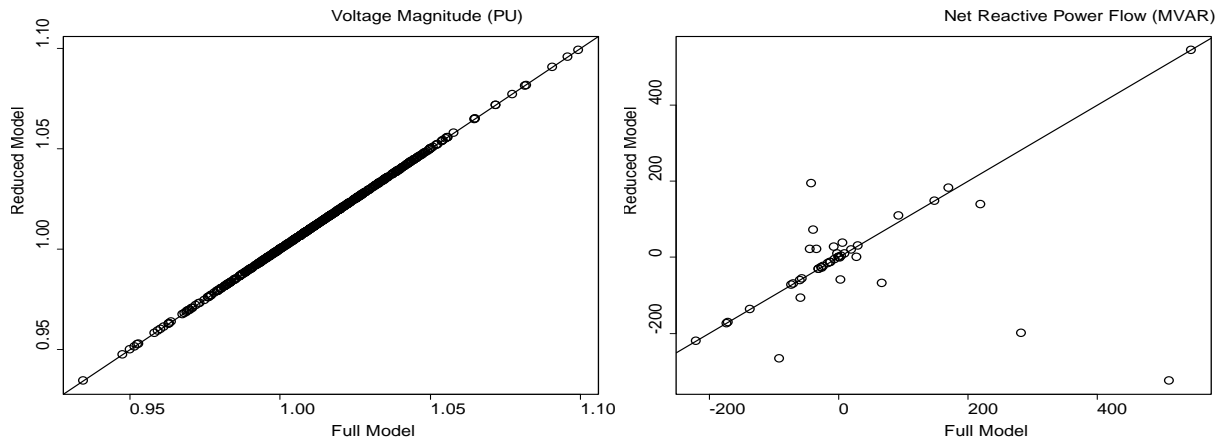


Figure 11-2. Validation of the 600-bus reduced model, comparing voltage and reactive power flow for retained busses

11.3 Future work

Future work would include refinement and validation of the sub-150-bus version of the model, including both steady state and dynamic validation against scenarios provided by FPL and the FRCC, and producing a notionalized version of the model, reviewed and approved for general use. Validated models (notionalized or not) could then be used for extensive studies of BPS behavior under widespread high-penetration PV impact scenarios, as well as major potential changes that may eventually affect the BPS such as more widespread distributed energy resources (DER) in general, and affects from high-penetration of other technologies such as plug-in electric vehicles (PEV's).

11.4 References

[1] Alquthami, T.S., et al, "Projected load and generation data in support of an open access dynamic model of the Florida grid", Power and Energy Society General Meeting, IEEE, 2010.

12 CONCLUSIONS

12.1 Key Findings

12.1.1 High Penetration PV

The four Florida utility feeders examined in detail all had high-penetration levels of PV. It is notable that in all cases, the high-penetration was the result of MW-scale PV installations, in three cases, due to a single large utility-scale installation, and, in the other case, due to two 1-MW plants and a few plants hundreds of kW in size. Aside from that, the feeders were reasonably varied in terms of load mix, voltage regulation devices and control strategies, topology, and PV system type and location.

Extensive studies on the Florida utility feeders, both analysis of field data and numerous simulation-assisted case studies lead to several clear conclusions:

There are a several factors that influence impact of high penetration levels of solar PV on a distribution circuit. Percent penetration does not correlate well with impact, as evidenced by the four Florida utility circuits examined in detail, ranging from 26% to 600% penetration. Influencing factors include circuit design, size and location(s) of PV, whether PV is central or distributed, types of regulation equipment present, if any, and their settings and control strategies, the size, distribution, shape, and type of load, and, the intermittency.

Reverse power flow, by itself, is not correlated with adverse impact.

The nature of the intermittency of the solar resource varies considerably geographically and with size and level of aggregation of PV, but, in any case, does not appear to be a major impact on daily circuit operation due to the relative difference in PV ramp rates under the highest variability conditions and the much faster dynamic response of electrical and electromagnetic systems. In any event, PV intermittency varies roughly on similar periodic scales as loads, and, thus, in most cases, presents no more challenge to system operation than do loads. This is evident in the PV and load responses shown in Figure 12-1.

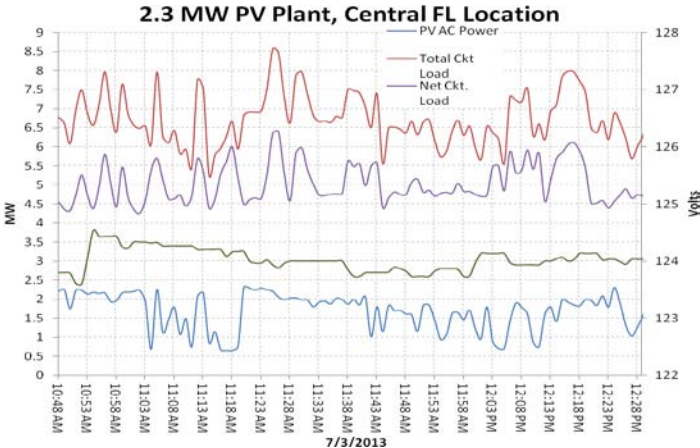


Figure 12-1. PV, load, and voltage variations, 2.3 MW

Modifications to settings or control strategies of traditional voltage regulation devices and systems will often help with accommodating high penetration PV, in terms of voltage profile and time-variation, and, in fact, having settings and control strategies for these the same as non-hi-penetration PV circuits can sometimes lead to poorer voltage regulation performance.

In every case examined, large PV plants participating in voltage regulation on a circuit were able to substantially improve voltage profile and time-series response. Interaction with existing devices and whether it increases or decreases their operation, or causes problems such as SVR wind-up, depends on many of the same factors as PV impact assessment in general

12.1.2 Tools

A reduced model approach has been developed and improved upon that provides some important advantages, including:

- Speedier model development

- Reduced chance of error in model development
- Simplified validation more fitting the limited field measurement locations available on a distribution circuit
- Simplified maintenance and support
- Faster simulation execution times, especially valuable for studies involving longer-term or multiple simulation runs
- Model size, in terms of nodes or busses, small enough to run in real-time on platforms such as RTDS
- Ability to run in real-time, in turn, provides the possibility of hardware-in-the-loop (HIL) testing of equipment or protection and control systems interacting with circuit simulations

The simplified feeder model development and the much faster execution times of the reduced model will be particularly valuable as the focus of high-penetration studies broadens from the individual feeder level to multiple feeders, substations, multiple substations, entire control areas, and the bulk power system. Scaling the scope of the study requires reducing the level of detail in order for simulation-assisted approaches to be practical, simply because of the computing power required.

A unique factor-screening parametric study approach to assessing impact and relative importance of different influencing factors was pioneered on this project. These types of studies utilized the open-use OpenDSS models, but, require longer simulation runs, more simulation runs, and more pre- and post-processing. Again, the reduced model approach improves the practicality of this due to the simulation execution times involved.

To facilitate the parametric study work several new indices have been developed including two (SALII and CALII) that would provide improved assessment of distribution circuit reliability with increased distributed generation, which where large voltage excursions would be considered in addition to interruptions and outages. And, the High Frequency Power Variability Index, HPVI, developed for this effort, is broadly applicable in assessing the high-frequency, intraday variability of solar PV irradiance and plant power output.

12.2 Future Work

Extensive investigations of high penetration PV impact on individual distribution feeders have been completed by the SUNGRIN team and other High-Penetration PV Deployment project teams, along with CEC-funded projects and others. Some major research needs going forward are:

- To investigate the wide area affects of high-penetration PV, across multiple feeders, substations, control areas and the bulk power system, including developing the necessary tools and techniques to effectively conduct simulation assisted studies across larger portions of the power system.
- To develop the next generation of advanced control approaches for distribution systems and up to the BPS for utility-integrated solutions that fully leverage the value and capability of solar PV as penetration continues to increase.
- To examine the collective results of all the high-penetration PV research projects over the past several years and, with the benefit of the full variety of circuits, tools, and approaches, develop more comprehensive and broadly applicable tools, insights, and conclusions.

APPENDICES

A. APPENDIX – ACRONYMS

AC	Alternating Current
ADSCOM	Administrative Subcommittee
AMSC	American Superconductor
ASC	Applied Superconductivity Center
ASME	American Society of Mechanical Engineers
ATS	Automatic Transfer Switch
BPA	Bonneville Power Administration
BPS	Bulk Power System
CAIDI	Customer Average Interruption Duration Index (defined in IEEE P1366)
CAIFI	Customer Average Interruption Frequency Index (defined in IEEE P1366)
caps	Capacitor banks
CAPS	Center for advanced Power Systems
CDF	Cumulative Distribution Function
CEC	California Energy Commission
CEII	Critical Energy Infrastructure Information
CHIL	Controller Hardware-in-the-Loop
COE	College of Engineering
CPUC	California Public Utilities Commission
D&NMTT	Data and Network Management Task Team
DC	Direct Current
DER	Distributed Energy Resources
DES	Distributed Energy Storage
DESS	Distributed Energy Storage System
DFT	Discrete Fourier Transform
DFR	Digital Fault Recorder
DG	Distributed Generation
DMS	Distribution Management System
DOE	(U.S.) Dept. of Energy
DPV	Distributed PV
dSVC	Distribution class Static VAR Compensator
EBSD	Electron Back-Scatter Diffraction
EDC	Economic Development Council
EERE	Energy Efficiency and Renewable Energy
EMS	Energy Management System
EMTP	Electromagnetic Transient Program
EPIRS	Electric Power Infrastructure Reliability and Security
EPRI	Electric Power Research Institute
EPS	Electric Power System
ES	Energy Storage
ESE	Energy Storage Elements

ESS	Energy Storage Systems
ETO	Emitter Turn-Off
FAMU	Florida A&M University
FAWN	Florida Automated Weather Network
FCL	Fault Current Limiter
FEAT	FRCC Event Analysis Team
FESC	Florida Energy Systems Consortium
FFT	Fast Fourier Transform
FIT	Feed-In Tariff
FMPA	Florida Municipal Power Agency
FOA	Funding Opportunity Announcement
FPL	Florida Power and Light
FRCC	Florida Reliability Coordinating Council
FRT	Fault Ride Through
FSEC	Florida Solar Energy Center
FSIG	Fixed Speed Induction Generator
FSU	Florida State University
GHI	Global Horizontal Irradiance
GPC	Gigahertz Processor Card
GRU	Gainesville Regional Utilities
GOES	Geostationary Operational Environmental Satellite
GW	Gigawatt
HIL	Hardware-in-the-Loop
HRSEM	High Resolution Scanning Electron Microscope
HTS	High Temperature Superconductivity
HV	High Voltage
IEEE	Institute of Electrical and Electronics Engineers
IP	In-Plane
IP	Intellectual Property
IVGTF	Integration of Variable Generation Task Force
JEA	Jacksonville Electric Authority
KSC	Kennedy Space Center
kVA	Kilovolt-amperes
kW	Kilowatt
LPV	Large PV
LTLSM	Low Temperature Laser Scanning Microscope
LVRT	Low Voltage Ride Through
MOI	Magneto Optical Imaging
MPPT	Maximum Power Point Tracking
MV	Medium Voltage
MVA	Million Volt-Amperes

MW	Megawatt
NARUC	National Association of Regulatory Utility Commissioners
NASA	National Aeronautics and Space Administration
NASPI	North American Synchrophasor Initiative
NCSU	North Carolina State University
NDA	Non-Disclosure Agreement
NEETRAC	National Electric Energy Testing Research and Applications Center
NERC	North American Electric Reliability Corporation
NHMFL	National High Magnetic Field Laboratory
NIC	Network Interface Card
NOAA	National Oceanic and Atmospheric Administration
NRECA	National Rural Electric Cooperative Association
NREL	National Renewable Energy Laboratory
OLTC	On-Load Tap Changer
OMS	Outage Management System
ONR	Office of Naval Research
ORNL	Oak Ridge National Laboratory
OUC	Orlando Utilities Commission
PCC	Point of Common Coupling
PCUE	Power Center for Utility Explorations
PEV	Plug-in Electric Vehicle
PHIL	Power Hardware-in-the-Loop
PI	Proportional Integral (controller)
PI™	Process Information (OSISoft real-time process information system)
PLD	Pulsed Laser Deposition
PLL	Phase-Locked Loop
PMU	Phasor Measurement Unit
POA	Plane of Array
PPA	Power Purchase Agreement
PQ	Power Quality
PSS®E	Power Systems Simulator for Engineers, aka PSS/E, PSSE
pu	Per unit
PV	Photovoltaic
PWM	Pulse Width Modulation
RITT	Research Implementation Task Team
RLC	Resistive-Inductive(L)-Capacitive
RMS	Root Mean Square
RPA	Reactive Power Allocation
RPAC	Reactive Power Allocation Coefficient
RSI	Renewable Systems Interconnection
RTDS™	Real Time Digital Simulator

SAIDI	System Average Interruption Duration Index (defined in IEEE P1366)
SAIFI	System Average Interruption Frequency Index (defined in IEEE P1366)
SAM	System Advisor Model
SCADA	Supervisory Control and Data Acquisition
SCB	Switched Capacitor Bank
SCE	Southern California Edison
SCFCL	Superconducting Fault Current Limiter
SEL™	Schweitzer Engineering Laboratories
SEM	Scanning Electron Microscope
SETP	Solar Energy Technologies Program
SG	Synchronous Generator
SGTF	Smart Grid Task Force
SI	System Integration
SIWG	Smart Inverter Working Group
SLA	Software License Agreement
SNL	Sandia National Laboratory
SOC	State of Charge
SOPO	Statement of Project Objectives
SSFCL	Solid State Fault Current Limiter
STATCOM	Static Compensator
STS	Static Transfer Switch
SUNGRIN	Sunshine State Solar Grid Initiative
SUNY	State University of New York
SVR	Step Voltage Regulator
SWG	Stability Working Group
TCP	Transmission Control Protocol
TF	Task Force
THD	Total Harmonic Distortion
TOU	Time of Use
TVA	Tennessee Valley Authority
UB	University at Buffalo
UCF	University of Central Florida
UFL	Universal File Stream Loader
UL	Underwriters Laboratory
USF	University of South Florida
VA	Volt-amperes
VAR	Volt-amperes (amps) Reactive (reactive power)
VVS	Variable Voltage Source
WG	Working Group

B. APPENDIX – OPEN USE MODEL DOCUMENTATION

Feeder component naming conventions

Component	Naming Convention	Description
Substation Bus	BXXXXX	BXXXXX – ‘B’ followed by five digit number for bus name
Bus	BXXXXXY	Y = [A,B,C,P] (Phase information)
Line Section	BXXXXXY_BXXXXXY	Name based on corresponding buses
Transformer	BXXXXXY_BXXXXXY_N	N- Integer indicating the number of transformer connected at that bus
Voltage regulator	BXXXXXY_BXXXXXY	Name based on corresponding transformer
Capacitor	BXXXXXY	Name based on corresponding bus
Capacitor control	BXXXXXY	Name based on corresponding capacitor
Load	BXXXXXY_N	Name based on corresponding bus
Generator	BXXXXXY_N	Name based on corresponding bus

C. APPENDIX – MODEL REDUCTION FUNCTIONS

No.	Reduction Step	Function Name	Description
1		sg_DispatchReduction.m	Main entry point for reduction process
2		sg_FeederReductionSetup.m	Feeder case setup
3		sg_findAdjacentBuses.m	Determine adjacent buses and lines at a bus
4		sg_GetTopologyTree.m	Build topology tree
5		sg_getObjectProperties.m	Determine an OpenDSS object's properties
6		sg_IDkeyBuses.m	Determine initial key and candidate bus lists
7		sg_modelResultsComparisonReduction.m	Compute data for comparison of models
8	Combine Loads	sg_openDssCombineLoads.m	Combines individual loads into aggregated loads
9		sg_openDssGetGenInfo.m	Extract feeder information on generators
10		sg_openDssGetLineInfo.m	Extract feeder information on lines
11		sg_openDssGetLoadInfo.m	Extract feeder information on loads
12		sg_openDssGetTransformerInfo.m	Extract feeder information on transformers
13	Move Elements	sg_openDssMoveElements.m	Move elements from a specified bus to another
14	Move line	sg_openDssMoveLine.m	Reconnect a line at a different bus
15	Remove bus	sg_openDssRemoveBus.m	Eliminate bus from the circuit, combines lines if necessary
16	Split bus	sg_openDssSplitBus.m	Split a load into part and reconnect at neighboring buses
17		sg_ProfileUpdate.m	Compute profile data for reduced circuit
18		sg_Reduction_Metric.m	Entry point for model reduction based on alternate metrics
19		sg_Reduction_Topology.m	Entry point for topology reduction algorithm
20		sg_voltageDropMetric.m	Computes voltage drop as index for reduction process



Prepared by

Florida State University
Center for Advanced Power Systems
2000 Levy Ave., Suite 140
Tallahassee, FL 32310